

# **Characterization of the substrate specificity of squalene-hopene cyclases (SHCs)**

## **Untersuchungen zur Substratspezifität von Squalen-Hopen Zyklasen (SHCs)**

Von der Fakultät 3: Chemie der Universität Stuttgart zur Erlangung der Würde eines Doktors der Naturwissenschaften (Dr. rer. nat.) genehmigte Abhandlung

Vorgelegt von Miriam Seitz

aus Rastatt

Hauptberichter: Prof. Dr. Bernhard Hauer

Mitberichter: Prof. Dr. Bernd Plietker

Vorsitzende: Prof. Dr. Cosima Stubenrauch

Tag der mündlichen Prüfung: 6. Februar 2013

Institut für Technische Biochemie der Universität Stuttgart

2012

Die vorliegende Arbeit entstand auf Anregung und unter Anleitung von Herrn Prof. Dr. Bernhard Hauer in der Zeit von Oktober 2009 bis Dezember 2012 am Institut für technische Biochemie an der Universität Stuttgart.

Im Rahmen dieser Dissertation wurden folgende Publikationen vorab veröffentlicht:

- **“Substrate specificity of a novel squalene-hopene cyclase from *Zymomonas mobilis*”**; M. Seitz, J. Klebensberger, S. Siebenhaller, M. Breuer, G. Siedenburg, D. Jendrossek, B. Hauer; *J. Mol. Cat. B: Enzymatic* **2012** (84) 72–77.
- **“Activation-Independent Cyclization of Monoterpenoids”**; G. Siedenburg, D. Jendrossek, M. Breuer, B. Juhl, J. Pleiss, M. Seitz, J. Klebensberger, B. Hauer; *Appl. Environ. Microbiol.* **2012** (78) 1055–1062.
- **“Synthesis of Heterocyclic Terpenoids by Promiscuous Squalene-Hopene Cyclases”**; M. Seitz, P.-O. Syrén, L. Steiner, J. Klebensberger, B. M. Nestl, B. Hauer; *ChemBioChem* **2013** (14) 436-439.
- **“Squalene hopene cyclases: highly promiscuous and evolvable catalysts for stereoselective C-C and C-X bond formation”**, S. C. Hammer, P.-O. Syrén, M. Seitz, B. M. Nestl, B. Hauer; *Curr. Opin. Chem. Biol.* **2013** (17) DOI: 10.1016/j.cbpa.2013.01.016.

## **Erklärung über die Eigenständigkeit der Dissertation**

Ich versichere, dass ich die vorliegende Arbeit mit dem Titel „Untersuchungen zur Substratspezifität von Squalen-Hopen Zyklasen (SHCs)“ selbständig verfasst und keine anderen als die angegebenen Quellen und Hilfsmittel benutzt habe; aus fremden Quellen entnommene Passagen und Gedanken sind als solche kenntlich gemacht.

## **Declaration of Authorship**

I hereby certify that the dissertation entitled “Characterization of the substrate specificity of squalene-hopene cyclases (SHCs)” is entirely my own work except where otherwise indicated. Passages and ideas from other sources have been clearly indicated.

Name/Name:           Miriam Seitz

Unterschrift/Signed: \_\_\_\_\_

Datum/Date:           \_\_\_\_\_

## Danksagungen

Mein erster und größter Dank gilt Prof. Dr. Bernhard Hauer, der mir ein sehr spannendes Thema zugetraut und es mir ermöglicht hat, meine Promotion innerhalb der letzten drei Jahre durchzuführen. Für die ausgezeichnete Betreuung möchte ich mich sehr bedanken.

Des Weiteren möchte ich besonders Dr. Bettina Nestl und Dr. Per-Olof Syrén danken, die mich durch ihre gute Betreuung sehr unterstützt, diese Arbeit sorgfältig korrigiert, mir viele wertvolle Ratschläge gegeben haben und mir immer sowohl fachlich als auch emotional zur Seite standen, sowie bei Dr. Janosch Klebensberger und Dr. Katja Koschorrek für ihre Betreuung. Auch dem „Team Zyklase“, bestehend aus Jörg Dominicus, Stephan Hammer, Per-Olof Syrén und Silvia Racolta sowie Sascha Siebenhaller, Michael Pohl und Lisa Steiner, die das Projekt mit gestaltet und vorangebracht haben, gilt ein herzlicher Dank für die tolle Zusammenarbeit, interessante Diskussionen und den stetigen Ideenaustausch. Des Weiteren möchte ich Dr. Gabi Siedenburg, Dr. Michael Breuer und Dr. Dieter Jendrossek für gute Zusammenarbeit danken. Jessica, Eric, Bernhard und Peter danke ich für das Korrekturlesen von meiner Arbeit.

Dem Bundesministerium für Bildung und Forschung (BMBF) und „KYROBIO: Developing biocatalysts for industrial chiral compounds“ gilt ein besonderer Dank für die Finanzierung des Projekts.

Meine letzten drei Jahre am ITB haben mich nicht nur auf fachlicher Seite, sondern auch persönlich sehr bereichert. Deswegen ist es mir wichtig, einige Leute, die mich auf meinem Weg begleitet haben, besonders zu erwähnen. Zuerst würde ich gerne Bettina und Bernd danken, die immer ein offenes Ohr für meine Sorgen hatten und auf deren Unterstützung ich mich stets verlassen konnte. Daniel, Sumire, Björn, Marko und Christian waren meine stetigen Wegbegleiter und haben mir so manches Mal sehr zur Seite gestanden. Stephan, Dennis, Sumire und Bettina möchte ich danken für die unvergessliche Biotrans-Konferenz, die ein absolutes Highlight meiner Zeit am ITB darstellt. Meine beiden Labor-Kollegen Christine und Jörg haben mich vor allem in der Endphase meiner Doktorarbeit stets motiviert, meine Sorgen angehört und mir immer geholfen. Hierfür möchte ich besonders danken. Die Liste mit lieben Leuten am ITB könnte an dieser Stelle noch eine Weile fortgesetzt werden. Aber statt alle einzeln aufzuzählen, möchte ich hier einfach allen



Kollegen danken, die täglich für gute Stimmung gesorgt und mir meine Arbeit damit sehr erleichtert haben. Danke für gute fachliche Diskussionen und Hilfsbereitschaft, für die Freundlichkeit und Freundschaft sowie für zahlreiche schöne Erlebnisse im und außerhalb des Instituts.

Auf persönlicher Seite möchte ich zuerst meinen Eltern danken für ihre liebevolle Erziehung und dafür, dass sie mich immer unterstützt und mir meine Ausbildung ermöglicht haben, die ich nun mit der Anfertigung meiner Doktorarbeit abschließe. Meinen Brüdern Niklas und Fabian und meiner Schwägerin Anita danke ich für unseren guten Zusammenhalt, für viele wichtige und lustige Gespräche und für ihre große Hilfsbereitschaft. Peters Familie, besonders Doris, möchte ich danken für ihre Herzlichkeit und für die jahrelange Unterstützung in allen Lebenslagen. Meiner kleinen Nichte Carolina und meinem kleinen Neffen Linus danke ich dafür, dass sie uns so viel Freude bereiten.

Den Rastatter Freunden möchte ich für viele schöne Erlebnisse danken, und dafür, dass sie so lustig sind wie eh und je, und dass wir es geschafft haben, uns nicht aus den Augen zu verlieren. Besonders meinen lieben Freundinnen Anja, Carolin und Virginia möchte ich für beinahe 20 Jahre Freundschaft danken, in denen sie immer ein offenes Ohr für meine Sorgen hatten.

Allen meinen Mitbewohnern, die ich in acht Jahren WG-Leben in Stuttgart hatte, und vor allem meinen derzeitigen Mitbewohnern Simon, Dennis und Peter danke ich für die Freundschaft und Fröhlichkeit, für aufmunternde und ernste Gespräche und den unermüdlichen Zusammenhalt während all der Jahre. Ein besonderer Dank gilt meiner Dienstagsgroupe und vor allem Tanja für unzählige tolle gemeinsame Erlebnisse.

Meinem Lacrosse-Team Neckarnixen und allen von Stuttgart Lacrosse e.V., mit denen ich einen großen Teil meiner Freizeit verbringe, danke ich für tolle Trainings, Spiele, Team-Events, Turniere, wichtige Unterhaltungen auf langen Autofahrten und vor für allem die Freundschaft, die wir teilen.

Zuletzt und am allermeisten danke ich meinem Freund Peter, mit dem ich seit dem ersten Semester gemeinsam durchs Leben gehe. Er hat mich stets in meinen Eigenschaften gestärkt, mich in schwereren Zeiten aufgemuntert und unterstützt, und schöne Tage zu etwas besonderem gemacht.

Miriam Seitz

# Table of content

1	<b>Zusammenfassung</b> .....	1
2	<b>Abstract</b> .....	4
3	<b>Theoretical Background</b> .....	7
3.1	<b>Occurrence and biosynthesis of terpenoids</b> .....	7
3.2	<b>Monoterpenoids</b> .....	12
3.3	<b>Sesquiterpenoids</b> .....	15
3.4	<b>Diterpenoids</b> .....	18
3.5	<b>Sesterpenoids</b> .....	20
3.6	<b>Triterpenoids</b> .....	22
3.6.1	Functions and occurrences .....	22
3.6.2	Biosynthesis of triterpenoids, reaction mechanisms and approaches for the evolution of the triterpene cyclases .....	23
3.6.3	Squalene-hopene cyclases .....	27
3.6.4	Substrate specificity of SHCs .....	36
3.7	<b>Organic syntheses of cyclic terpenoids</b> .....	38
3.7.1	Ambroxan and sclareolide .....	39
3.7.2	Caparrapioxide .....	44
3.7.3	Sclareoloxide and hexahydrochromene .....	46
3.7.4	Ambraoxide, ambreinolide and unsaturated ambraoxide .....	47
3.7.5	Isopulegol and menthol .....	48
4	<b>Aim of the project</b> .....	52
5	<b>Results</b> .....	53
5.1	<b>Squalene-hopene cyclases: Cloning, expression, enzyme preparation and biotransformations</b> .....	53
5.1.1	Cloning, expression and partial purification .....	53
5.1.2	Biotransformations – Elaboration of a reliable standard protocol .....	56
5.2	<b>Substrate specificity of SHCs</b> .....	68
5.2.1	Alcohols .....	69
5.2.2	Ketones .....	71
5.2.3	Carboxylic acids .....	72

5.2.4	Aldehydes .....	73
<b>5.3</b>	<b>Comparison of the substrate specificities of <i>ZmoSHC1</i>, <i>ZmoSHC2</i> and <i>AacSHC</i> .....</b>	<b>75</b>
5.3.1	Enhanced conversions .....	78
5.3.2	Limits of substrate specificity .....	79
<b>5.4</b>	<b>Directed mutagenesis .....</b>	<b>80</b>
5.4.1	Selection of spots for single mutants and screening .....	80
5.4.2	Creation and screening of the loop deletion mutant .....	81
<b>6</b>	<b>Discussion .....</b>	<b>82</b>
<b>6.1</b>	<b>Squalene-hopene cyclases: cloning, expression, enzyme preparation and biotransformations .....</b>	<b>82</b>
6.1.1	Biotransformations with whole cells .....	82
6.1.2	Biotransformations with partially purified SHCs .....	84
6.1.3	Stability experiments .....	85
6.1.4	Substrate and product inhibition .....	87
6.1.5	Internal standard experiments .....	89
6.1.6	pH Studies .....	90
<b>6.2</b>	<b>Substrate specificity of SHCs .....</b>	<b>90</b>
<b>6.3</b>	<b>Comparison of the substrate specificity of <i>ZmoSHC1</i>, <i>ZmoSHC2</i> and <i>AacSHC</i> .....</b>	<b>92</b>
6.3.1	Enhanced conversions .....	98
6.3.2	Limits of substrate specificity .....	99
<b>6.4</b>	<b>Directed mutagenesis .....</b>	<b>100</b>
6.4.1	Selection of spots for single mutants and screening .....	100
6.4.2	Creation and screening of the loop deletion mutant .....	102
<b>7</b>	<b>Conclusion .....</b>	<b>105</b>
<b>8</b>	<b>Outlook .....</b>	<b>106</b>
<b>9</b>	<b>Materials and methods .....</b>	<b>108</b>
<b>9.1</b>	<b>Instruments .....</b>	<b>108</b>
<b>9.2</b>	<b>Software .....</b>	<b>109</b>
<b>9.3</b>	<b>Consumables .....</b>	<b>110</b>
<b>9.4</b>	<b>Chemicals .....</b>	<b>110</b>
<b>9.5</b>	<b>Media, buffers and Kits .....</b>	<b>112</b>

<b>9.6</b>	<b>Molecular biological devices.....</b>	<b>113</b>
<b>9.7</b>	<b>Cell culture and enzyme expression.....</b>	<b>114</b>
<b>9.8</b>	<b>Protein biochemical methods.....</b>	<b>115</b>
9.8.1	Partial purification of the membrane bound protein fraction.....	115
9.8.2	Protein determination.....	116
<b>9.9</b>	<b>Biotransformations.....</b>	<b>116</b>
9.9.1	Biotransformations with whole cells.....	116
9.9.2	Biotransformations with partially purified SHC.....	117
9.9.3	Sample preparation.....	118
9.9.4	Preparative biotransformations and product isolation.....	119
<b>9.10</b>	<b>Analysis and evaluation.....</b>	<b>121</b>
9.10.1	GC-FID.....	121
9.10.2	GC-MS.....	123
9.10.3	New products – characterization with NMR.....	125
9.10.4	IR and HREIMS analyses.....	131
9.10.5	Determination of log P values.....	132
9.10.6	Quantification.....	133
<b>10</b>	<b>Literature.....</b>	<b>135</b>
<b>11</b>	<b>Supplementary data.....</b>	<b>157</b>
<b>11.1</b>	<b>Abbreviations.....</b>	<b>157</b>
<b>11.2</b>	<b>Sequences and other informations about the SHCs.....</b>	<b>161</b>
11.2.1	Wildtype SHCs.....	162
11.2.2	Mutants.....	163
<b>11.3</b>	<b>Multiple sequence alignments.....</b>	<b>165</b>
11.3.1	SHCs from strains containing two SHCs.....	165
<b>12</b>	<b>Curriculum vitae.....</b>	<b>168</b>

# 1 Zusammenfassung

Die zyklischen Terpenoide stellen eine große Gruppe von Naturstoffen mit verschiedensten biologischen Funktionen dar. Bis heute konnten etwa 60.000 verschiedene zyklische Terpenoide, die aus Gerüsten von zehn bis über 30 Kohlenstoffatomen aufgebaut sind, identifiziert werden.<sup>1,2</sup> Unter dieser großen Anzahl von zyklischen Stoffen finden sich viele bekannte Duft- und Aromastoffe, wie zum Beispiel Menthol oder Limonen, Verbindungen, die als pharmazeutisch wirksame Inhaltsstoffe in Medikamenten Anwendung finden, wie etwa der gegen Tumor wirksame Stoff Taxol oder das gegen Malaria angewendete Artemisinin oder auch die als Membranbestandteile und Hormone bekannten Steroide.<sup>3-6</sup> All diese interessanten Naturstoffe werden durch Zyklisierung von wenigen linearen Vorläufermolekülen gebildet. Diese Zyklisierungsreaktionen werden von Terpenoid Zyklasen katalysiert.<sup>1,7</sup>

Der Schwerpunkt der vorliegenden Arbeit liegt auf einer Unterfamilie dieser Enzymgruppe der Terpenoid Zyklasen, den Squalen-Hopen Zyklasen (SHCs).<sup>8-10</sup> Unter den über 300 annotierten SHCs wurde die SHC vom thermophilen Bakterium *Alicyclobacillus acidocaldarius* (*AacSHC*) am besten untersucht. Neben der Kristallstruktur wurde auch der komplexe Mechanismus aufgeklärt, nach dem das lineare C<sub>30</sub> Substrat Squalen zu den pentazyklischen Produkten Hopen und Hopanol zyklisiert wird.<sup>11-13</sup> Der Mechanismus dieser Reaktion, bei der neun Stereozentren und 13 kovalente C-C Bindungen spezifisch entstehen, gilt als einer der komplexesten, die man in der Chemie der Naturstoffe bislang entdecken konnte.<sup>13</sup> Neben *AacSHC* wurden in vorangehenden Arbeiten auch einige andere SHCs teilweise charakterisiert.<sup>14,15</sup> Von besonderem Interesse ist hierbei der gegen hohe Alkohol- und Zuckerkonzentrationen tolerante Stamm *Zymomonas mobilis*, der als einer der besten Hopanoid-produzierenden Bakterienstämme bekannt ist und zwei Gene enthält, die für SHCs codieren: *ZmoSHC1* und die in vorherigen Arbeiten partiell charakterisierte *ZmoSHC2*.<sup>14,15</sup>

Es war gezeigt worden, dass SHCs neben dem natürlichen Substrat Squalen auch einige andere lineare Terpenoide als Substrate akzeptieren und diese zyklisieren. Zum Beispiel konnten verkürzte Squalen-Analoga von *AacSHC* zyklisiert werden und auch der C<sub>16</sub>-Alkohol Homofarnesol wurde in den entsprechenden zyklischen Ether Ambroxan umgesetzt.<sup>16-19</sup> Diese Ergebnisse ließen darauf schließen, dass die SHCs eine vielversprechende

Enzymfamilie zur Katalyse von sehr verschiedenen, komplexen Zyklisierungsreaktionen darstellen könnten und deswegen entschieden wir uns dazu, die Substratbreite der SHCs näher zu untersuchen.

Um die Squalen-Hopen Zyklasten *ZmoSHC1* und *ZmoSHC2* zu charakterisieren und ihre biokatalytischen Aktivitäten mit der von *AacSHC* vergleichen zu können, wurden die für diese Enzyme codierenden Gene kloniert und heterolog in *Escherichia coli* exprimiert. Die Expression funktioneller Enzyme wurde durch Umsetzung des natürlichen Substrates Squalen bestätigt. Um die Enzyme direkt miteinander vergleichen zu können, wurde ein Protokoll für die partielle Aufreinigung der membrangebundenen SHCs ausgearbeitet und optimiert. Für diese Aufreinigung sowie für die Umsetzung der hydrophoben Substrate in wässrigem Milieu musste ein geeignetes Detergenz verwendet werden. *ZmoSHC1* wurde des Weiteren näher charakterisiert, wobei die pH- und Temperaturabhängigkeit der katalytischen Aktivität, die biokatalytische Stabilität des Enzyms über eine längere Zeitdauer sowie Inhibierungseffekte untersucht wurden. Die drei Enzyme wurden auf Aktivität gegenüber unnatürlichen Substraten mit C-Kettenlängen von C<sub>10</sub>-C<sub>18</sub> getestet. Ein besonderer Fokus wurde hierbei auf Substrate gelegt, die funktionelle Gruppen enthalten, wie zum Beispiel Hydroxyl-, Carboxy- oder Ketogruppen, die, wie für die Hydroxylgruppe von Homofarnesol gezeigt, an der Zyklisierungsreaktion teilnehmen könnten. Interessanterweise wurden diese funktionellen Gruppen in den finalen Ring der polyzyklischen Produkte integriert, wodurch Produkte mit neuen, attraktiven Eigenschaften entstanden.<sup>20-27</sup> Homofarnesol konnte in den zyklischen Ether und bekannten Duftstoff Ambroxan umgesetzt werden.<sup>16,20</sup> Die entsprechende Carbonsäure Homofarnesolsäure wurde ebenfalls als Substrat akzeptiert und es wurde das zyklische Lakton Sclareolid erhalten. Der tertiäre C<sub>15</sub> Alkohol Nerolidol wurde zum bizyklischen Caparrapioxid umgesetzt. Des Weiteren wurden auch zwei Ketone als Substrate akzeptiert und in zyklische Enolether umgesetzt.

Im Rahmen der vorliegenden Arbeit wurden die neuen Produkte nach präparativer Biotransformation und Aufreinigung charakterisiert. Nicht nur die Tatsache, dass diese Substrate sehr viel kürzere Kohlenstoff-Ketten als das „natürliche“ Substrat Squalen besitzen und über verschiedene funktionelle Gruppen verfügen, die an den Zyklisierungsreaktionen teilhaben und zu interessanten Produkten umgesetzt werden, sondern auch die unterschiedlichen Aktivitäten der SHCs gegenüber dieser Substrate sind bemerkenswert. Es konnte gezeigt werden, dass *ZmoSHC1* über besondere Eigenschaften verfügt, da

unerwartete Umsetzungsraten bei der Katalyse mit diesem Enzym bestimmt wurden. Während die Zyklisierung von Squalen von *ZmoSHC1* nur sehr gering katalysiert wurde, wurde eine gute Aktivität gegenüber der Reaktion von Homofarnesol zu Ambroxan ermittelt. Alle anderen beschriebenen Substrate wurden in geringen, aber signifikanten Raten umgesetzt. Ein vollkommen anderes Aktivitäts-Muster wurde bei Umsetzungen mit *AacSHC* erhalten. Hier wurde neben sehr guter Umsetzung von Squalen eine viel geringere Aktivität gegenüber allen anderen Substraten bestimmt. Vom Enzym *ZmoSHC2* wurden nur Squalen und Farnesylaceton mit sehr geringer Aktivität als Substrate akzeptiert, alle anderen Substrate wurden nicht umgesetzt.

Anhand dieser Ergebnisse kann gefolgert werden, dass SHCs als vielseitige Biokatalysatoren für komplexe Zyklisierungsreaktionen verwendet werden können, da diese Enzyme eine unerwartete Substrataktivität mit anderen Substraten als Squalen zeigen. In der vorliegenden Arbeit werden diese und weitere Ergebnisse im Detail beschrieben. Neben der erwähnten Untersuchung der Aktivität der verschiedenen SHCs gegenüber unterschiedlichen Substraten wurden auch Mutanten hergestellt und untersucht, die zu einer Erklärung der Aktivitätsunterschiede zwischen den verschiedenen Squalen-Hopen Zyklasen verhelfen sollten. Diese Charakterisierung der Triterpen Zyklasen und die Diskussion ihrer besonderen Eigenschaften führen zu neuen Schlussfolgerungen über das Potenzial von SHCs, als fähige Biokatalysatoren für noch nie gezeigte Reaktionen eingesetzt werden zu können.

## 2 Abstract

Cyclic terpenoids form a large group of natural products with various biological functions. About 60,000 different cyclic terpenoids have been identified by now, containing scaffolds of ten to more than 30 carbon atoms.<sup>1,2</sup> Among this huge amount of different cyclic compounds, there are many well-known flavors and fragrances, such as menthol or limonene, compounds which are widely used for pharmaceutical purposes like the antitumor compound Taxol and the anti-malaria agent artemisinin, or common membrane constituents and hormones such as the sterols.<sup>3-6</sup> All of these natural products are derived from cyclization reactions of few linear precursor molecules catalyzed by terpenoid cyclases.<sup>1,7</sup>

The main focus of the present work rests on one very interesting family of the terpenoid cyclases, the squalene-hopene cyclases (SHCs).<sup>8-10</sup> Among the over 300 annotated SHCs, most extensive studies had been carried out characterizing the SHC from the thermophilic bacterium *Alicyclobacillus acidocaldarius* (*AacSHC*), solving the crystal structure and the complex cyclization mechanism of the C<sub>30</sub> precursor squalene into the pentacyclic products hopene and hopanol.<sup>11-13</sup> This reaction constitutes one of the most complex reaction mechanisms found in nature, including the stereospecific formation of nine stereocenters and 13 covalent bonds.<sup>13</sup> Besides *AacSHC*, several SHCs were partially characterized in previous works.<sup>14,15</sup> Our interest was triggered by the ethanol and sugar tolerant strain *Zymomonas mobilis* which is known as one of the most potent hopanoid producers. *Zymomonas mobilis* contains two genes encoding for SHCs: *ZmoSHC1* and the formerly partially characterized *ZmoSHC2*.<sup>14,15</sup>

It could be shown that the SHCs are also capable of cyclizing other linear terpenoids. For example, it was found that truncated squalene analogs were accepted as substrates by *AacSHC* and also the alcohol homofarnesol could be converted into the corresponding cyclic ether ambroxan.<sup>16-19</sup> These results indicate that SHCs represent a promising family for catalysis of very different and complex cyclization reactions. Thus, we decided to investigate the SHCs' potentials regarding their substrate specificities.

In order to characterize the squalene-hopene cyclases *ZmoSHC1* and *ZmoSHC2* and compare them with *AacSHC* especially regarding their biocatalytic activities towards unnatural substrates, the SHCs were cloned and heterologously expressed in *Escherichia coli*.



Functional expression was confirmed by conversion of the natural substrate squalene. For the direct comparison, a protocol for partial purification of the membrane-anchored SHCs was elaborated and optimized. For this partial purification as well as for the conversion of the hydrophobic substrates in aqueous milieu a suitable detergent had to be selected. *ZmoSHC1* was characterized in more detail, retrieving information about pH- and temperature-dependence of the activity and the biocatalytic stability over a long period of time as well as inhibitory effects.

All of the three enzymes were tested with unnatural substrates of C<sub>10</sub>-C<sub>18</sub> carbon chain lengths. A special focus was laid on substrates containing functional groups such as hydroxyl-, carboxy- or keto-groups expected to participate in the cyclization reaction, as shown for the hydroxyl-group of homofarnesol. Several of the substrates were accepted and cyclic products were generated. Interestingly, the functional groups were integrated in the final ring closure and to products with new properties were obtained.<sup>20-27</sup> Homofarnesol conversion yielding the cyclic ether ambroxan, which is known as a expensive and rare flavor compound, was observed as reported in the literature.<sup>16,20</sup> Also the corresponding carboxylic acid, homofarnesoic acid, could be converted into the cyclic lactone sclareolide. The C<sub>15</sub> tertiary alcohol nerolidol was accepted as substrate and the bicyclic ether caparrapioxide was formed. Lastly, two ketones were accepted as substrates leading to cyclic enol ether products.

Within the present work, all of these new products were characterized after preparative biotransformation and product isolation. Not only the facts that these substrates are much shorter than the natural substrate squalene and possess different functional groups which take part in the cyclization reaction and that useful products containing new properties are formed, but also the different activities of the SHCs towards these substrates are remarkable. Thus, it could be shown that *ZmoSHC1* exhibits special biocatalytic properties, as the substrate activity pattern was unexpected. While squalene was converted very poorly, good activity was found towards the reaction of homofarnesol to ambroxan. All of the other substrates were converted in low but significant rates into the corresponding cyclic products. A completely different substrate activity pattern was observed using *AacSHC* as biocatalyst. Besides very good squalene conversion, much lower activities towards all of the other substrates were found. Using *ZmoSHC2*, only very low conversion rates were found for squalene and farnesylacetone and no conversion of any of the other substrates.

Based on these observations, it can be concluded that *ZmoSHC1* represents a versatile biocatalyst for complex cyclization reactions, as it shows unexpected substrate activity towards other substrates than squalene. In the present work, these and further detailed results are described. Besides the examination of the SHCs' activities towards different substrates there were also several mutants created in order to find explanations for the differences between the SHCs regarding their substrate activities. This characterization of the triterpenoid cyclase *ZmoSHC1* and discussion of their special properties leads to new conclusions about the potential of SHCs to serve as potent biocatalysts for new reactions.

### 3 Theoretical Background

The family of terpenoids represents one of the largest groups of natural products with various biological functions. For many years, scientists have been fascinated by these compounds. A lot of research focuses on them, trying to identify and understand their occurrence, formation, significance, functionalities and their possible benefits for us. Pioneering research on terpenoids started almost one century ago.<sup>28-31</sup> What is special about this class of compounds? Why do they draw the attention of chemists, biochemists, physicists and biologists?

In 1990, Guy Ourisson, a famous chemist in the field of natural products, in particular related to terpenoids, published an essay with the following introduction.<sup>32,33</sup>

“Terpenoids are a ravishment and a nightmare. A nightmare for the student trying to memorize hardly different structures and crazy trivial names, and a ravishment when he discovers that a few basic rules are enough to “understand” thousands of structures and to exclude from serious consideration many, that would otherwise apparently fit the available structural data. A ravishment also, when we see the white of betulin in the bark of birches, the orange, yellow, crimson or red of carotenoids in a basket of peppers or in a flight of flamingoes; a ravishment when used in the proper combination in a spice or a perfume, to lure a beetle (or ourselves) to a prospective mate, but a nightmare, when one is confronted with the nagging question: **“Why such a diversity? Would nature not have worked, had it been simpler?”**

In this short paragraph Guy Ourisson describes scientists’ fascination and respect towards the terpenoids with few words. This present thesis about this exciting field of natural products will maybe not answer but advance the discussion triggered by Ourisson’s questions and describe the current state of knowledge on terpenoids.

#### 3.1 Occurrence and biosynthesis of terpenoids

Terpenoids, also called isoprenoids, are present in all organisms. They are very abundant and offer a great structural diversity, acting as primary or secondary metabolites in bacteria,

plants and higher organisms. It is not easy to set a clear borderline between primary and secondary metabolites, as they cannot be differentiated clearly on the basis of precursor molecules, chemical structures or biosynthetic origin. Thus, the classification is made by the role they play in the organisms they are coming from. Primary metabolites are mostly small size molecules playing a role in essential metabolic processes within an organism, such as growth regulation, respiration or photosynthesis. The compounds called natural products are secondary metabolites, compounds which are influencing ecological interactions between an organism and its environment. To give an example, plant secondary metabolites can be compounds with functions against herbivores or pathogens, defending the plant or attracting pollinators and seed-dispersing animals.

Many of these natural products are utilized as flavors, pigments, polymers, fibers, glues, waxes, drugs or agrochemicals. Plant natural products can mainly be divided into three groups of compounds: terpenoids, alkaloids and phenylpropanoids. Just to give one famous representative from each group, Fig. 3.1 shows three compounds: the sesquiterpenoid artemisinin, which is one of the most potent anti-malarian drugs, the alkaloid caffeine and the flavoring phenylpropanoid vanillin.<sup>3,34-36</sup>

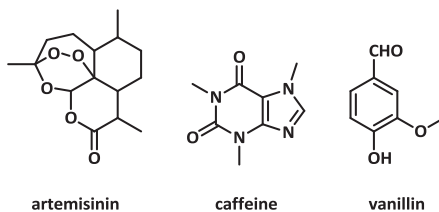


**Fig. 3.1: Common representatives of the three groups of important natural products: the terpenoid artemisinin, the alkaloid caffeine and the phenylpropanoid vanillin.**

Each of these three groups of natural products possesses a great amount of different derivatives. Besides the 30,000 alkaloids<sup>37</sup> and 8,000 phenylpropanoids<sup>34</sup>, the largest and most diverse group of natural compounds is formed by the terpenoids with about 60,000 identified compounds.<sup>32,37-40</sup> One of the most special facts of this large group of natural products is that they all originate from two very small and very simple precursors: The C<sub>5</sub> units isopentenyl diphosphate (IPP) and dimethylallyl diphosphate (DMAPP), as shown in Fig. 3.2.<sup>2</sup>



**Fig. 3.2: The terpenoid precursors: isopentenyl diphosphate (IPP) and dimethylallyl diphosphate (DMAPP).**

These two C<sub>5</sub> precursors can be formed *via* two different biosynthesis pathways, the mevalonate-dependent (MAD)<sup>41</sup> or the mevalonate-independent (MAI)<sup>34,42–45</sup> route. Investigations unveiled that in most organisms just one of both pathways is occurring for biosynthesis of the isoprenoid precursors. The MAI pathway is found especially in lower organisms like bacteria and is also common in plants. In contrast to this, archaea, fungi and animals are just operating *via* MAD.<sup>34,35,44</sup>

It is hardly believable that from these two molecules many thousands of different products can be created bearing very different properties and sizes. The first reactions on the biosynthetic routes to these important natural compounds are head-to-tail condensation reactions of IPP and DMAPP catalyzed by prenyltransferases (Fig. 3.3). These reactions yield geranyl diphosphate (GPP). Subsequent reactions elongate the chains step by step, leading to linear molecules of increasing chain lengths, ending up as monoterpenoids (C<sub>10</sub>), sesquiterpenoids (C<sub>15</sub>) and diterpenoids (C<sub>20</sub>). Longer chains are derived by head-to-head condensation reactions of two FPP or GPP units leading to tri- (C<sub>30</sub>), tetra- (C<sub>40</sub>) or polyterpenoids (C<sub>n</sub>).<sup>1,7,46–48</sup>

Pioneering work on the terpenoid chemistry started in the 19<sup>th</sup> century with first publications of O. Wallach in the 1880s, leading to the “isoprene rule” which was defined later by Ruzicka and coworkers.<sup>49–51</sup> Besides the “empirical isoprene rule” revealing that “the carbon skeleton of the terpenes is composed of isoprene units linked in regular or irregular arrangement”, the “biogenetic isoprene rule” was defined including that “the carbon skeleton of the biological end product is not necessarily identical to the carbon skeleton of the precursor”.<sup>51</sup> This means that in general all isoprenoids are derived from isoprene.

However, there are also natural products persisting of a chemical structure that cannot be traced back to isoprene directly, since they were modified during the formation of the final product.<sup>51</sup> Later, the isoprene rules, especially the biogenetic isoprene rules, were discussed in more detail. Explanations for the stereochemistry of the formed products were defined suggesting how cyclization could occur, especially regarding the triterpenes.<sup>29,52</sup> Over the

following years, a lot of work was done on mechanistical studies, especially for ring forming reactions as it became more and more obvious that the large diversity of the family of terpenoids is not only due to the formation of the growing linear carbon chains.<sup>28</sup> Besides the mentioned publications of Ruzicka *et al.*, more pioneering work in the field of the biosynthesis of terpenoids was performed by Elias J. Corey and coworkers.<sup>53–55</sup> In these works, which were started in the 1960s and resumed in the 1990s, special focus was laid on the complex cyclization of the C<sub>30</sub> 2,3-oxidosqualene.<sup>56–59</sup>

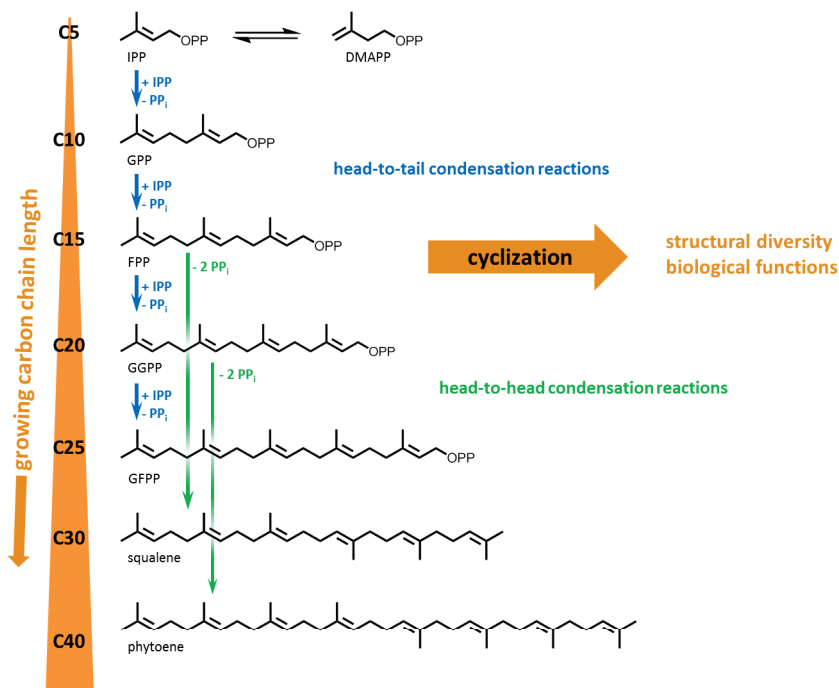


**Fig. 3.3:** Terpenoid chains are elongated by prenyltransferases creating geranyl diphosphate (GPP), farnesyl diphosphate (FPP), geranylgeranyl diphosphate (GGPP) and geranylgeranyl diphosphate (GFPP) by head-to-tail condensation reactions of isopentenyl diphosphate (IPP) and dimethylallyl diphosphate (DMAPP); the triterpene squalene is formed by head-to-head condensation of two FPP molecules and the tetraterpene phytoene from two GGPP units, respectively.

The linear terpenoids represent the precursors for manifold subsequent reactions leading to cyclic products with innumerable different properties and biological functions. In nature, the cyclization reactions are carried out by a large variety of enzymes accepting linear molecules

as precursors: the terpenoid cyclases. These enzymes are able to increase the number of products extensively and implement the biological functionalities and special properties of the terpenoids.

The cyclization of linear terpenoids can occur *via* two different mechanisms. Thus, the terpenoid cyclases are divided into two classes of enzymes regarding the mechanism of the catalyzed cyclization reaction (Fig. 3.4). For the first group of these enzymes, class I cyclases, the substrate has to be diphosphate-activated and a reactive carbocation is created by Lewis acid (e.g.  $Mg^{2+}$ ) triggered cleavage of the diphosphate group. The respective class I substrates are mainly the “smaller” substrates, such as mono-, sesqui- and diterpenes. Class II cyclases also generate a first, highly reactive carbocation. However, the substrate is not diphosphate-activated but the carbocation is formed by Brønsted acid-catalyzed protonation of a C=C double bond or an epoxide group of the substrate. The substrates which are cyclized *via* class II reaction mechanism are the longer terpenes, such as di-, ses- and triterpenes.<sup>1,2,46</sup>

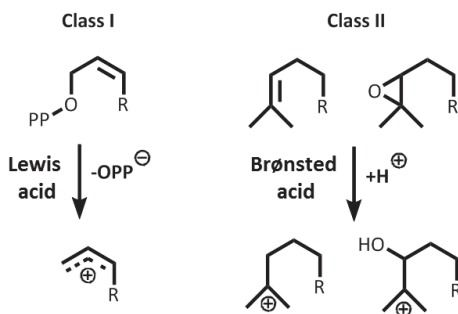


**Fig. 3.4: Differences between class I and class II cyclase-catalyzed initiation of the cyclization reaction.**

In order to distinguish between class I and class II-catalyzed cyclization, the type of the substrate and the first step of the reaction creating the first, highly reactive carbocation are the decisive factors to take into account, because the following steps are similar for both class I and class II cyclizations. During the cyclization procedure, the positive charge is passed through the molecule stabilized by  $\pi$ -electrons of aromatic residues in the active site of the cyclase. The stereochemically defined scaffold of the end product is formed and the final carbocation is either deprotonated forming a C=C-double bond or the positive charge is

quenched by nucleophilic attack of a water molecule or another nucleophile.<sup>60,61</sup> As one example, the class II cyclization of the C<sub>30</sub> precursor squalene to the pentacyclic products hopene and hopanol is shown in Fig. 3.5. The initiation of the cyclization reaction is performed by protonation of a terminal C=C double bond by an aspartate residue in the active site of the cyclase creating the initial, highly reactive carbocation. Subsequently, the product scaffold is formed and the terminal carbocation (C<sub>22</sub>-hopanyl cation; shown in square brackets), is deprotonated (blue arrows), or quenched by nucleophilic attack of a water molecule (red arrows) resulting in two different products.

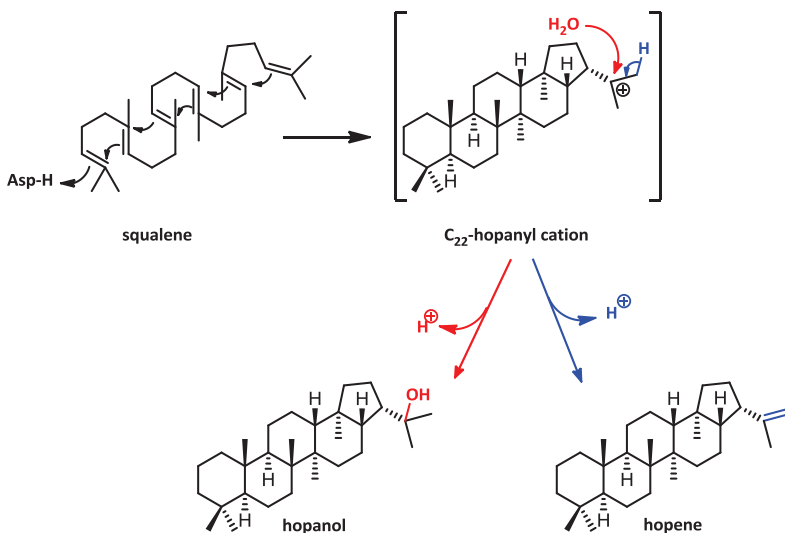


Fig. 3.5: Cyclization of squalene to the pentacyclic products hopene and hopanol.

In the following section, the focus of the introduction will be laid on the different cyclic terpenoids and the enzymes able to cyclize linear terpenoids. Their occurrences, properties and their catalyzed reactions will be discussed in detail. They will be explained step by step, sorted by increasing size of their natural substrates.

### 3.2 Monoterpenoids

As most of the monoterpenoids occurring in nature are cyclic, a lot of investigation was done in the field of these C<sub>10</sub> compounds. Although they can be traced to few skeletons, they possess a large diversity due to the occurrence of many derivatives resulting from creation



of positional isomers and stereochemical variants.<sup>62</sup> Originating from geranyl diphosphate (GPP), the monoterpenoids are formed by the monoterpene synthases. This family of enzymes is known to be able to catalyze the synthesis of acyclic monoterpenes, such as myrcene and ocimene, as well as cyclic monoterpenoids like limonene.<sup>4</sup> Most of the knowledge of the functionalism of the monoterpene synthases was derived by studying the (+)- and (-)-bornyl diphosphate synthases, (+)- and (-)-pinene synthases, limonene synthase, and (-)-*endo*-fenchol synthase.<sup>7,62</sup> All of the studied monoterpene synthases display the ability to generate multiple products at the same active site. One explanation for this finding is that the stabilization of the reactive carbocations in the active site can occur in more than one way and, thus, the enzymes are able to generate a variety of products.<sup>4</sup>

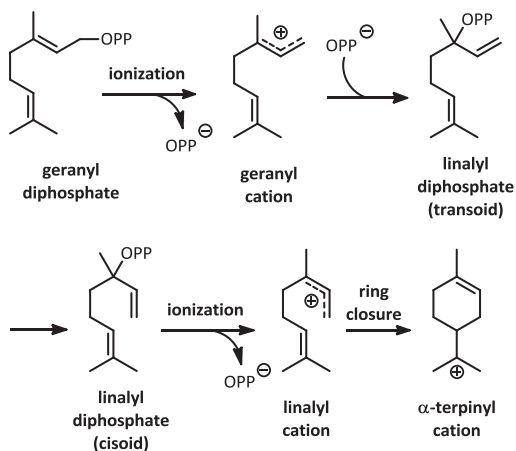


**Fig. 3.6: Cyclization of geranyl diphosphate leading to the  $\alpha$ -terpinyl cation as basic scaffold for cyclic monoterpenoids.<sup>1,4</sup>**

The monoterpene cyclization starts with stereoselective binding of GPP in the active site, followed by ionization by metal-dependent migration of the diphosphate leaving group and binding of the resulting linalyl diphosphate (Fig. 3.6, Fig. 3.7). Prior to cyclization, linalyl diphosphate is isomerized into its *cisoid* form and the cyclization is carried out after a second ionization of the linalyl diphosphate forming the  $\alpha$ -terpinyl cation as universal intermediate for formation of cyclic monoterpenes.<sup>1,4,7</sup>

The cyclization of GPP leading to limonene is exemplary for monoterpene cyclization. Although this reaction does not seem complex, the limonene synthase is one of the most-

studied monoterpene synthases and has become the “prototype” for these enzymes.<sup>63</sup> It is found in peppermint and spearmint and the native enzyme’s main product is limonene accompanied by formation of side products like myrcene, (-)- $\alpha$ -pinene and (-)- $\beta$ -pinene. Limonene represents the precursor of menthol and carvone.<sup>7</sup> Especially (-)-menthol is characteristic for the flavor of the essential oil of peppermint (*Mentha piperita*) as it constitutes about 40 % of the major compound of the essential oil.<sup>35</sup>

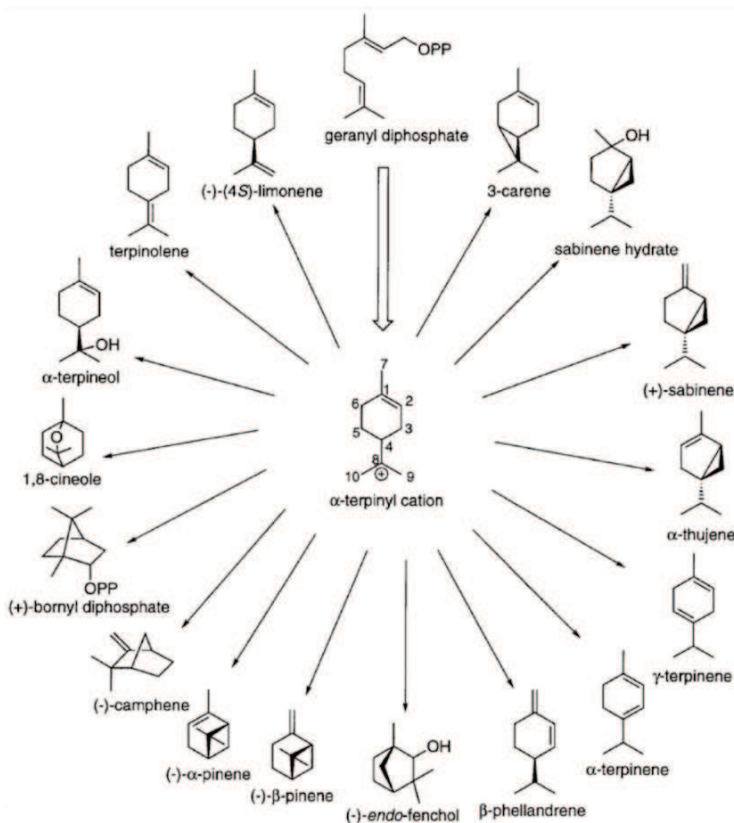


Fig. 3.7: Cyclic monoterpenoids derived from the  $\alpha$ -terpinyl cation.<sup>7</sup>

Although the physiological functions of monoterpenoids in nature remain mostly unknown, some functionalities were found, such as pollinator attraction, competitive phytotoxicity and defense against phytophagous insects and microbial pathogens.<sup>62</sup> Several studies suggest medicinal use of essential oils that contain many monoterpenoid constituents. One example

is caraway oil with the main constituents carvone and limonene which exhibit repellent properties.<sup>64</sup> Regarding our interest in these groups of natural products cyclic monoterpenoids are attractive as they are often volatile and common fragrances and flavors.<sup>7,46,62</sup>

Concerning the structure and amino acid sequences of the monoterpene synthases, it has been observed that there is one motif common for both prenyltransferases, monoterpene synthases and sesquiterpene synthases: the so called DDxxD motif represents the crucial position for the creation of the first reactive carbocation.<sup>7,65</sup> This highly conserved and aspartate-rich motif is the best-known structural motif and is found in almost all of the characterized terpene synthases. It was discovered that this region is participating in the binding of the metal ions responsible for catalysis of the diphosphate cleavage. Profound mutational and biochemical characterization of the (+)-bornyl diphosphate synthase and other monoterpene synthases bargained a lot of information about the mechanism, the functions and evolution of the residues in the active site, reviewed in detail by several groups.<sup>1</sup>

### 3.3 Sesquiterpenoids

Cyclic sesquiterpenoids are formed by metal-directed cyclization of farnesyl diphosphate (FPP) catalyzed by sesquiterpene cyclases.<sup>1</sup> The formation of linear FPP as a common precursor for all cyclic sesquiterpenoids proceeds *via* head-to-tail condensation of DMAPP with two IPP units catalyzed by farnesyl diphosphate synthases.<sup>66</sup> The sesquiterpene cyclases show a similar reaction mechanism as observed for the monoterpene synthases. However, the structural diversity of the generated products is greatly increased. Due to the fact that FPP contains three C=C double bonds, in comparison to the two C=C double bonds of the monoterpene precursor GPP, and that its carbon chain offers a higher flexibility, there are more possibilities for reactions.<sup>4,7</sup>

The initiation of the cyclization reaction occurs by cleavage of the diphosphate leaving group, and the reactive farnesyl cation is created. The following steps vary according to the product that will be formed. They include different ring closures forming up to ten- or eleven-membered rings, as shown for formation of (*E,E*)-gammacadienyl or (*E*)-humulyl cation (Fig. 3.8).<sup>67</sup> Also cyclic products containing carbon rings of smaller sizes can be

formed, as demonstrated for the formation of the bisabolyl cation which contains a six-membered ring, or the cycloheptenyl cation, where a seven-membered ring is formed by the sesquiterpenoid cyclases (Fig. 3.8).<sup>67</sup>

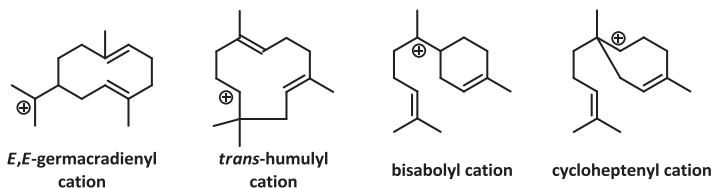


**Fig. 3.8: Intermediates in the cyclization of sesquiterpenoids.**

Most of the studied sesquiterpene cyclases generate multiple products while just some of them lead to one principal product. These observations are explained as follows: The highly reactive carbocations generated in the first steps of the cyclization reactions are very unstable and quenched at an early stage of the reaction cascade. Either several different or one single product can be formed depending on structural differences of the enzymes. In case of multiple product formation incomplete evolution of the active site is suggested as a reason. Another explanation could be the simplification for the evolution of new functions.<sup>1,4,7</sup>

Both microbial and plant sesquiterpene cyclases have been investigated deeply. Whereas the primary structures differ, many similarities are described regarding the tertiary structures and the electrophilic reaction cascade mechanisms. One of the best described sesquiterpene cyclases is the trichodiene synthase from *Fusarium sporotrichioides* with solved reaction mechanism as well as structure-function relationships which enables the comparison with the monoterpene synthases.<sup>4,7,68-70</sup> Besides this, also a large number of other sesquiterpene synthases has been characterized, expanding the knowledge of structural and mechanistic characteristics of this class of enzymes.<sup>4,7,71</sup>

Many cyclic sesquiterpenes were shown to exhibit useful properties. Examples for industrially used monocyclic sesquiterpenes are damascones and ionones which belong to the family of rose ketones and are fragrances occurring in essential oils.<sup>4,72,73</sup> Other sesquiterpenoids have pharmaceutical use, such as abisic acid, which is used as growth regulator.<sup>74</sup> The monocyclic bisabolol, and the bicyclic compounds petasin and isopetasin are antiphlogistic and spasmolytic (Fig. 3.9).<sup>75</sup>

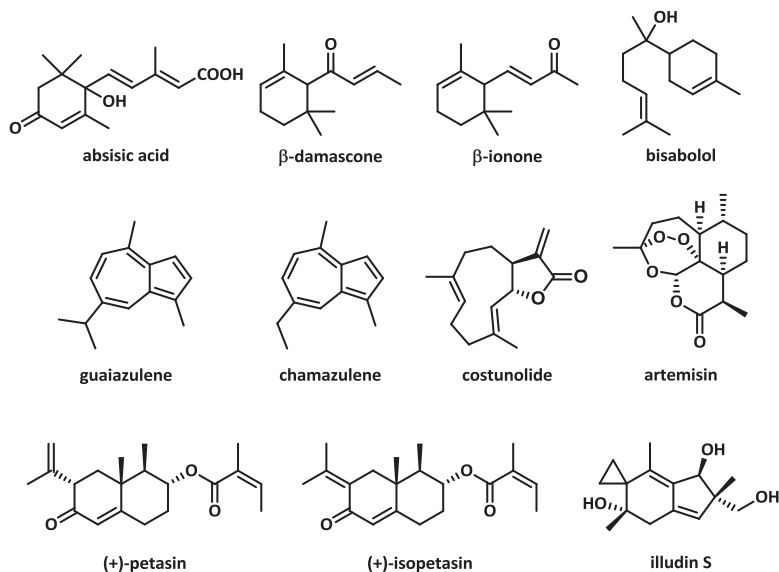


Fig. 3.9: Cyclic sesquiterpenoids which are used as flavor compounds or pharmaceuticals.

Guaiazulene and chamazulenes are inflammatory. In addition to this, guaiazulene represents a flavor compound of essential oils, as it is a component of chamomile oil and occurs as a pigment in corals.<sup>76–78</sup> The germacranolides, represented in Fig. 3.9 by costunolide, are a large group of sesquiterpenoid lactones which also show antitumor effects. Illusin S is a representative of tricyclic sesquiterpenoids. It occurs in different fungi and is highly toxic, but when used in therapeutical concentrations, it exhibits antibiotic and antitumor properties.<sup>36,79</sup> Artemisinin is a well-known anti-malarial sesquiterpenoid which was found in annual wormwood (*Artemisia annua*).<sup>3,80,81</sup> There are plenty of more examples for pharmaceutically useful sesquiterpenoids, such as the antibiotics and mycotoxines from the trichothecane family<sup>67</sup>, the immunosuppressive and antibiotic ovalicin from bergamote oil<sup>67,82</sup>, the pentalenolactones which offer antibiotic, antitumor and anti-inflammatory properties<sup>67,83</sup>, the eudesmane derivatives with their antifeedant, antibacterial, cytotoxic features<sup>84</sup> and many others.

### 3.4 Diterpenoids

Diterpenes are  $C_{20}$  compounds formed from geranylgeranyl diphosphate (GGPP). More than 1000 diterpenes are known fitting into 20 major and four less common bi-, tri-, tetra and pentacyclic skeletons. Many diterpenoids are derived from the only acyclic diterpene phytol by ring closures, oxidations and substitutions.<sup>74</sup> Similar to other classes of terpenoids there are hydrocarbons, alcohols, aldehydes, ketones and carboxylic acids all known in this group. The formation of most cyclic diterpenes is catalyzed by diterpene synthases but in contrast to the cyclization of mono- and sesquiterpenes, the cyclization of diterpenes can either occur *via* class I or class II mechanism.

On the one hand, the substrate GGPP can be ionized by the cleavage of the diphosphate group, similar to the initiation of the cyclization of mono- and sesquiterpenes catalyzed by mono- and sesquiterpene synthases.<sup>7,85</sup> On the other hand, some diterpene cyclases also show the ability to catalyze the cyclization of GGPP by a protonation-initiated mechanism, forming the initial reactive carbocation intermediate by protonation of the terminal C=C double bond of GGPP. In addition, there are also some types of diterpene cyclases which are able to catalyze cyclizations *via* both mechanisms.<sup>7,86</sup> The formation of different products is traced to subsequent reaction steps, such as hydride and methyl shifts, Wagner-Meerwein rearrangements and further cyclizations as discussed for mono- and sesquiterpene cyclizations, as well as internal de- and reprotonations.

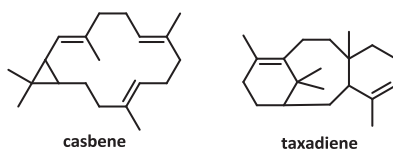
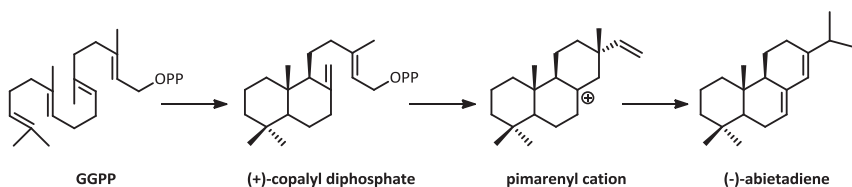


Fig. 3.10: Cyclic diterpenes.

Examples for ionization-dependent diterpene cyclases are the casbene and the taxadiene synthases. Accepting GGPP as substrate and starting the cyclization by Lewis-acid assisted cleavage of the diphosphate, the products formed are the antimicrobial and antifungal casbene and the antitumor compound taxadiene, respectively (Fig. 3.10).<sup>85,87,88</sup>

Other diterpene synthases that were characterized did not show the presence of the DDxxD motif, which is characteristic for class I enzymes. The first carbocation is not generated by

ionization but by means of protonation of a C=C double bond of the substrate. This observation was in line with the mechanism assumed for the cyclases of longer chain terpenes, such as the triterpene cyclases. In this case, another aspartate-rich motif is conserved, the DxDD motif. The cyclization reaction is initiated by Brønsted acid-catalyzed protonation of a terminal C=C double bond of the substrate, generating the highly reactive carbocation.<sup>89</sup> One example for a diterpene cyclase which is able to catalyze reactions *via* both mechanisms is the abietadiene synthase: firstly, the protonation-induced cyclization of GGPP leads to enzyme-bound (+)-copalyl diphosphate, then, the pimarenyl cation is created by departure of the diphosphate followed by cyclization. Finally, the scaffold of (-)-abietadiene is created by reprotonation, methyl migration and deprotonation (Fig. 3.11).<sup>90</sup>



**Fig. 3.11: Cyclization of GGPP to (-)-abietadiene catalyzed by abietadiene synthases.**

Besides the already mentioned bioactive compounds casbene and taxadiene there are many other diterpenoids known to exhibit a variety of physiological functions. Paclitaxel, also called Taxol, is a derivative of taxadiene and known to be antileucemic. It is described as one of the most promising medications for cancer.<sup>5</sup> Taxol is found in nature in the bark from the trees *Taxus brevifolia* (Pacific yew) and *Taxus baccata* (European yew).<sup>74</sup> The previously discussed (-)-abietadiene is just occurring in low amounts and its use has not yet been investigated so far.<sup>90</sup> Another group of interesting diterpenoids is represented by the steviosides. They have recently become a hot topic in Germany, as they can be used as sweeteners. The diterpenoid glycosides can be isolated from *Stevia rebaudiana* and exhibit a 300-fold sweeter taste than sugar (Fig. 3.12).<sup>74,91</sup>

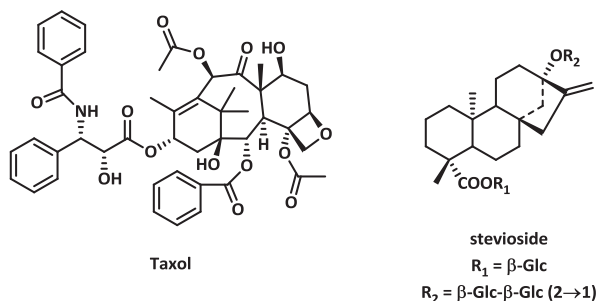


Fig. 3.12: Diterpenes with biological activity.

### 3.5 Sesterpenoids

The group of sesterpenoids, derived from the linear  $C_{25}$  precursor geranylgeranyl diphosphate (GGPP), is probably the least investigated. This could be due to their rare occurrence as secondary metabolites or to their lack of value for humans. However, some research was done on the ophiobolins in the 1960s. Ophiobolins are the only cyclic sesterpenoids where a cyclization mechanism has been suggested, but there are no enzymes discussed catalyzing the reaction. Studies suggest that the GGPP cyclization is initiated by cleavage of the diphosphate and the cyclization reaction proceeds subsequently as shown in Fig. 3.13.<sup>92-96</sup>

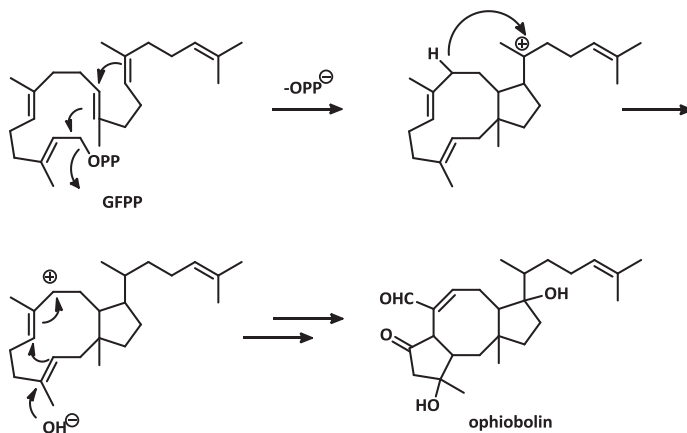
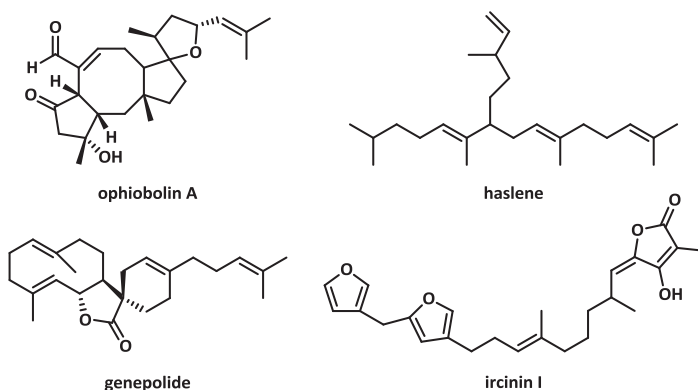


Fig. 3.13: Biosynthetic pathway forming the ophiobolin scaffold from GGPP.<sup>92-94</sup>



When this mechanism for orphiobolin biosynthesis was described, the gap between cyclic diterpenoids derived from GGPP and triterpenoids coming from squalene could be diminished. The structure of this group of compounds is indeed interesting, as the complex cyclization leading to the 5-8-5 ring product scaffold is unique (Fig. 3.13).<sup>92-95</sup>

Produced by pathogenic fungi, representatives of this group display phytotoxic properties.<sup>95,97,98</sup> In lower concentrations, they can be valuable in drugs. Ophiobolin A (Fig. 3.14), in particular, is known to possess antibacterial, antitumor and nematocidal functions showing inhibitory effects against *Staphylococcus aureus*, *Aspergillus flavus*, *Candida albicans*, *Torulopsis cremoris* and *Torulopsis petrophilum*.<sup>99,100</sup>



**Fig. 3.14: Sesterpenoids found in nature.**

Other common sesterpenoids are the genelopides, which are formally  $\gamma$ -lactones and were recently found in Mountain wormwood (*Artemisia umbelliformis*). Their biosynthesis is not clearly understood but it is suggested that these compounds are Diels-Alder adducts of costunolide and myrcene and that their formation is catalyzed by Diels-Alderase. They could be used for production of wormwood liqueurs (Fig. 3.14).<sup>101</sup> Ircinin-1 and Ircinin-2 and other furanoterpenes are forming a special class of sesterpenes. They were found in marine sponges and it was shown that these compounds are cytotoxic.<sup>102,103</sup> The linear sesterpene group of the haslenes has been shown to exhibit cytostatic properties.<sup>99,104</sup>

## 3.6 Triterpenoids

### 3.6.1 Functions and occurrences

The class of triterpenoids is probably the largest and most ancient of all of the groups of different terpenoids. As they are found in all kinds of membranes bearing different structures, they are widely distributed all over the world. Thousands of different triterpenes with about 80 different carbon skeletons have been identified by now.<sup>6</sup> Basically, the triterpenoids can be divided into several groups, among which the sterols, hopanes, oleananes, ursanes, lupanes, fernanes and arboranes should be mentioned (Fig. 3.15).<sup>6,105,106</sup>

The most frequent and best investigated triterpenoids are the tetracyclic sterols, represented in Fig. 3.15 by lanosterol, cycloartenol and cholesterol, and the pentacyclic hopanoids with a common hopane scaffold. The other pentacyclic triterpenoids are based on the oleanane, ursane, lupane, fernane and arborane skeletons, occurring in different kinds of organisms.<sup>6,107–110</sup>

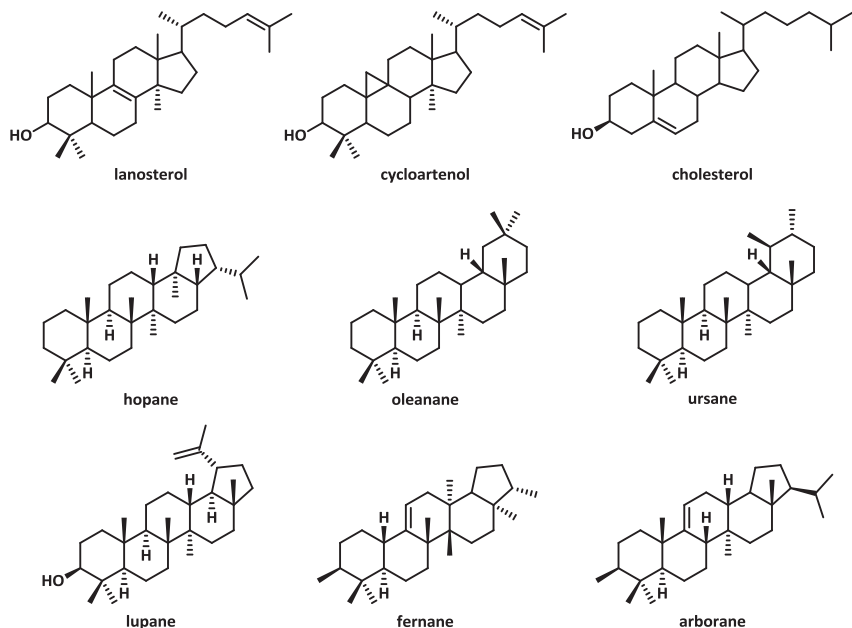


Fig. 3.15: Scaffolds of cyclic triterpenes occurring in nature: sterols (lanosterol, cycloartenol, cholesterol), hopanes, oleananes, ursanes, lupanes, fernanes and arboranes.

The importance of steroids in eukaryotic organisms is displayed by their roles as hormones, membrane constituents and precursors of other steroids.<sup>111,112</sup> Squalene is known as the key intermediate for their biosynthesis in plants and animals, leading to other metabolites with a variety of different functions and structures. They contain side chains characteristic for different types of organisms, such as plants or mammals.<sup>6,112</sup>

In this work, special focus is laid on the group of hopanoids. For many years, scientists investigated their function dependent occurrence in different organisms. They also tried to explain their contents in different organisms depending on the environmental conditions.<sup>113-115</sup> Their occurrence as “structural equivalents of sterols” was discussed several times, as these two classes of compounds provide several similar properties. They both play an important role as membrane constituents, regulating the fluidity of cell membranes.<sup>111,115,116</sup>

In the following chapter (3.6.2), the biosynthesis of the cyclic triterpenoids will be described, explaining the backbone of the triterpene cyclases and the reaction mechanisms by which the cyclic triterpenoids are created. In chapter 3.6.3, a special class of bacterial triterpene cyclases, the squalene-hopene cyclases, will be introduced in detail, as they represent the centerpiece of this work.

### **3.6.2 Biosynthesis of triterpenoids, reaction mechanisms and approaches for the evolution of the triterpene cyclases**

The basis for formation of triterpenoids is the common C<sub>30</sub> precursor squalene which is generated by a prenyltransferase-catalyzed head-to-head condensation reaction of two FPP units (Fig. 3.3). Squalene is ubiquitous in nature and in its linear form it is especially found in olives, shark liver oil, and rice bran.<sup>99</sup> The cyclic triterpenoids are derived by cyclization of squalene or 2,3-oxidosqualene which is formed from squalene by squalene epoxidases (Fig. 3.16). From these two precursors all of the polycyclic triterpenoids, such as hopanoids and steroids, are derived.<sup>6</sup>

The anaerobic formation of hopanoids is catalyzed by squalene-hopene cyclases (SHCs). In contrast to this, the cyclization of 2,3-oxidosqualene is catalyzed by oxidosqualene cyclases (OSCs) leading to steroids. SHCs and OSCs are closely related but it was shown that they differ in their folding due to minimal structural differences.<sup>6</sup> The fact that the formation of 2,3-oxidosqualene requires molecular oxygen led to the conclusion that steroids could just

be formed when the atmosphere yet contained oxygen. From these considerations, the theory that the steroid biosynthetic pathway was evolved from the hopanoid biosynthesis via minor mutations of the cyclase, was established.<sup>6,115–121</sup> In addition to this, the occurrence of steroids in ancient sediments seemed to give valuable informations as biomarkers for the oxidation of the atmosphere and the first appearance of cyanobacteria starting to produce oxygen.<sup>122</sup>

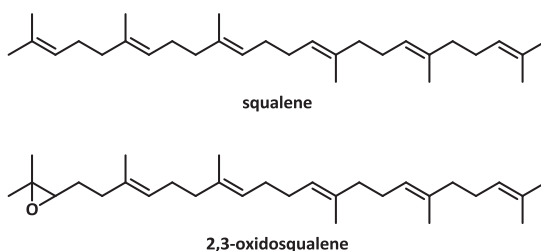


**Fig. 3.16: The precursors for polycyclic triterpenoids: squalene and oxidosqualene.**

In principle, the distribution of SHCs and OSCs was suspected to be relatively clear: The hopanoids were found in prokaryotic organisms, especially in bacteria, while the steroids were found in eukaryotic organisms. One approach was discussed leading to the conclusion that hopanoids present in organic matter indicate prokaryotic existence, while steroids can be used as biomarkers for the appearance of higher organisms.<sup>6</sup> However, this general declaration was disproved when the first steroids were found in prokaryotes<sup>113,123,124</sup>, and especially when later also an OSC was found in the bacterial strain *Methylococcus capsulatus*.<sup>6,125–127</sup> It was also discovered that some plants, e.g. ferns, gymophytes, lichens, fungi, are able to synthesize both steroids and hopanoids.<sup>6,128</sup> A new theory was postulated arguing that earliest enzymes are expected to catalyze the simplest and energetically most favored reactions and that during evolution these enzymes developed to more potent catalysts, being able to overcome more and more energetic barriers generating specific products which are beneficial for the hosts. Thus, it was considered that SHCs and OSCs, evolved independently outgoing from a common ancestor.<sup>129,130</sup>

However, it seems to be obvious that both steroids and hopanoids are similar regarding their functions in the different organisms and, thus, that SHCs and OSCs have many properties in common. Besides the sequence identity of SHC and OSC families of usually over 31 %, also important positions in the active cavity of these cyclases are often very similar. For example,

the prokaryotic SHC from *Alicyclobacillus acidocaldarius* (*AacSHC*) and the human lanosterol synthase OSC (*HsaOSC*) possess 20 % identical residues, what means that these cyclases are homologous.<sup>6</sup> Studies on the crystal structure similarities revealed that both *AacSHC* and *HsaOSC* consist of two connected ( $\alpha/\alpha$ ) barrels enclosing large hydrophobic cavity (Fig. 3.14).<sup>131</sup> The entrance to the active cavity is suggested to be placed in one of the two barrels, whereas the center of the active site, where the cyclization reaction is initiated, is located in the second barrel.<sup>8</sup>

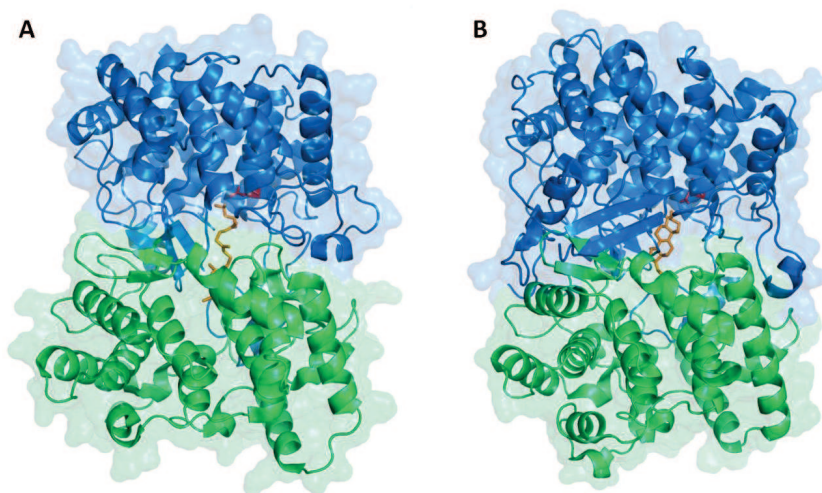


**Fig. 3.17:** Crystal structures of A) *AacSHC* and B) *HsaOSC*; the two ( $\alpha/\alpha$ ) barrel domains are colored in blue and green; the catalytic aspartate (part of the catalytic motifs xxDC / DxDD) in red and the substrate analog azasqualene / the product lanosterol are colored in orange.

It was shown that both enzymes possess conserved amino acid motifs and that many of them are representative structural domains in their crystal structures.<sup>11,130,132</sup> An explanation for this high conservation can be seen by considering the high similarity of the substrates they accept and the products they form. For these highly complex cyclization reactions a precise stereochemical conformation is required. The initial protonation of the substrate is performed by an aspartate residue (D376 for *AacSHC* and D455 for *HsaOSC*), which is part of a conserved motif. Also more  $\pi$ -electron rich positions responsible for stabilization of the carbocation intermediates and the protection against premature quenching of an intermediate, for example by water, are often homologous for both enzymes.<sup>11,132</sup> This was

figured out by numerous mutational studies performed by several groups solving the reaction mechanisms of the cyclization cascades and identifying the crucial positions responsible for the stabilization of the carbocations.<sup>13,123,133–136</sup> Several amino acid sequence repeats of the length of 16 amino acids each were found both in SHCs and OSCs. These QW motifs were shown to occur up to six times in the SHCs and four times in OSCs and are supposed to be responsible for the stability of these cyclases.<sup>10,135–137</sup>

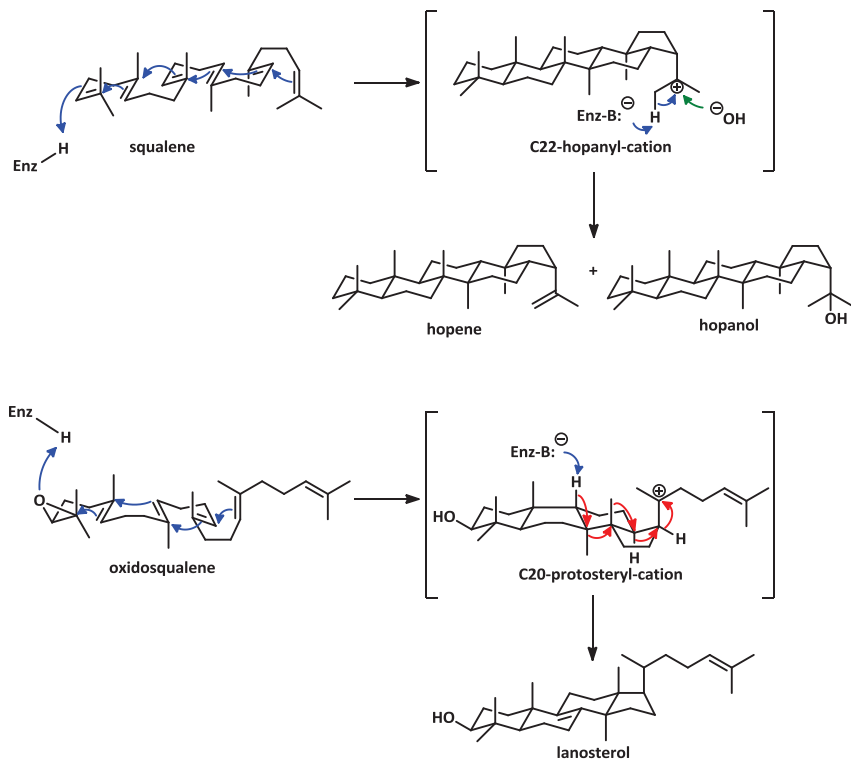


**Fig. 3.18:** Reaction mechanisms for the cyclization of squalene to hopene and hopanol and oxidosqualene to lanosterol; the nucleophilic attacks are marked as blue arrows; the methyl and hydride shifts in red and the nucleophilic attack of hydroxyl is marked in green, respectively.

However, there also have to be mentioned several differences between SHCs and OSCs. They both accept a similar substrate, just differing in the presence or absence of an epoxide ring at the 2,3-position. However, it was shown that in the case of squalene cyclization in

*Aac*SHC, the substrate is placed in the active cavity in chair-chair-chair conformation, whereas 2,3-oxidosqualene is positioned in the active site of *Hsa*OSC in chair-boat-chair conformation (Fig. 3.18).<sup>9,58,130,132</sup> For the initial protonation of the substrates it was observed that the relevant motif, the DxDD motif for SHCs and the xxDC motif for OSCs differ in strength. While the SHCs' DxDD motif is strongly electrophilic and is also able to protonate the 2,3-oxidosqualene, the xxDC motif of the OSCs is weaker and no conversion of the SHCs' substrate squalene was observed with OSCs.<sup>130,138,139</sup> Regarding the cyclization steps following the initial protonation, there are several approaches discussed, suggesting the cyclization steps to occur in concerted manner or as multistep reactions *via* different intermediates.<sup>9,58</sup> While SHCs cyclize the substrate by electrophilic additions to the double bonds of the carbocation intermediates, cyclization of the substrate by OSCs is accompanied by hydride and methyl shifts subsequent to the cyclization step. OSC-catalyzed cyclization of oxidosqualene in plants yields lanosterol (Fig. 3.18).<sup>9</sup> The alkylations of the side-chains of the products are complex and play an essential role with respect to the biological functionalities.<sup>6</sup> Alkylation of the hopanoid ring system was reported for some bacteria but it remains unclear when the methylation occurs and usually requires the presence of a C=C-double bond or an aromatic ring.<sup>140</sup>

### 3.6.3 Squalene-hopene cyclases

Squalene-hopene cyclases (SHCs) are catalysts for the class II cyclization of the linear triterpenoid squalene to hopene and hopanol, which is one of the most complicated reactions known in biochemistry (Fig. 3.18). Most today's knowledge has been derived from characterization of a squalene-hopene cyclase of the thermophilic organism *Alicyclobacillus acidocaldarius* (formerly *Bacillus acidocaldarius*). But also other SHCs have been investigated and partially characterized, such as *Methylococcus capsulatus* SHC<sup>125,139</sup>, *Zymomonas mobilis* SHC2<sup>14,141,142</sup>, or *Bradyrhizobium japonicum* SHC<sup>14,143</sup>.

#### 3.6.3.1 *Alicyclobacillus acidocaldarius* SHC (*Aac*SHC)

The crystal structure of *Aac*SHC was solved in the 1990s, revealing new insights into the biocatalysis of squalene cyclization (Fig. 3.17 A).<sup>6,11,144</sup> The active site of the enzyme is placed in the large central cavity and is enclosed by loops with aromatic residues that are estimated to be responsible for the binding of squalene in the required conformation and for the stabilization of the substrate during the cyclization process. The central active site cavity

consists of a large non-polar surface accompanied by a small polar area.<sup>6,144,145</sup> Mutational analyses of the active site led to detailed information about the amino acid residues playing an important role for the complex cyclization mechanism. At the top position of the central cavity, the catalytic DxDD motif is located; in particular, Asp376 was shown to be crucial for initial protonation of the C=C-double bond.<sup>13,146</sup> After the protonation, the first ring and probably also the second ring is suggested to be cyclized in concerted manner, followed by rearrangements of five-membered rings and Markovnikov-like ring closure reactions forming the third and fourth ring. After formation of the fifth ring, the final carbocation is deprotonated or quenched with water (Fig. 3.18).<sup>146</sup>

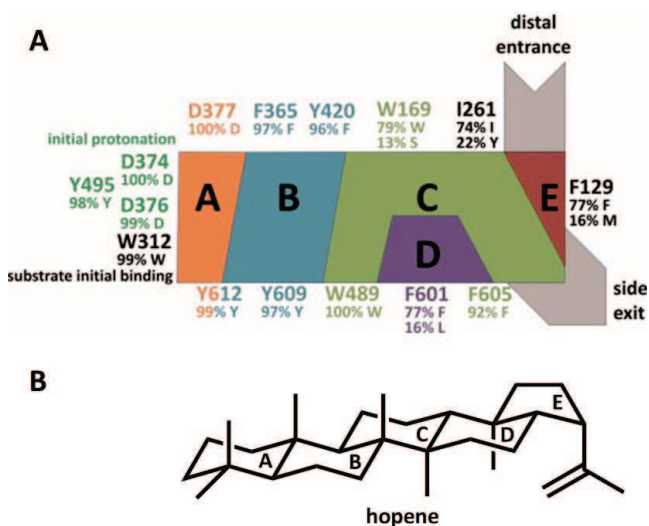
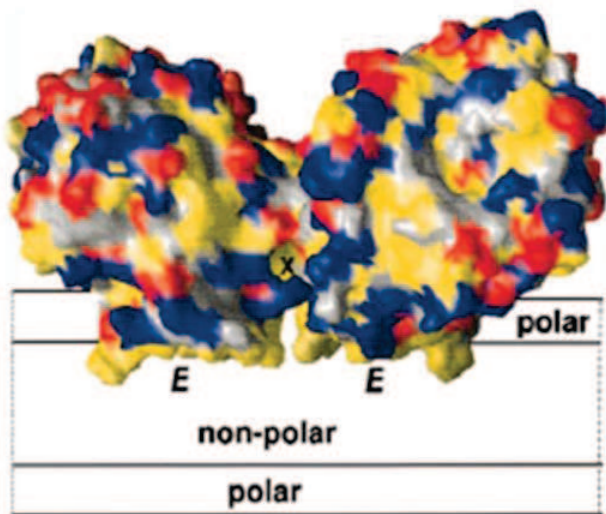


Fig. 3.19: A) Schematic model of the SHCs' active site displaying the amino acids which are crucial for the catalysis of squalene cyclization. The numbering of the amino acids refers to AacSHC and the values show the conservation of these residues in accordance to all 325 aligned SHCs. The letters indicate the product's ring formed in this part of the active site. B) The indication of the five rings is shown exemplarily for hopene.<sup>10</sup>

The amino acids which had been shown to be crucial for squalene cyclization with AacSHC were recently compared with the corresponding amino acids of other SHCs from the SHC database (TTCED<sup>10</sup>) containing 325 SHCs. These amino acid residues were shown to be highly conserved, as displayed in Fig. 3.19.



*Aac*SHC is a monotopic membrane-anchored enzyme and it is assumed that the entrance into the active cavity is reached from the inner, non-polar part of the bacterial membrane, as shown in Fig. 3.20. This makes sense, as squalene is an unpolare substrate and the products are known to be membrane constituents and could be directly placed in the membrane after cyclization.



**Fig. 3.20: Draft of the membrane-anchored dimer *Aac*SHC: the access to the active site is suggested to be from the non-polar membrane.<sup>58</sup>**

The fact that *Aac*SHC and presumably also other SHCs are membrane-associated enzymes complicates experimental work. After cell disruption soluble proteins from the cell lysate can be removed easily by centrifugation. However, membrane-anchored proteins remain in the cell debris and have to be solubilized using surfactants, such as Triton™ X-100, CHAPS, or Tween® 20 (Fig. 3.21), as suggested by numerous studies in this field.<sup>147,148</sup> Within this solubilization step, lipid components of the membrane are disrupted and the membrane proteins are achieved in an aqueous solution complexed with detergents.<sup>149</sup>

But although solubilization is possible by selecting a suitable surfactant, the protocol for biotransformations has to be worked out carefully. Different facts have to be considered, such as the critical micelle concentrations (cmc) of the selected detergent, effects of the

detergent on protein determination assays or on extraction after the biotransformations and disturbance of analytical systems such as GC.

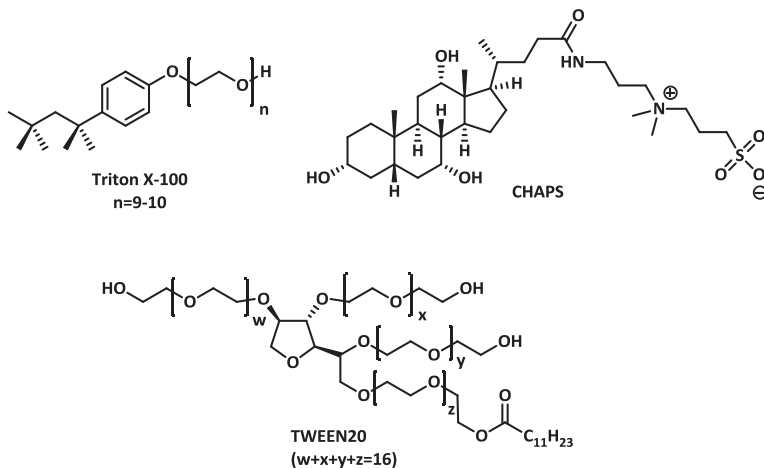


**Fig. 3.21: Detergents that can be used for solubilization of membrane associated proteins.**

Plenty of mutational and biochemical analyses was performed on the SHCs during the last decades, revealing information about the biochemical catalysis performed by these cyclases. Especially the ability of this enzyme to accept other substrates than squalene triggered our interest. The reported activity of *Aac*SHC towards unnatural substrates will be described in 3.6.4.

### 3.6.3.2 *Zymomonas mobilis* SHCs (*Zmo*SHC1 and *Zmo*SHC2)

While *Aac*SHC had been investigated profoundly in many previous studies, less focus had been laid on other SHCs, such as the SHCs from the ethanol-producing bacterial strain *Zymomonas mobilis*.<sup>15</sup> *Zymomonas mobilis* is a gram-negative bacterium which is remarkable because of its high amount of hopanoids with different side chains. It was assumed that this high hopanoid content is implicated in the high ethanol and sugar tolerance of *Zymomonas mobilis*.<sup>14,15,142,150-152</sup> In 1995, a SHC of *Zymomonas mobilis* (*Zmo*SHC2) was heterologously expressed and its activity towards squalene was shown.<sup>15</sup> The complete genome of *Zymomonas mobilis* was sequenced in 2005 and, besides *Zmo*SHC2, a second SHC could be described in this strain (*Zmo*SHC1). While the crystal structures of *Zmo*SHC1 and *Zmo*SHC2

remain unknown, multiple sequence alignments of these SHCs with *AacSHC* can reveal information (Fig. 3.22 and 11.1).

```

ZmoSHC1  MGLDRNSLSLLMKKIFGAKTSKPSADSTLIGDILKRRNRPEPTAKVDTKIFNMGNSLNLVLSACDWLIGQKPFQGHVWGVAESNASHEAWCL
ZmoSHC2  MIVST-----SSAFHSD-----LSSDVEFIQKATRALLEKQQQGHVVELEADATFPAYLL
AacSHC   M-----AEQLVEAP-----AYAFLLDRAVEYLLSCQDEGVYWGVLGNVTEAEYLL
          *           *           *           *           *           *           *           *           *           *
ZmoSHC1  ALWFLGL-EDHFLRPLGNALLEMQREDGWSGVYFAGNGDINATVEAYAAALSLGVSADNPVLKGAAWIAEKGLKNIKVFTRWIALIGEWPEKFP
ZmoSHC2  LKHYLGEPEDELEAKIQRVLERIQEGHGGWSLYFG-GDLDLSATVKAYFALRMIQDSDPAHMLRARNELIARGGAMRANVTRIQALFGAMSWEHVP
AacSHC   LCHILDR-VDRDMEKIKRRYLLHQREDGTWALYFG-GPPDLDTTIEAYVALKYIQMSRDEEPMKALRFIQSQGGIESSRVFTRMWLALVGEYVPEKVP
          *   *           *   *   *   *   *   *   *   *   *   *   *   *   *   *   *   *   *   *   *   *   *
ZmoSHC1  NLPPEIWFDPNFVFSIYNFAWRATMVPVIAILSARRPSRPLRPQRLDELFPGEARFDEYLEKK---EGIDLWSQFFRTDRGLHVQSNLLKRRS
ZmoSHC2  QMPVELMLPEWFPVHINKMAYWARTVLVPLLQALKPVARNRRGLVDEL-----FVPDVIPTLQ-ESGDP IWRFFSALDKVLHKVEP--YWPKN
AacSHC   MVPEIIMFLGRKMPLNIYFEGSWARATVVALSIVMSRQPVFPLERARVPEL-----YETDVFERRRGAKGGGW--IPFDALRALHGVRK--LSVHP
          *   *   *   *   *   *   *   *   *   *   *   *   *   *   *   *   *   *   *   *   *   *   *
ZmoSHC1  LREAAIRHVLWHLIRHQADGGWQGTQPPWYGLMALHGEGYQLYHPVMAKALSALD---DPQWRHDESSSWIQATNSPVDTMLALMALKDA---KA
ZmoSHC2  MRAKAIHSCVHFVYERLANGEDLGAIYPAIANSVMYDALGYDENPERAIARRAVEKIMVLDCTEDQGRKRYVQCCLSPDWDTALVAHMLVGGDEA
AacSHC   FRAAERIRALDWLERQAGDGSWGTQPPWYALIALKILDMT-QHPAFIKWEGLE---LYGVELDYGWGF-QASIPVNDTGLAVLALRAAGLPAD
          *   *   *   *   *   *   *   *   *   *   *   *   *   *   *   *   *   *   *   *   *   *   *
ZmoSHC1  EDRFTPEMDKAADWLLARQV-KVKGDSIKLPDVEGGWAFEYANDRYPDDDTAVALLALSYYDKKEWQKKGVEDAITRGVNWLIAMQSECGWGAFD
ZmoSHC2  EKSAI----SALSWLKPQQLDVKGDWARRRDLRPGGWAFAQYRNDYYPDDDTAVVTMAMDRAKLSLHDD-FEESKARAMEWTIGMQSDNGWGAFD
AacSHC   HDRLIV---KAGEWLLDRQI-TVFGDVAWRPHLKPGGFAFQFDNVYYPDDDTAVVWALNLTLLPDRRRR---DAMTKGFRWVGMQSSNGWGAFD
          .. *   *   *   *   *   *   *   *   *   *   *   *   *   *   *   *   *   *   *   *   *   *   *
ZmoSHC1  KDNNRSLSKIPFCDGEGSIDPFSVDVTAHVLEAFGLGLSRDMFVIQKADIVYRSEQAEGAWFRGWNYYIGTGVLPALAAIGEDMTPYITKACD
ZmoSHC2  ANNSYTYLNNIPFDHGLLDLPTTVDSARCVSMMAQAGISITDPMKAADVLLKEQEDDGSWFRGWNYYIGTWSALCALNVAALPHDLAVQKAVA
AacSHC   VDNISDLPHNIPFDGEGVDDPFSDEVTAVHLECFGSGFYDDAWKVIKRAVELRKRQKFDGSGFRGWNYYIGTGVAVSALKAVGIDTREPVIQKALD
          : *   *   *   *   *   *   *   *   *   *   *   *   *   *   *   *   *   *   *   *   *   *   *
ZmoSHC1  WLVAHQEDDGGWGESCSSEYMEIDISIGKGP--TPSQTAWALMGLIAANRPDEYEAIAKGCYHLIRQEQDGSWKEEFTTGTGEPGYGVTGKLDDDPALS
ZmoSHC2  WLKTIQEDDGGWGENDCSYA-LDYSGYEPMDSATQAWALGLMVGAEANS-EAVTKGINWLAQDDEGLWKEDEYSGGDFPR
AacSHC   WVEQHQPDDGGEDCRSYEDPAYAKGA--STPSQTAWALMALIAGGRAES-EAARRGVQLVETQRPDGGWDEPYTGTGEPG-----
          *   *   *   *   *   *   *   *   *   *   *   *   *   *   *   *   *   *   *   *   *   *   *
ZmoSHC1  KRLLQGAELSRAPMIRYDFYRQFFPIALSRAERLIDLNN-----
ZmoSHC2  -----VEYLRVHGYSKYFPLWALARYENLKKANQPIVHYGM
AacSHC   -----DFYLCGYMYRHVFPFLALGRYKQAIERR-----
          *   *   *   *   *   *   *   *   *   *   *   *   *   *   *   *   *   *   *   *   *   *   *

```

Fig. 3.22: Multiple sequence alignment of *ZmoSHC1*, *ZmoSHC2* and *AacSHC*. The aspartate residues in the active site (DxDD motif) are highlighted in blue, the residues which are predicted to interact in with the squalene analog in the active site of *AacSHC* and the corresponding residues in *ZmoSHC1* and *ZmoSHC2* are marked in grey, the 26 amino acid insertion in *ZmoSHC1* is marked in yellow and the N-terminal residue of *ZmoSHC1* is highlighted in green.

The global sequence identities were determined as 33.6 % (*ZmoSHC1* with *ZmoSHC2*), 40.6 % (*ZmoSHC1* with *AacSHC*) and 37.2 % (*ZmoSHC2* with *AacSHC*), respectively (see also chapter 11.1).<sup>153</sup> As many of the amino acid residues in the active sites of these SHCs which have been reported to be in direct contact with the substrate in case of *AacSHC* are corresponding, one could expect similar behaviors of the SHCs regarding their enzymatic performances. But also several obvious differences already discovered in the multiple sequence alignment of the SHCs should be pointed out. First of all, *ZmoSHC1* shows a residue of about 45 amino acids length at the N-terminal end of the sequence. Another difference is the 26 amino acid long insertion at the C-terminal end of *ZmoSHC1*. As the crystal structure of *ZmoSHC1* is unknown, a homology model of *ZmoSHC1* was designed for a better

understanding of the insights of this enzyme. The homology model of *Zmo*SHC1 created by Benjamin Juhl and Alexander Steudle (ITB) is displayed in Fig. 3.23, highlighting the N-terminal residue in grey and the insertion at the C-terminal end in yellow.

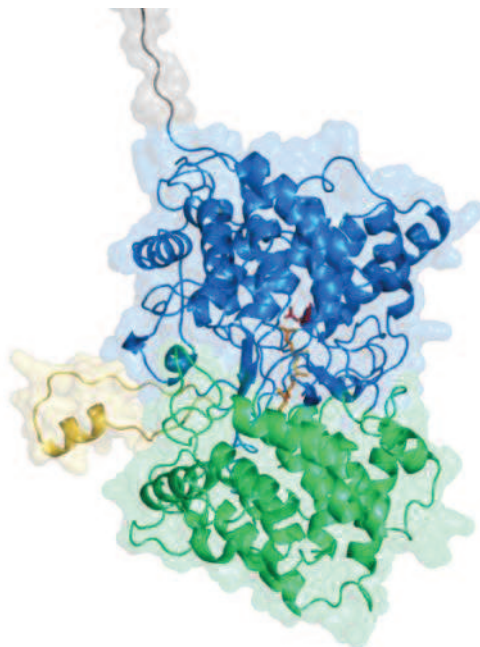


**Fig. 3.23: Homology model of *Zmo*SHC1. The domains are colored in blue and green, the loop region in yellow and the long residue at the N-terminal end in grey; the catalytic aspartate is colored in red and the substrate analog azasqualene in orange.**

### 3.6.3.3 Other SHCs

By now, 325 SHCs have been identified by annotation. The phylogenetic tree highlighting SHCs discussed in this work is shown in Fig. 3.24.

Some of these representatives were emphasized due to their occurrence in different branches of the tree and their origin from thermophilic bacterial strains which could be interesting for stability reasons. These SHCs are namely *Gth*SHC from *Geobacillus thermodentrificans*<sup>154</sup>, *Mca*SHC from *Methylococcus capsulatus*<sup>155</sup> and *Te*SHC from *Thermosynechococcus elongatus*<sup>156</sup>. Other SHCs were highlighted due to their global proximity to *Zmo*SHC1 and *Aac*SHC, such as *Aaci*SHC from *Alicyclobacillus acidoterrestris*<sup>136</sup>, *Ace*SHC from *Acidothermus cellolyticus*<sup>157</sup>, *Cac*SHC from *Catenulispora acidiphila*<sup>158</sup>, *Sco*SHC

from *Streptomyces coelicolor*<sup>159</sup>, *SscSHC* from *Streptomyces scabiei*<sup>160</sup>, *SsvSHC* from *Streptomyces sviveus*<sup>161</sup>, *SthSHC* from *Spherotheca thermophilus*<sup>162</sup>, *SviSHC* from *Saccharomonospora viridis*<sup>163</sup>, and *TtuSHC* from *Teredinibacter turnerae*<sup>164</sup>. An overview of these SHCs and the determined global sequence identities are shown in Table 3.1. For more detailed information see 11.2 and the supplementary data on CD-ROM.

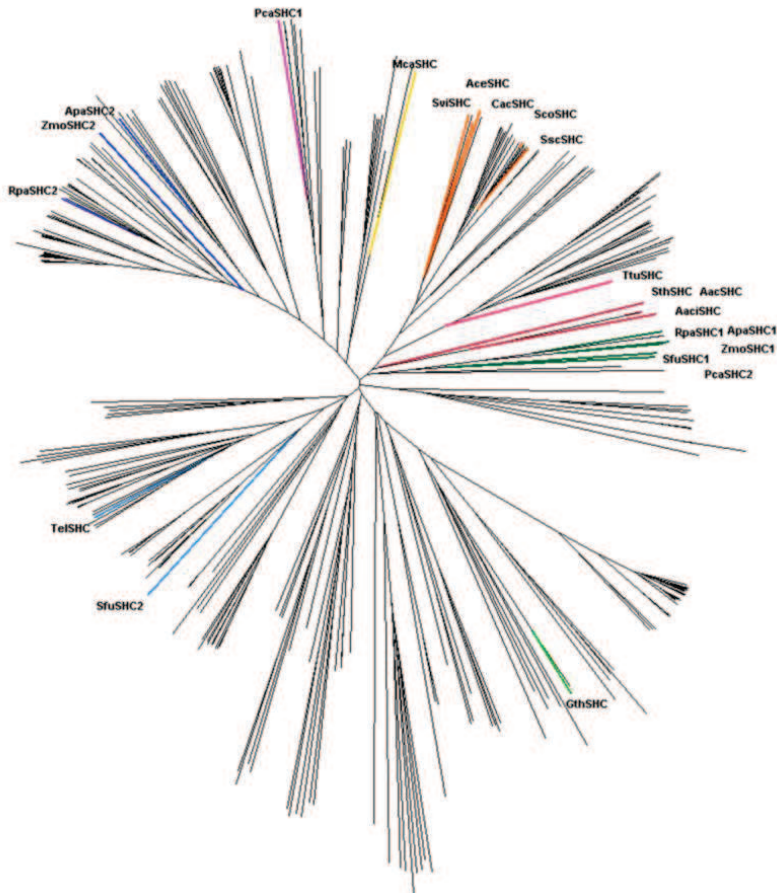


**Fig. 3.24:** Phylogenetic tree of the 325 identified SHCs. Several SHCs are highlighted.

Remarkably, there are several strains which contain two SHCs, as the already described *Zymomonas mobilis* which possesses *ZmoSHC1* and *ZmoSHC2* (Table 3.2). The differences between these two enzymes were already discussed; the amino acid sequence of *ZmoSHC1*

is longer, revealing 67 amino acids more than *ZmoSHC2* and shows a long residue at the N-terminal end of the protein and a 26 amino acid insertion at the C-terminus. *Acetobacter pasteurians*<sup>165</sup> is another bacterial strain with two SHCs (*ApaSHC1* and *ApaSHC2*, alignment see 11.3.1 b), showing similar characteristics like *Zymomonas mobilis*.

**Table 3.1: Overview of several SHCs highlighted in the phylogenetic tree (Fig. 3.24).**

Name	Strain	amino acids	molecular weight [kDa]	global sequence identity [%] with		
				<i>ZmoSHC1</i>	<i>ZmoSHC2</i>	<i>ApaSHC</i>
<i>AacSHC</i>	<i>Alicyclobacillus acidocaldarius</i> <sup>89</sup>	637	71.6	41	37	-
<i>AaciSHC</i>	<i>Alicyclobacillus acidoterrestris</i> <sup>136</sup>	634	70.8	39	35	63
<i>AceSHC</i>	<i>Acidothermus cellolyticus</i> <sup>157</sup>	633	70.2	39	40	51
<i>CacSHC</i>	<i>Catenulispora acidiphila</i> <sup>158</sup>	644	71.0	39	39	48
<i>GthSHC</i>	<i>Geobacillus thermodentrificans</i> <sup>154</sup>	617	69.5	29	32	32
<i>McaSHC</i>	<i>Methylococcus capsulatus</i> <sup>155</sup>	654	74.0	31	48	38
<i>ScoSHC</i>	<i>Streptomyces coelicolor</i> <sup>159</sup>	680	75.2	41	39	47
<i>SscSHC</i>	<i>Streptomyces scabiei</i> <sup>160</sup>	664	73.2	42	40	49
<i>SsvSHC</i>	<i>Streptomyces sviveus</i> <sup>161</sup>	669	74.2	41	39	49
<i>SthSHC</i>	<i>Spherobacter thermophilus</i> <sup>162</sup>	617	68.5	39	36	47
<i>SviSHC</i>	<i>Saccharomonospora viridis</i> <sup>163</sup>	640	71.6	41	40	49
<i>TelSHC</i>	<i>Thermosynechococcus elongatus</i> <sup>156</sup>	642	72.7	37	40	43
<i>TtuSHC</i>	<i>Teredinibacter turnerae</i> <sup>164</sup>	671	75.5	51	35	44

First of all the sequence of *ApaSHC1* is longer than *ApaSHC2*, containing 64 amino acids more. Secondly, *ApaSHC1* exhibits a long residue at the N-terminal end, which had already been observed for *ZmoSHC1*. And lastly, *ApaSHC1* contains a 26 amino acid insertion at the C-terminal end, similar to *ZmoSHC1*. Similar observations regarding this insertion were made for *RpaSHC1* and *RpaSHC2* from *Rhodopseudomonas palustris*<sup>166</sup> and *SfuSHC1* and *SfuSHC2*

from *Syntrophobacter fumaroxidans*<sup>167</sup>. These SHCs do not possess a residue at the N-terminal end. The last strain with two SHCs which is described here, *Pelobacter carbinolicus*<sup>168</sup>, shows slight differences. In this case, the shorter of the SHCs, *Pca*SHC2, contains a loop region at the C-terminus. In contrast to this, *Pca*SHC1 contains two small insertions in the center of the sequence, as shown in 11.3.1 e). Regarding their global sequence identities with *Zymomonas mobilis* SHCs, *Pca*SHC2 shows a higher identity with *Zmo*SHC1 (48 %) whereas *Pca*SHC1 is more similar to *Zmo*SHC2 with a global sequence identity of 41 %. For more detailed information see 11.2 and the supplementary data on CD-ROM.

**Table 3.2: Overview of SHCs from strains containing two SHCs.**

Name	Strain	amino acids	molecular weight [kDa]	Residue?	Loop?	global sequence identity [%] with		
						<i>Zmo</i> SHC1	<i>Zmo</i> SHC2	<i>Aac</i> SHC
<i>Zmo</i> SHC1	<i>Zymomonas mobilis</i> <sup>169,170</sup>	725	81.7	yes (45 aa)	yes (26 aa)	-	34	41
<i>Zmo</i> SHC2		658	74.1	no	no	34	-	37
<i>Apa</i> SHC1	<i>Acetobacter pasteurianus</i> <sup>165</sup>	720	80.1	yes (41 aa)	yes (26 aa)	78	33	40
<i>Apa</i> SHC2		656	72.9	no	no	33	54	39
<i>Rpa</i> SHC1	<i>Rhodopseudomonas palustris</i> <sup>166</sup>	685	77.3	no	yes (26 aa)	61	34	44
<i>Rpa</i> SHC2		654	72.6	no	no	33	57	39
<i>Sfu</i> SHC1	<i>Syntrophobacter fumaroxidans</i> <sup>167</sup>	710	79.2	no	yes (24 aa)	48	34	41
<i>Sfu</i> SHC2		688	78.1	no	no	37	35	42
<i>Pca</i> SHC1	<i>Pelobacter carbinolicus</i> <sup>168</sup>	737	82.2	no	no	35	41	36
<i>Pca</i> SHC2		695	77.5	yes (26 aa)	yes (24 aa)	48	35	42

For *Apa*SHC1 and *Rpa*SHC1 the high global sequence identities of 78 % and 61 % to *Zmo*SHC1 have to be emphasized. Analog to this, their second SHCs, *Apa*SHC2 and *Rpa*SHC2 show good similarity with *Zmo*SHC2. Regarding the placement of the mentioned SHCs in the phylogenetic tree (Fig. 3.24), it has to be noted that the loop-containing SHCs, namely *Apa*SHC1, *Rpa*SHC1, *Sfu*SHC1 and *Pca*SHC2) are all placed close to *Zmo*SHC1. This can be

observed analogously for the second SHCs *ApaSHC2* and *RpaSHC2* which are located in proximity to *ZmoSHC2*. However, *SfuSHC2* and *PcaSHC1* are positioned in completely different branches as *ZmoSHC2*. Additionally, their global sequence identities with *ZmoSHC2* are about 35 %, which is relatively low.

Regarding the sequences of the insertions observed for *ZmoSHC1*, *ApaSHC1*, *RpaSHC1*, *SfuSHC1* and *PcaSHC2*, their high similarity has to be mentioned. This is illustrated in Fig. 3.25 showing an alignment of the 24 to 26 amino acid long sequences.

```

ZmoSHC1      GYGVGQTIKLDDPALSKRLLQGAELS
ApaSHC1      GYGVGQTIKLDDPAISKRLMQGAELS
RpaSHC1      GYGVGQTIKLNDPLLSKRLMQGPELS
SfuSHC1      GYSVGERIRLRD--MGASLKQGTELQ
PcaSHC2      GYGVGERTNLKE--AGATLDQGCELA
              **.**: .* : . * ** **

```

Fig. 3.25: Alignment of the loops of *ZmoSHC1*, *ApaSHC1*, *RpaSHC1*, *SfuSHC1* and *PcaSHC2*.

### 3.6.4 Substrate specificity of SHCs

As already mentioned, it was shown that SHCs are not highly substrate specific and cyclize both squalene and 2,3-oxidosqualene.<sup>6</sup> In several works it could be shown that besides this also diverse linear terpenoids were converted into cyclic products by *AacSHC*. Hoshino *et al.* showed the cyclization of the C<sub>15</sub> alcohol farnesol and the C<sub>25</sub> alcohol geranylgeraniol as well as the cyclization of two C<sub>20</sub> and C<sub>25</sub> terpenes. The reactions of these truncated squalene analogs catalyzed by *AacSHC* led to bi-, tri- and tetracyclic products (Fig. 3.26, Fig. 3.27).<sup>17</sup>

Even 18 years before, in 1986, Neumann *et al.* already had shown the cyclization of the C<sub>16</sub> alcohol homofarnesol to the heterocyclic flavor compound ambroxan. In this pioneering work, the group also presented the cyclization reactions of a homofarnesyl-ether and the cyclization of the C<sub>11</sub> homogeneraniol (Fig. 3.27).<sup>16</sup> Also more bulky substrates, such as pyrrole- and indole-containing terpenes have been shown to be accepted as substrates and also the cyclization of 26- and 27-methylidenesqualene to novel unnatural C<sub>31</sub> polyprenoids as well as 2,3-dihydrosqualene and squalene 2,3-epoxide was observed with *AacSHC*.<sup>18,19,171</sup>



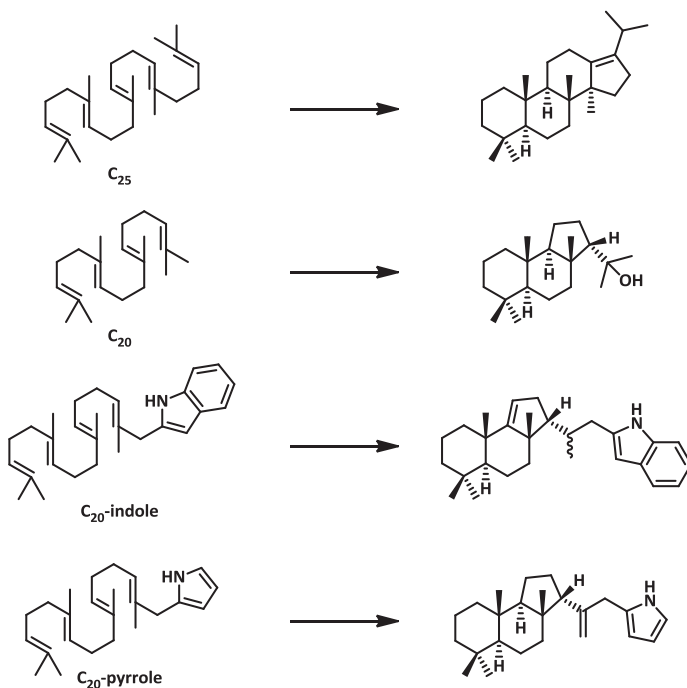


**Fig. 3.26:** Biotransformations catalyzed with *Aac*SHC: The linear sesterpene (C<sub>25</sub>; (6*E*,10*E*,14*E*)-2,6,10,15,19-pentamethylcosa-2,6,10,14,18-pentaene) and the diterpene (C<sub>20</sub>; (6*E*,10*E*)-2,6,10,15-tetramethylhexadeca-2,6,10,14-tetraene) were converted to the corresponding cyclic products.<sup>17</sup> The C<sub>20</sub>-indole containing substrate and the C<sub>20</sub>-pyrrole were also converted into cyclic products.<sup>18,19</sup>

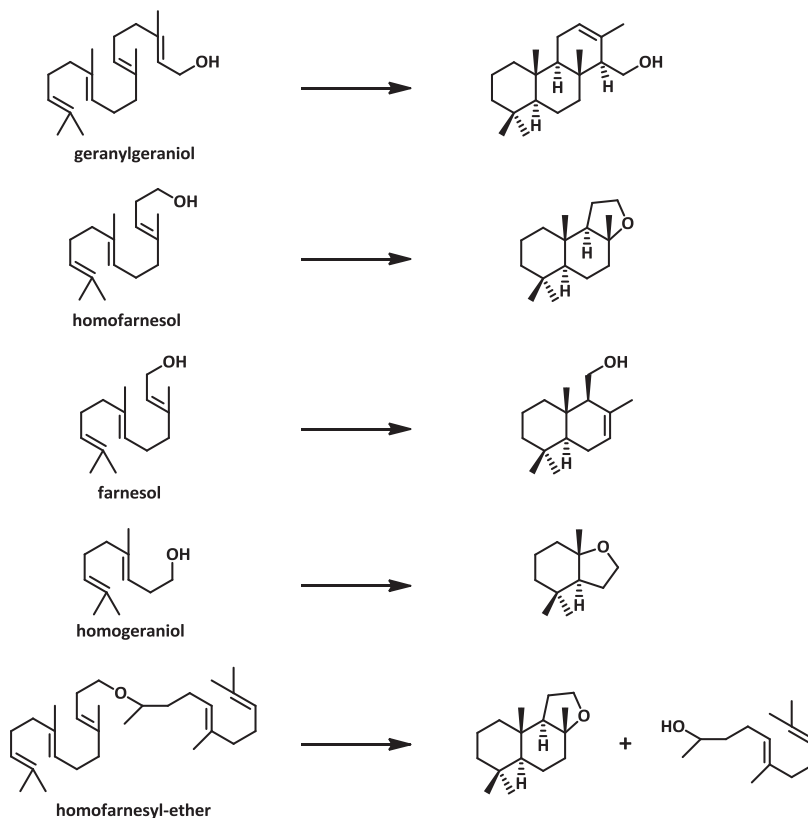


Fig. 3.27: Cyclization reactions of terpenoid alcohols shown with *Aac*SHC: geranylgeraniol (C<sub>20</sub>), homofarnesol (C<sub>16</sub>), farnesol (C<sub>15</sub>) and homogeraniol (C<sub>11</sub>) were converted into the cyclic products.<sup>16,17</sup> Homofarnesyl-(1,5,9)-trimethyl-4,8-dodecadienyl-ether was converted to ambroxan and the corresponding alcohol.<sup>16</sup>

### 3.7 Organic syntheses of cyclic terpenoids

Inspired by nature, many organic chemists started to investigate on cyclization reactions catalyzed by traditional catalysts.<sup>172</sup> Pioneering work on polyolefin cyclizations was performed by the groups of Stork and Eschenmoser in the 1950s.<sup>28,29</sup> The cyclization of polyenes such as farnesic acid catalyzed by mixtures of Brønsted acids like sulfuric acid, formic acid or acetic acid, was demonstrated. Mechanistical studies on the cyclization of squalene and analogs were especially performed by the group of E. J. Corey and first studies

for Lewis and Brønsted acid catalyzed non-enzymatic biomimetic polyene tetra- and pentacyclization of polyprenic acetals or chiral terminal epoxides of polyprenes were described.<sup>173–176</sup> From these publications in the 1960s until now, the mechanism of the squalene cyclization was elucidated leading to biomimetic approaches for the *in vitro* synthesis of steroids and further cyclic terpenoids of common interest.<sup>55,59,177</sup>

Outgoing from these first total syntheses, both yields and stereoselectivity were improved during the last decades. Later, the enantioselective formation of bi- and tricyclic terpenoids from linear precursors was described with Lewis acid-assisted chiral Brønsted acids as catalysts (chiral LBAs, Fig. 3.28). Using this artificial cyclase, the enantioselective synthesis of the flavor compound ambroxan or the bicyclic ether caparrapioxide was described.<sup>178,179</sup>

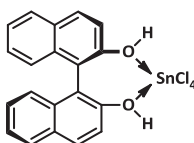


Fig. 3.28: Lewis acid-assisted chiral Brønsted acid (LBA).<sup>179</sup>

Recently, the enantioselective polycyclization of different achiral polyene precursors leading to tri-, tetra- and pentacyclic products was shown *via* a proton-initiated mechanism catalyzed by a chiral LBA containing  $\text{SbCl}_5$  as Lewis acid.<sup>180</sup> However, the enantiospecific formation of certain cyclic products remains challenging.

### 3.7.1 Ambroxan and sclareolide

In nature, ambroxan is found as metabolite of the sperm whale (*Physeter macrocephalus L.*), occurring in the concretions in its gut, in the ambra. The ambra is composed of several constituents, such as (+)-ambrein (Fig. 3.29).

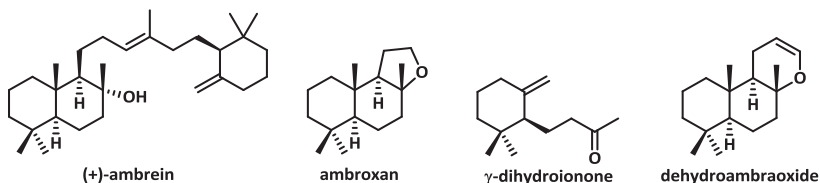
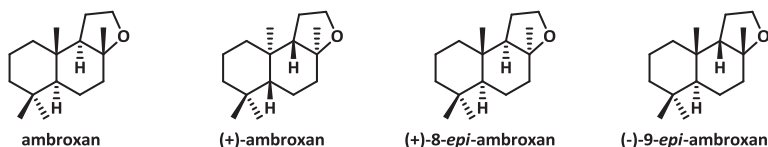


Fig. 3.29: The major constituents of the ambra.

Due to the exposure to sunlight and air, ambrein is decomposed to several odorous compounds, such as (-)-ambroxan, which will just be named ambroxan in the present work,  $\gamma$ -dihydroionone or dehydroambroxide (Fig. 3.29).<sup>20,181</sup>

With a price of about \$ 1,000 / kg ambroxan is the most valuable flavor compound among the amber odorants and has been used in the flavor and fragrance industry for a long time.<sup>20,182</sup> Until today, ambroxan is widely used in the perfume industry with a production of about 30 tons per year.<sup>20</sup>



**Fig. 3.30: Stereoisomers of ambroxan.**

The special organoleptic properties of ambroxan make this compound desirable. Its odor is described as musk-like, woody, warm or animalic. In contrast to this, the odor of (+)-ambroxan is described as exotic and spicy. Although the four isomers shown in Fig. 3.30 seem to be very similar, both their odors and especially the odor threshold are differing. The most powerful flavors are representing ambroxan and (-)-epi-ambroxan.<sup>183-186</sup>

The second product discussed in this chapter, sclareolide, or also called norambreinolide, is a tricyclic lactone occurring in nature as a component of *Arnica angustifolia*, *Sideritis nutans*, and *Kyllinga erecta*.<sup>21</sup> However, it occurs in much smaller amounts than the above mentioned sclareol. Sclareolide possesses several bioactive properties.<sup>187</sup> It is described to have phytotoxic, cytotoxic and antifungal properties. In addition to this, it can be used as an additive in foodstuffs enhancing the organoleptic properties and it is assumed to be an useful supplement for weight loss.<sup>21,22</sup>

Sclareolide is the most important intermediate in the chemical route from sclareol to ambroxan and other natural products, such as (-)-hyatellaquinone, a marine compound that was found to be an inhibitor of the reverse transcriptase of Human Immunodeficiency Virus (HIV) and, thus, can be pharmaceutically used (Fig. 3.31).<sup>188,189</sup> Another example for the use of sclareolide was described for the synthesis of  $\gamma$ -bicyclohomofarnesal, a strong odor compound.<sup>190</sup> (+)-Zerumbin B was also synthesized from sclareolide, representing a pharmaceutical compound valuable for several uses, such as its use against stomach ache,

chest pain or fever.<sup>21,191,192</sup> Another pharmaceutical product that was shown to be generated from sclareolide is ottensinin, used for lumbago or convulsions (Fig. 3.31).<sup>193</sup>

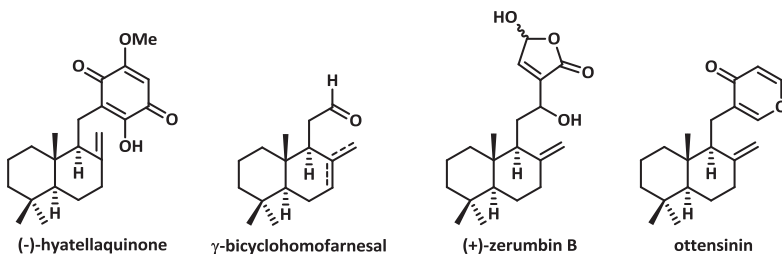


**Fig. 3.31: Compounds generated from sclareolide in organic synthesis.**

Ambroxan and sclareolide consist of 16 carbon atoms and do not obey the “empiric isoprene rule” and, thus, are not easily available from natural sources.<sup>49–51</sup> However, both substrates can be synthesized *via* different routes from farnesol, farnesylchloride or other substrates.<sup>179</sup>

Due to excessive whaling, natural ambroxan is disappearing from the world market, and an alternative access had to be found.<sup>186</sup> In order to do this, many organic chemists investigated the chemical synthesis of ambroxan from starting materials that are easy available. First approaches were established in the 1950s by Hinder and Stoll from the company Firmenich, producing to ambroxan from the natural compound sclareol which is derived from clary sage (*Salvia sclarea*).<sup>20,194,195</sup>

After conversion of sclareol to sclareoloxide using sodium permanganate under acidic conditions (Fig. 3.32, route a), an oxidized intermediate is formed by ozonolysis.<sup>20,194,195</sup> Saponification leads to sclareolide, one of the important key intermediates in the partial synthesis of ambroxan. Reduction with  $\text{LiAlH}_4$  finally yields ambroxan. Using this synthetic route, the thermodynamically favored (-)-9-*epi*-ambroxan is formed as a side product. An alternative route from sclareol to sclareolide uses chrome trioxide or  $\text{KMnO}_4$  as catalyst.<sup>196</sup> A similar route was patented in 1962 starting with oxidation of sclareol to the corresponding hydroxyketone using potassium permanganate under alkaline reaction conditions prior to conversion into sclareoloxide with glacial acetic acid (Fig. 3.32, route b).<sup>196</sup> Further oxidation was described with sodium permanganate or chromic acid yielding the oxidized intermediate which could afterwards be saponified to sclareolide. As side product, acetoxy acid is formed. One big drawback of this route is the toxicity of chromic acid and the difficulties in the

removal of the  $\text{MnO}_2$  which is formed. In addition to this, the oxidation of sclareoloxide is time consuming, resulting in a total process time of approximately 20 h.

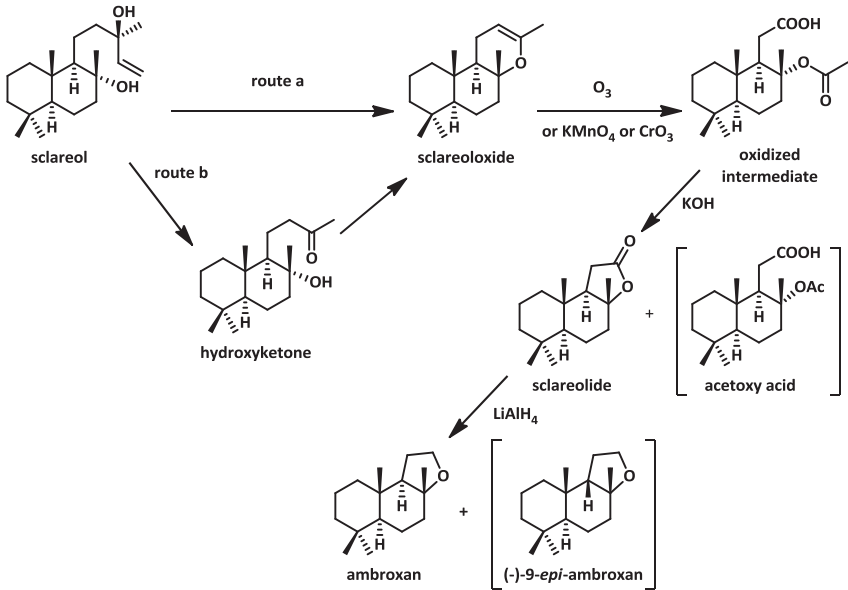


**Fig. 3.32: Semi-synthetic routes to ambroxan from sclareol:** After oxidation to sclareoloxide with  $\text{KMnO}_4$  under acidic conditions (route a) or with  $\text{KMnO}_4$  to the corresponding hydroxyketone and further oxidation with glacial acetic acid (route b), the intermediate sclareoloxide can be oxidized *via* ozonolysis<sup>20,194,195</sup>, with sodium permanganate or chromic acid<sup>196</sup>, leading to an oxidized intermediate. Saponification yields sclareolide which can be reduced to ambroxan. As side products, acetoxy acid and 9-*epi*-ambroxan can be formed.

An improvement of this process was developed and patented in the 1990s by the company Henkel where the process could be improved using sodium hypochlorite for the oxidation of sclareol to the corresponding hydroxyketone and / or sclareoloxide prior to oxidation to sclareolide using peracids or peracid salts.<sup>197,198</sup> This process was found to be much faster, leading to yields of 65 – 70 % after just about 3 h. Oxidation of sclareol to the hydroperoxide under acidic conditions prior to cyclization to ambroxan in presence of a redox catalyst ( $\text{Fe}^{2+} / \text{Cu}^{2+}$ ) is another method which was established and patented.

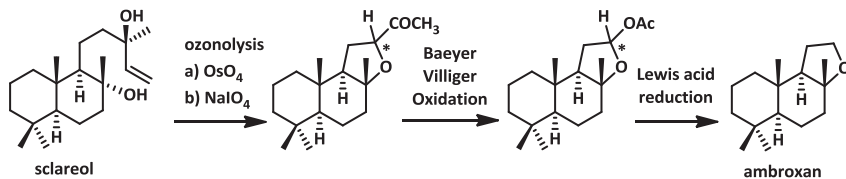


**Fig. 3.33:** Synthetical route from sclareol to ambroxan starts by ozonolysis using osmium tetroxide<sup>199</sup> or the sodium periodate.<sup>200</sup> Ambroxan is achieved after Baeyer-Villiger oxidation and Lewis acid-catalyzed reduction.

Another route was discovered and patented using osmium tetroxide or sodium periodate for ozonolysis of sclareol (Fig. 3.33).<sup>199,200</sup> The disadvantage of this process is the rather time consuming oxidation step, which needs several days, and the toxicity of osmium tetroxide.<sup>201</sup> A biochemical approach was discovered using the microorganisms *Hyphozyma roseoniger*, *Cryptococcus albidus*, *Cryptococcus laurentii* or *Bensingtonia ciliata* for the reaction described in Fig. 3.34.<sup>202,203</sup> The formed diol can be cyclized to ambroxan using toluene-*p*-sulfonylchloride in pyridine.<sup>204</sup>

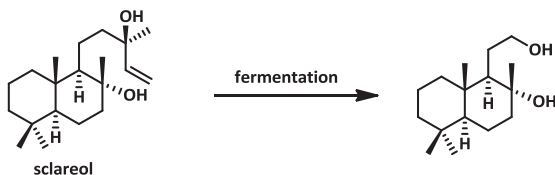


**Fig. 3.34:** Fermentation of sclareol leading to the corresponding diol shown with several microorganisms.<sup>202,203</sup>

As alternative precursors to the access of ambroxan from sclareol, several routes have been discovered from natural products. An overview is given in Fig. 3.35. For example, one access of ambroxan was found from linalool *via* nerolidol and homofarnesoic acid or homofarnesol followed by polyene cyclization.<sup>179</sup> The formation of ambroxan from communic acids was published in 1993 and recently reviewed.<sup>187</sup> Another access was found from (+)-*cis*-abienol or  $\beta$ -ionone.<sup>194,195,205–207</sup>

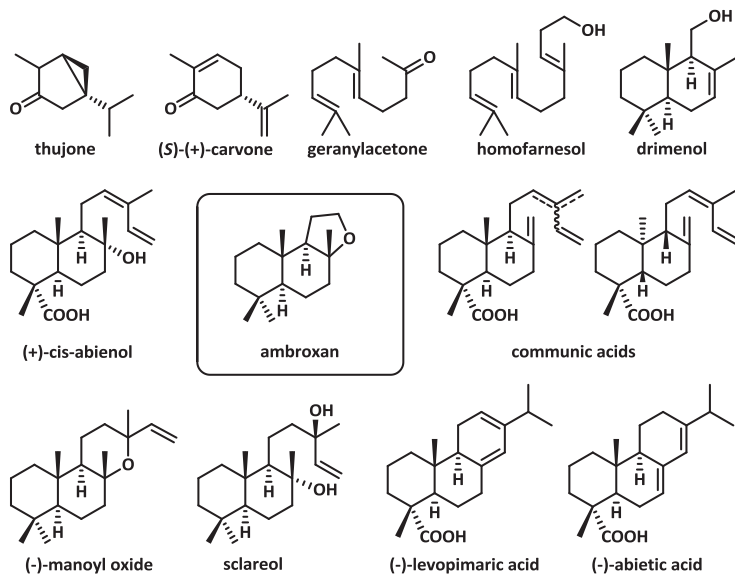


Fig. 3.35: Precursors for organic synthesis of ambroxan: (S)-(+)-carvone<sup>208</sup>, drimenol<sup>209</sup>, geranylacetone<sup>186</sup>, (-)-manoyl oxide<sup>204</sup>, thujone<sup>210</sup>, (-)-abietic acid<sup>211</sup>, (-)-levopimaric acid<sup>212</sup>, communic acids<sup>207</sup>, homofarnesol<sup>179</sup> and (+)-cis-abienol<sup>213</sup>.

### 3.7.2 Caparrapioxide

The caparrapioxides (Fig. 3.36) have been found to occur in nature in the defense secretion of the termite species *Amitermes evuncifer*<sup>214</sup>, in the sea hare *Aplysia dactylomela*<sup>215</sup> and in the extract of sun-cured Greek tobacco (*Nicotiana tabacum*)<sup>216</sup>. Due to their unusual structural features they are interesting compounds that offer special biological activities.<sup>217</sup> It was described that (-)-8-*epi*-caparrapioxide exhibits an ambergris, wooden flavor.<sup>24</sup>

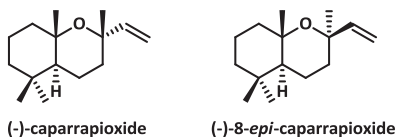
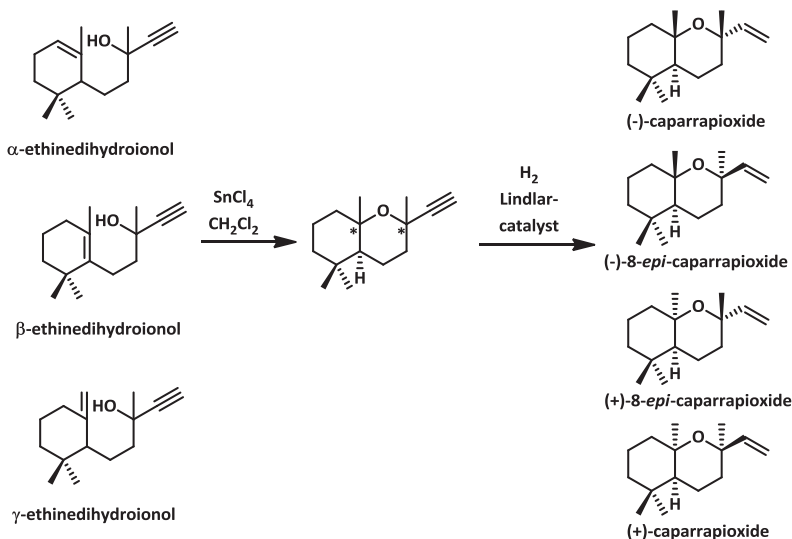


Fig. 3.36: Structures of the nerolidol cyclization products: (-)-caparrapioxide and (-)-8-*epi*-caparrapioxide.

However, the synthesis of these compounds was found to be challenging due to the complicated polycyclization reaction. In 1976, Lombardi *et al.* were the first in synthesizing



both caparrapioxides and presenting the first NMR data for each stereoisomer. The reaction started from ethinedihydroionol catalyzing the ring closure by  $\text{SnCl}_4$  prior to partial hydrogenation in presence of a Lindlar catalyst (Fig. 3.37).<sup>178,218</sup>



**Fig. 3.37:** Process for production of caparrapioxides from ethinedihydroionol.<sup>218</sup>

The separation of the caparrapioxide isomers was performed *via* bromation. As the equatorial vinyl group of (-)-caparrapioxide was found to be bromated much faster than the axial vinyl group of (-)-8-*epi*-caparrapioxide, the mixture was separated on silica gel column.<sup>219,220</sup> After the separation, the (-)-caparrapioxide could be recovered using zinc powder.<sup>220</sup>

In the following years, investigation on the chemical synthesis of the caparrapioxides proceeded further.<sup>217,219,220</sup> Enantiospecific synthesis was shown from farnesol or nerolidol using Lewis acid-assisted chiral Brønsted acid (LBA) catalysis.<sup>178</sup> While the synthesis starting from farnesol required several steps, nerolidol could be converted directly. The drawbacks of this route are the low yields of maximal 32 % and the long reaction times of one day. The preparation of the chiral LBAs is described to be easy but requires several steps from commercially available binaphthol (BINOL).<sup>221</sup>

### 3.7.3 Scclareoloxide and hexahydrochromene

The in nature manifold occurring<sup>222–226</sup> and commercially available ketones farnesylacetone and geranylacetone can be converted into the cyclic enol ether compounds sclareoloxide and a derivative of hexahydrochromene (named hexahydrochromene in the present work) which can both be of economic interest (Fig. 3.38).

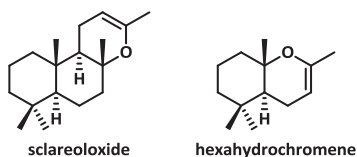


**Fig. 3.38: Cyclic enol ethers sclareoloxide and hexahydrochromene.**

Enol ethers in general are a versatile class of compounds used in organic chemistry, as they are able to participate in olefin metathesis reactions.<sup>227</sup> In addition to this, sclareoloxide embodies an attractive compound representing a valuable precursor or intermediate for the production of many flavor components as being an intermediate in the synthesis of drimane sesquiterpenoids and ambroxan (Fig. 3.32).<sup>182,228</sup> This tricyclic enol ether also provides access to puupehenones, which appeared to be an important group of marine metabolites of mixed biosynthesis (Fig. 3.39).<sup>229</sup>

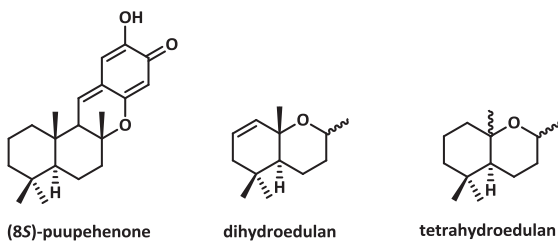


**Fig. 3.39: Examples for bioactive products that can be synthesized from sclareoloxide and hexahydrochromene: (8S)-puupehenone, dihydroedulan and tetrahydroedulan.**

These products are of interest, as they exhibit various biological activities as well as antimicrobial, antifungal<sup>230,231</sup> and cytotoxic<sup>232</sup> activities and they have been found to be inhibitors for the replication of the HIV virus<sup>25,26</sup>. The cyclization product of geranylacetone, hexahydrochromene, enables an access for production of edulans, which show rose-like aromas.<sup>27</sup> Dihydroedulans have been found to be valuable flavor compounds, occurring for

example in passion fruit (*Passiflora edulis*, Fig. 3.39).<sup>233</sup> It can also be a valuable precursor for production of octahydrobenzopyran (also called tetrahydroedulan) derivatives which are compounds that exhibit amber odor.<sup>24,234</sup>

The development of such a cyclization reaction is very interesting from the chemical point of view, as the created products are difficult to achieve in traditional chemical synthesis. The synthesis of sclareoloxide has been described by oxidation of sclareol, as already discussed in chapter 3.7.1 on the route to ambroxan (Fig. 3.32) or by degradation of manoyl oxide (Fig. 3.35).<sup>20,194–196,228</sup>

### 3.7.4 Ambraoxide, ambreinolide and unsaturated ambraoxide

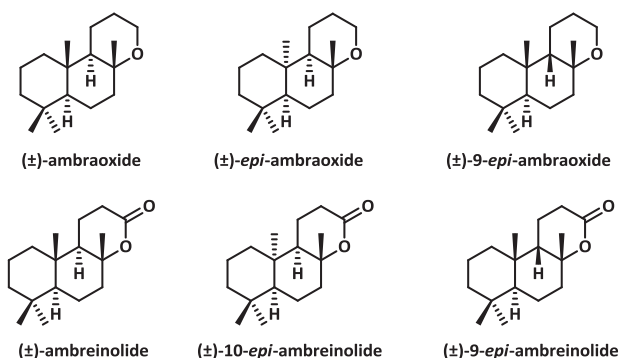


**Fig. 3.40:** Cyclic products of bishomofarnesol: (±)-ambraoxide, (±)-*epi*-ambraoxide and (±)-9-*epi*-ambraoxide; and cyclic products derived from bishomofarnesoic acid: (±)-ambreinolide, (±)-10-*epi*-ambreinolide and (±)-9-*epi*-ambreinolide.

Ambraoxide and ambreinolide are useful compounds in the tobacco and perfume industry.<sup>235,236</sup> Cyclization of the corresponding aldehyde, bishomofarnesal, leads analogously to an unsaturated ambraoxide, a compound which has also been reported to offer a strong ambergris odor and, thus, representing another valuable product.<sup>237</sup>

As already mentioned for their C<sub>16</sub> homologs, these C<sub>17</sub> compounds also do not follow the “empiric isoprene rule” and, thus, are not easily found from natural sources and have to be synthesized.<sup>49–51</sup> One possible educt is farnesol, for example.<sup>238–243</sup> Bromation to farnesylbromide followed by substitution with diethyl malonate and ester cleavage,

bishomofarnesoic acid is achieved after decarboxylation. Reduction leads to bishomofarnesol which can be oxidized further to bishomofarnesal (Fig. 3.41).

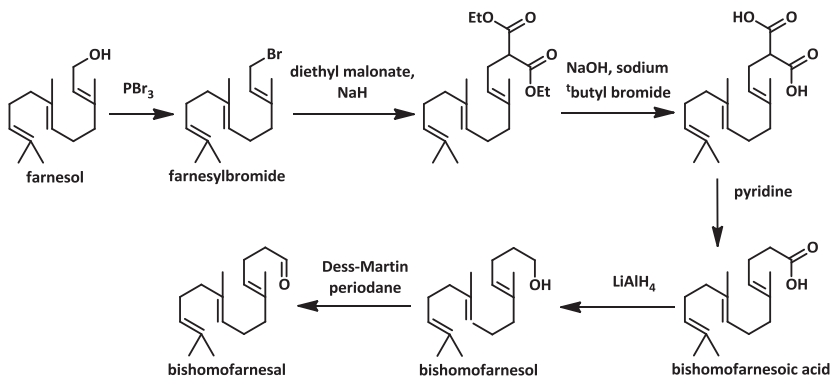


**Fig. 3.41: Synthesis of the  $\text{C}_{17}$  substrates bishomofarnesoic acid, bishomofarnesol and bishomofarnesal starting from farnesol.**

Several routes for the syntheses of the tricyclic products were described, such as synthesis of ambreinolide from manool.<sup>244,245</sup> Another access was presented by superacid-catalyzed cyclization of bishomofarnesoic acid or bicyclobishomofarnesoic acid (Fig. 3.42)<sup>246</sup> or from dihydro- $\beta$ -pseudoionone.<sup>235</sup> Ambraoxide can be derived by reduction of ambreinolide.<sup>235</sup> The natural product isoabienol can both be oxidized with potassium permanganate to ambreinolide and converted into unsaturated ambraoxide by ozonolysis.<sup>247,248</sup> Ambraoxides were also synthesized from the natural compound larixol.<sup>236</sup> An overview of the substrates used in the syntheses is given in Fig. 3.42.

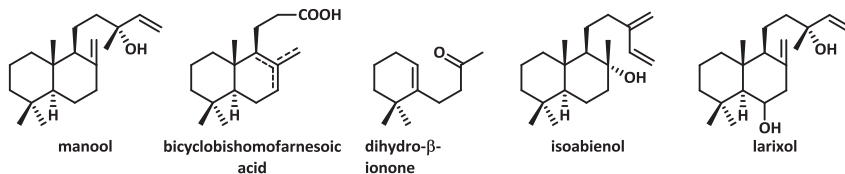


**Fig. 3.42: Educts for the syntheses of the tricyclic ambergris products.**<sup>247,248</sup>

### 3.7.5 Isopulegol and menthol

Cyclization of racemic citronellal leads to eight isopulegol isomers due to the presence of three stereocenters (Fig. 3.43).

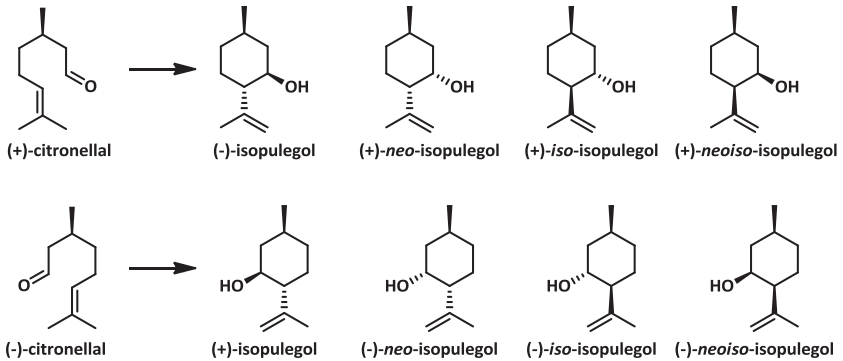


Fig. 3.43: Cyclization of citronellal showing the different isopulegol isomers.<sup>249</sup>

The cyclic isopulegol is present in several essential oils, for example in the leaves and peel of *Citrus medica* L.<sup>250,251</sup> The monocyclic monoterpene alcohol was shown to exhibit depressant and anxiolytic-like properties and is suggested to exhibit anti-tumor effects.<sup>251–253</sup> Isopulegol is an important intermediate in the synthesis of the flavor compound menthol. Among the different isomers of menthol, (-)-menthol is the most desired one, as it exhibits a unique flavor and is widely used in products like chewing gum or toothpastes and also for pharmaceutical applications because of its cooling effect.<sup>254,255</sup>

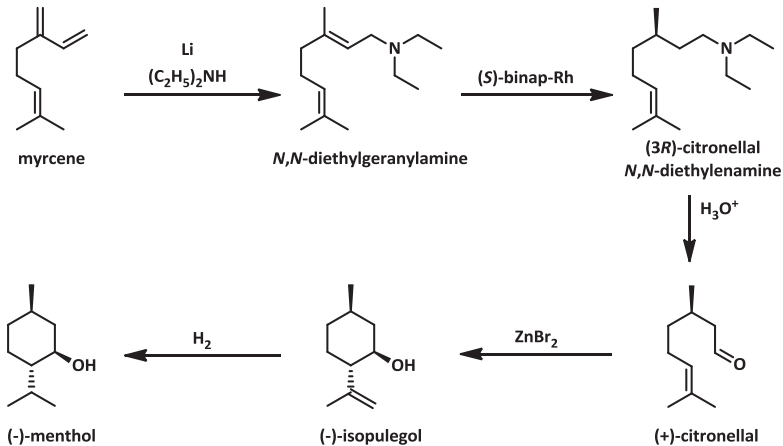


Fig. 3.44: Takasago process starting from myrcene.<sup>255</sup>

Citronellal can be cyclized to isopulegol using different chemical catalysts, such as zirconia<sup>256–258</sup> or other Lewis acids, for example  $\text{ZnBr}_2$ ,  $\text{AlCl}_3$ ,  $\text{BF}_3$ ,  $\text{SbCl}_3$ .<sup>259</sup> Green synthesis of

(-)-isopulegol from (+)-citronellal was reported using  $\text{SiO}_2/\text{ZnCl}_2$  as catalysts under solvent-free conditions.<sup>260</sup> (-)-Isopulegol is an intermediate in the industrial synthesis of (-)-menthol via the Takasago process.<sup>261</sup> This process starts with lithium-catalyzed addition of diethylamine to myrcene yielding diethylgeranylamine. Isomerization catalyzed by a chiral rhodium phosphine catalyst ((*S*)-binap-Rh) forms *N,N*-diethylenamine. This intermediate is hydrolyzed to (+)-citronellal and cyclized to (-)-isopulegol under presence of  $\text{ZnBr}_2$ . In the last step, hydrogenation leads to the final product (-)-menthol.<sup>255</sup> The crucial step of this synthetic route is the formation of 96-99 % enantiomeric pure *N,N*-diethylenamine leading to (+)-citronellal of a higher optical purity than it can be obtained from natural sources such as citronella oil (Fig. 3.44).<sup>255,262</sup>

Another method for the production of (-)-menthol was established from *m*-cresol and propylene in the Haarmann and Reimer-process (Fig. 3.45).<sup>254,255</sup> Hydration of thymol yields a mixture of menthol isomers. A racemic mixture of (-)-menthol and (+)-menthol is derived by fractional distillation. The menthyl benzoates are achieved by *trans*-esterification with methyl benzoate and can be separated by selective crystallization. The desired product (-)-menthol is derived after hydrolysis. Several recycles lead to a 90 % overall yield of (-)-menthol.<sup>254,255</sup>

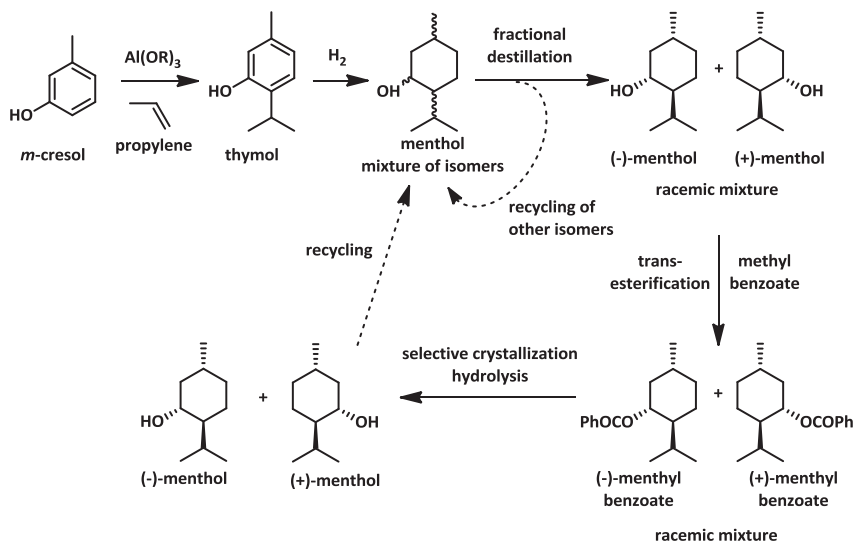


Fig. 3.45: Haarmann and Reimer-process for the production of menthol.

Another process for the industrial production of (-)-menthol from citral was established by BASF SE.<sup>263-266</sup> Rectification of citral concentrates Z-citral which is reduced to (+)-citronellal by use of a rhodium catalyst which is soluble in the reaction mixture, such as  $\text{Rh}(\text{OAc})_3$  for example. (+)-citronellal is cyclized to (-)-isopulegol in presence of  $\text{ZnBr}_2$ . Further reduction catalyzed by a heterogenous nickel- and copper-containing catalysts furnishes (-)-menthol (Fig. 3.46).

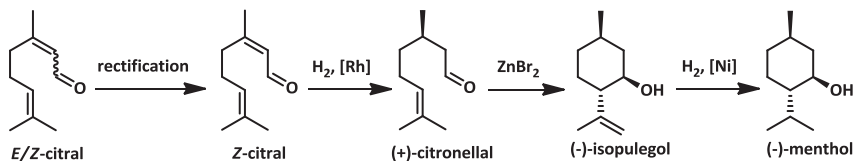


Fig. 3.46: BASF SE-process for industrial production of (-)-menthol from citral.

## 4 Aim of the project

In the scope of the present work, the SHCs *AacSHC*, *ZmoSHC1* and *ZmoSHC2* were selected as model squalene-hopene cyclases aiming to explore the substrate specificity of these enzymes. After cloning of the SHCs into the expression strain, a reproducible system for protein expression, enzyme purification and biotransformation was established. A special focus was laid on the partial purification of the membrane-anchored SHCs by use of detergents. The conditions for the biotransformations were selected carefully in order to generate a system enabling comparison both of the activity of different enzymes towards one substrate as well as the activity of the same enzymes for catalysis of different cyclization reactions.

Unnatural substrates on terpenoid basis were selected containing different carbon chain lengths and different functionalities regarding the positions relevant for initiation or termination of the cyclization reactions. Thirteen different substrates of carbon chain lengths of ten to 18 bearing different functional groups, such as alcohol-, carboxy-, keto- or aldehyde-groups, were tested. Cyclization of eight of these unnatural substrates could be confirmed and unknown products were characterized after preparative biotransformations.

The activities of the SHCs towards the unnatural substrates were explored and discussed, revealing a new understanding of the properties of this class of enzymes. The studies exhibited new insights into the substrate specificity and possible applications of the SHCs, since the cyclic products possess attractive properties, as they are flavors or fragrances, intermediates in the synthesis of other compounds or difficult to achieve in traditional organic syntheses. Among the three mentioned SHCs, special focus was laid on *ZmoSHC1* because of its individual substrate activity pattern and remarkable differences regarding its amino acid sequence in contrast to the other SHCs. As one of the most obvious differences is displayed by the 26 amino acid insertion at the C-terminal end of *ZmoSHC1* ("loop"), mutational analysis of this insertion was performed. The deletion mutant was generated, characterized and compared to the wildtype SHCs.



## 5 Results

### 5.1 Squalene-hopene cyclases: Cloning, expression, enzyme preparation and biotransformations

#### 5.1.1 Cloning, expression and partial purification

The SHCs were cloned in the expression vector pET-22b(+) as described in section 9.6 (Fig. 5.1). The genes were verified by sequencing (GATC-Biotech AG).

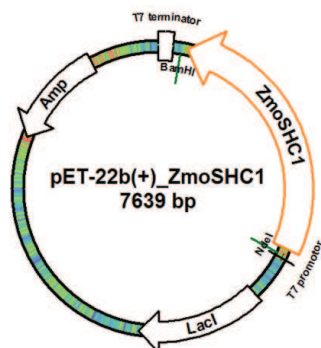


Fig. 5.1: Vector map for pET-22b(+)\_ZmoSHC1, showing the restriction sites *Bam*HI and *Nde*I.

The expression was optimized to the parameters described in detail in 9.7 (30°C, 4 h, 0.2 mM IPTG). The following expressions were carried out as described and controlled by SDS-PAGE (Fig. 5.2).

For partial purification of the SHCs, the cells were disrupted by ultrasonification and the cell membranes were subsequently incubated with a buffer containing 1 % Triton X-100 (1 g/100 mL) as detergent, solubilizing the membrane-anchored SHCs from the cell membranes. The procedure described in 9.8.1 yielded partially purified enzyme solution. The fractions were controlled on SDS-Gels (see Fig. 5.3 and for the protocol 9.8.2) and densitometric evaluation revealed cyclase contents of 90-95 % of the total protein which was determined as 3.5 to 6 mg/mL. As shown in Fig. 5.3 and Fig. 5.4, the purification was successful, although a high amount of enzyme remained in the pellet fraction.

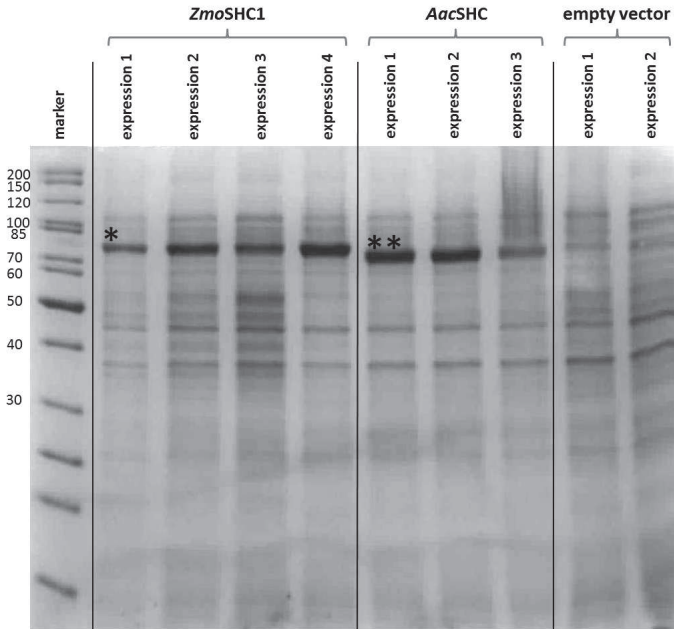


Fig. 5.2: SDS-gel showing cells expressing *ZmoSHC1* and *AacSHC*. The negative control for empty vector cells is shown on the two lanes on the right. The bands for 81 kDa *ZmoSHC1* are marked with \*, the bands for 74 kDa *AacSHC* are marked with \*\*.

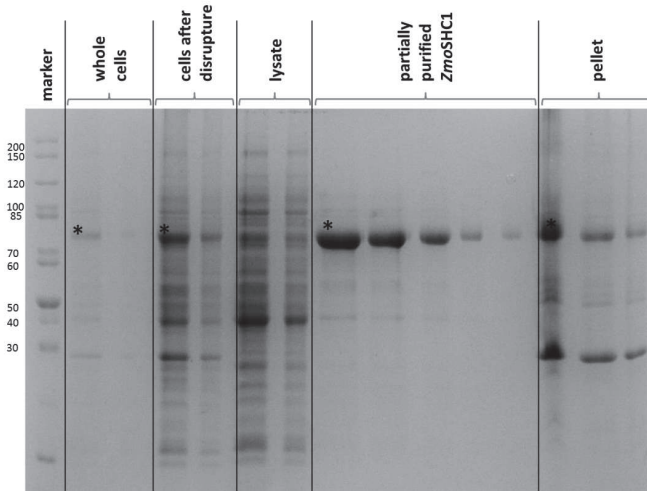


Fig. 5.3: SDS-gel showing the different steps during partial purification of *ZmoSHC1*. The bands for 81 kDa *ZmoSHC1* are marked with \*.

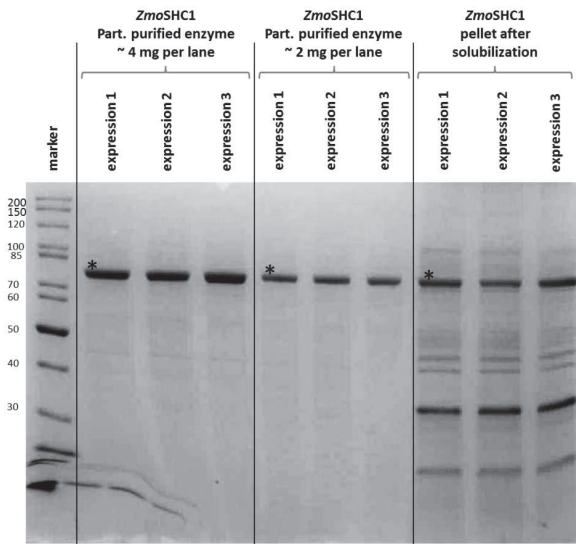


Fig. 5.4: SDS-gel showing partially purified *ZmoSHC1* from different expression set ups in two dilutions and the pellet remaining after the solubilization. The bands for 81 kDa *ZmoSHC1* are marked with \*.

As shown in Fig. 5.4, comparable solutions of partially purified SHC were derived from different expressions of the same SHC as well as from different SHCs. Thus, this partially purified enzyme could be used for biotransformations of varying enzymes and their activities could be compared to each other.

### 5.1.2 Biotransformations – Elaboration of a reliable standard protocol

As a starting point of the studies, the three cyclization reactions displayed in Fig. 5.5 were selected as model reactions for the development of a comparable and stable biotransformation system. These reactions were namely the cyclization of the natural substrate squalene to the membrane constituents hopene and hopanol, the conversion of the C<sub>16</sub> alcohol homofarnesol to the tricyclic flavor compound ambroxan and the biotransformation of the C<sub>10</sub> monoterpene citronellal to the menthol precursor isopulegol.

In the subsequent pages, optimization of the biotransformations leading to a reproducible and comparably setup is described in detail.

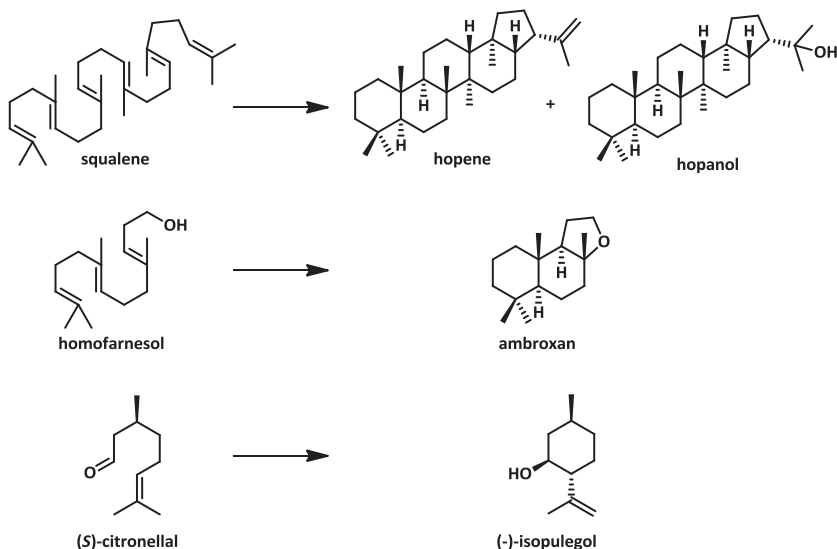


Fig. 5.5: Model reactions catalyzed by SHCs: squalene to hopene and hopanol, homofarnesol to ambroxan and (S)-citronellal to (-)-isopulegol.

### 5.1.2.1 Biotransformations with whole cells

First of all, biotransformations using whole cells expressing *ZmoSHC1*, *ZmoSHC2* and *AacSHC* were carried out with the three model substrates squalene, homofarnesol and citronellal.

**Table 5.1: Conversion of the different substrates (10 mM) after 20 / 5 h using whole cells expressing *ZmoSHC1*, *ZmoSHC2* and *AacSHC* (OD<sub>600</sub> = 10 / 80). The results are given as percentage of the product peaks in relation to the total GC peak areas; the ratio of hopene/hopanol for conversion of < 0.5 % was determined as <sup>a</sup>6.6 and <sup>b</sup>7.1.**

substrate	<i>ZmoSHC1</i>		<i>ZmoSHC2</i>		<i>AacSHC</i>	
	OD <sub>600</sub> = 10, 20 h	OD <sub>600</sub> = 80, 5 h	OD <sub>600</sub> = 10, 20 h	OD <sub>600</sub> = 80, 5 h	OD <sub>600</sub> = 10, 20 h	OD <sub>600</sub> = 80, 5 h
squalene	0.3 ± 0.2	n.d.	2.2 ± 1.1 <sup>a</sup>	< 0.1	96.9 ± 1.9 <sup>b</sup>	0.3 ± 0.2
homofarnesol	22.9 ± 6.8	29.2 ± 7.8	n.d.	n.d.	3.4 ± 0.5	11.3 ± 1.9
(S)-citronellal	0.8 ± 0.1	13.3 ± 5.4	n.d.	n.d.	n.d.	2.6 ± 0.4

The cells were applied in two different cell densities of OD<sub>600</sub> = 80 and OD<sub>600</sub> = 10 and the incubation times were varied between 5 and 20 h (see 9.9.1 a). The results are shown in Table 5.1.

Functional expression of all of the three SHCs was confirmed by conversion of at least one of the three model substrates.

### 5.1.2.2 Biotransformations with partially purified cyclase

In order to achieve conversion rates comparable for different enzymes, partially purified cyclase was used for biotransformations (see 9.9.2 a). The fractions were diluted to the same protein content. All of the three enzymes were functional, as they could at least convert one of the three substrates. The best conversion was shown for squalene with *AacSHC*. *ZmoSHC1* showed very low activity towards squalene and much higher activity towards homofarnesol. The results are shown in Table 5.2.

**Table 5.2: Conversion of the different substrates (10 mM) after 20 h using 0.1 mg/mL partially purified *ZmoSHC1*, *ZmoSHC2* and *AacSHC*. The results are given as percentage of the product peaks in relation to the total GC peak areas; the ratio of hopene/hopanol for conversion of > 0.5 % was determined as <sup>a</sup>7.9 and <sup>b</sup>5.5.**

substrate	<i>ZmoSHC1</i>	<i>ZmoSHC2</i>	<i>AacSHC</i>
squalene	0.2 ± 0.0	1.8 ± 1.0 <sup>a</sup>	79.0 ± 9.9 <sup>b</sup>
homofarnesol	9.5 ± 0.6	n.d.	n.d.
(S)-citronellal	0.4 ± 0.1	n.d.	n.d.

### 5.1.2.3 Stability experiments

One very important aspect for enzymatic systems is the biocatalytic stability. In order to examine the stability of the novel enzyme *ZmoSHC1*, several tests were performed. Both the whole cell system and the partially purified SHC were explored.

As first parameters, the incubation time and temperature were examined by measuring biotransformation of 10 mM of homofarnesol at different temperatures (30 / 37 / 42°C) with whole cells expressing *ZmoSHC1* (cell density OD<sub>600</sub> = 5) after 12, 24, 48, 72 and 96 h (see 9.9.1 b). As shown in Fig. 5.6, stability of the setup at 30°C with highest conversion rates during the first 24 h of the experiment could be confirmed. Lower conversion and loss of activity after 12 h was observed at 37°C. No cyclization of homofarnesol could be determined at all when the incubation temperature was 42°C.

In continuation, the biocatalytic stability of partially purified *ZmoSHC1* was analyzed. In this setup, the substrate was not added to the samples right at the beginning but after a certain pre-incubation time. Partially purified *ZmoSHC1* (approx. 1 mg/mL) was provided in reaction tubes and after 0 / 12 / 24 / 48 / 72 and 96 h of incubating at 30 / 37 / 42°C, homofarnesol was added to a final concentration of 10 mM. The biotransformations were carried out for 5 h. After extraction, the conversion rates were determined (for more details see 9.9.2 b). The results are shown in Fig. 5.7.

Without any pre-incubation, the highest activity could be observed at 42°C. As the pre-incubation time increased, the activity of *ZmoSHC1* decreased significantly. At 30°C and 37°C, the enzymatic activity was stable, still representing similar rates after 120 h of pre-incubation. The activity at 37°C was slightly higher than at 30°C (Fig. 5.7).

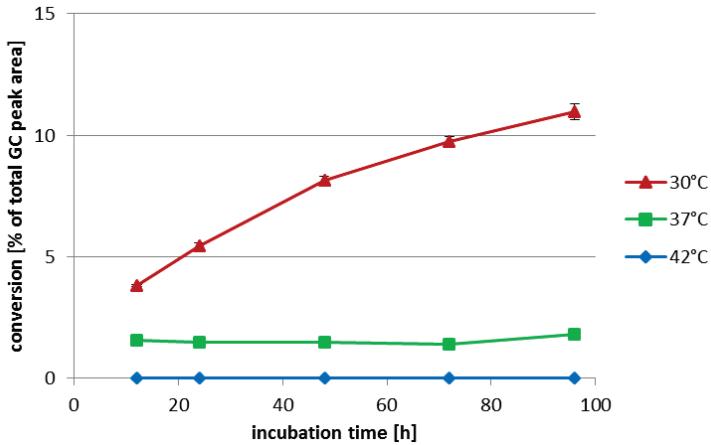


Fig. 5.6: Stability test with whole cells ( $OD_{600} = 5$ ) expressing *ZmoSHC1* showing the conversion of 10 mM homofarnesol after 12-96 h at 30°C (red) / 37°C (green) and 42°C (blue), respectively. The values are shown as percentage of total GC peak areas.

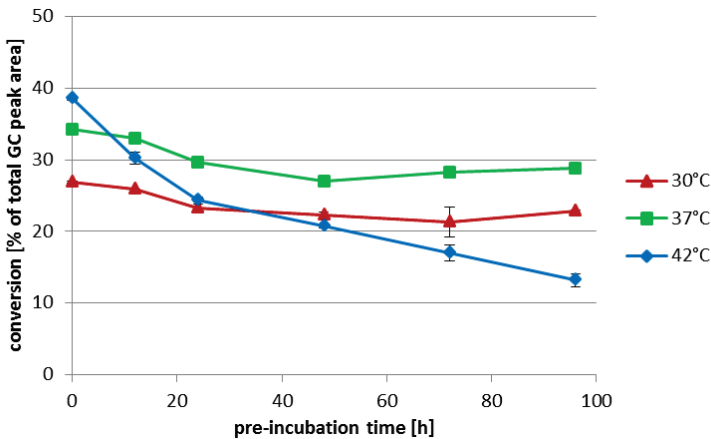
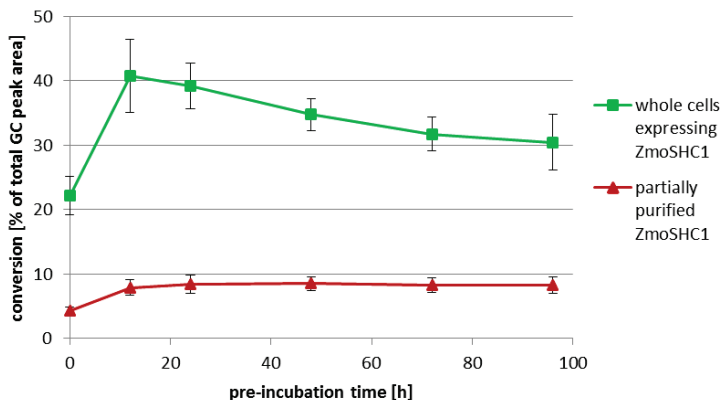


Fig. 5.7: Stability test with partially purified *ZmoSHC1* (approx. 1 mg/mL) showing the conversion of 10 mM homofarnesol after 5 h relative to the pre-incubation time after 12-96 h at 30°C (red) / 37°C (green) and 42°C (blue), respectively. The values are shown as percentage of total GC peak areas.

However, the two previously discussed stability experiments had been carried out under the conditions used right in the beginning of this work. Afterwards, the buffer system was changed from Tris/HCl to the temperature-independent citrate-buffer and the enzyme

concentration of the partially purified SHC was adjusted properly, as the solution used in the previously described stability assays was very concentrated. Thus, the observations were only taken as qualitative results. In order to derive reproducible values, two additional tests were performed.



**Fig. 5.8: Stability tests with whole cells expressing *ZmoSHC1* (green) and 0.1 mg/mL partially purified *ZmoSHC1* (red) showing the conversion of 10 mM of homofarnesol after 5 h relative to the pre-incubation time at 30°C. The values are shown as percentage of total GC peak areas.**

Similar to the previously carried out experiment with partially purified *ZmoSHC1*, mixtures of cells or partially purified enzyme and buffers were incubated for a distinct period. Then the substrate (homofarnesol, final concentration 10 mM) was added and after 5 h of additional incubation, the conversion was determined. This experiment was carried out both with cells expressing *ZmoSHC1* ( $OD_{600} = 80$ , see 9.9.1 c) as well as with partially purified *ZmoSHC1* (0.1 mg/mL final concentration, see 9.9.2 c). A high cell density was chosen in order to obtain a high activity as the incubation was just carried out for 5 h. The experiments were carried out at 30°C.

Under the given conditions, the partially purified cyclase demonstrated stability over 96 h (Fig. 5.8, red line). The conversion rate was found to be 7.9 % after 12 h of pre-incubation and 8.3 % after 96 h of pre-incubation. The highest activity of 8.5 % was found after 72 h. Interestingly, without any pre-incubation, the activity was low (4.3 %). For whole cell biotransformations, the conversion rate was determined as 22.2 % without any pre-incubation, which was just about half as high as after 12 h of pre-incubation (40.7 %). Then



the activity decreased constantly. After 96 h of pre-incubation, a rate of 30.5 % was determined.

In order to explore the stability of cells expressing *ZmoSHC1* in different cell densities, another assay screening for long time biotransformations was generated. Different cell densities ( $OD_{600} = 1 / 5 / 10 / 20 / 30$ ) were selected to convert 10 mM of the substrate homofarnesol in a time period of 24 / 48 / 72 / 96 / 120 h (see 9.9.1 d). The results obtained from this experiment are displayed in Fig. 5.9. Low cell density ( $OD_{600} = 1$ ) did not lead to a significantly higher conversion with longer incubation time (1.7 % after 24 h to 1.9 % after 120 h). For cell densities of  $OD_{600} = 5$ , the rate increased slightly from 6.7 % (24 h) to 10.5 % (120 h). Using whole cells expressing *ZmoSHC1* of a cell density of  $OD_{600} = 10$ , the conversion raised from 14.7 % to 24.9 % and with cells of a density of  $OD_{600} = 20$  from 26.9 % to 48.4 %, respectively. A similar pattern was found for the experiment carried out with cells of the density  $OD_{600} = 30$ ; the rate increased from 35.4 % (24 h) to 65.6 % (120 h).

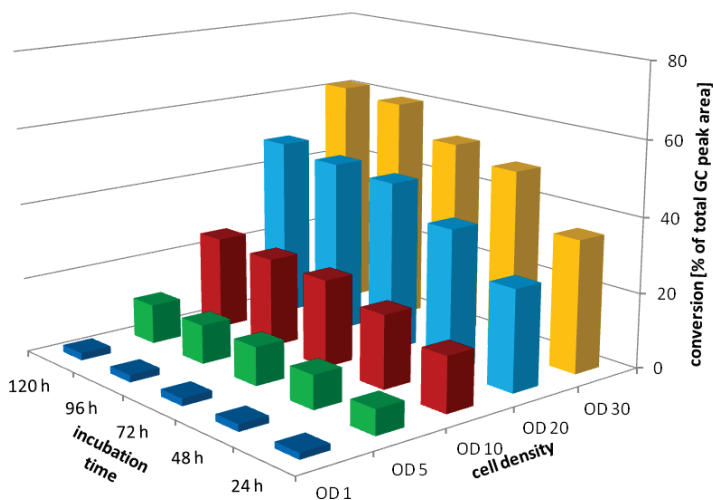


**Fig. 5.9:** Stability experiments with cells expressing *ZmoSHC1*. The conversion of 10 mM of homofarnesol was performed for 24 - 120 h at 30°C with different cell densities ( $OD_{600} = 1$  to  $OD_{600} = 30$ ). The values are shown as percentage of total GC peak areas.

#### 5.1.2.4 Substrate and product inhibition

Enzymatic activity can be influenced negatively by inhibiting effects of substrates and / or products. In order to test possible effects of the compounds on the activity of the SHCs, different experiments were carried out.

In the first experimental setup, a substrate mixture of homofarnesol and squalene was added to both cells expressing *ZmoSHC1* and *AacSHC* ( $OD_{600} = 10 / 80$ ) (see 9.9.1 e). The activities of the whole cell systems in the two different cell densities were tested with 5 mM homofarnesol and 5 mM squalene. Analogously, partially purified *ZmoSHC1* and *AacSHC* (0.1 mg/mL) were tested. As shown in Fig. 5.10, both homofarnesol and squalene were converted with *ZmoSHC1* and *AacSHC*.

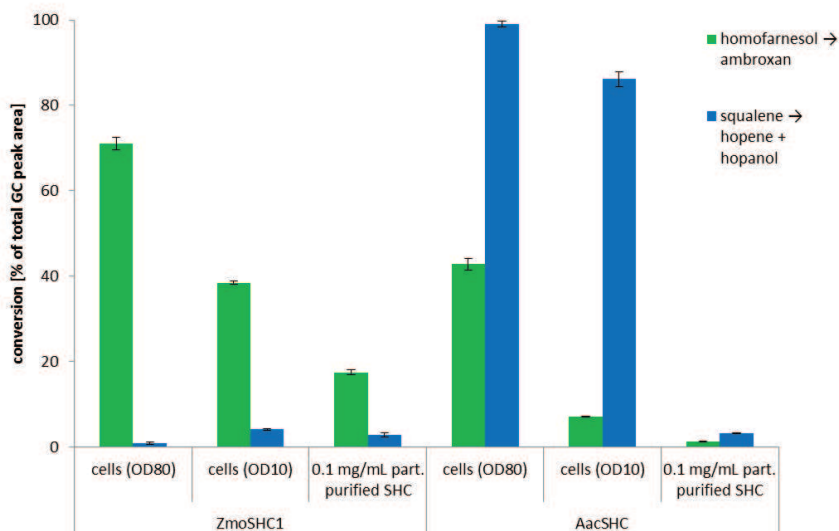


**Fig. 5.10:** Conversion of 5 mM homofarnesol and 5 mM squalene using cells expressing *ZmoSHC1* and *AacSHC* ( $OD_{600} = 80 / OD_{600} = 10$ ) and partially purified *ZmoSHC1* and *AacSHC* (0.1 mg/mL) in 20 h. The conversions of homofarnesol are shown as green, squalene as blue bars, respectively. The results are shown as percentages of the product GC peak areas in relation to the sum of all GC peak areas.

Regarding the results obtained from biotransformations carried out with whole cells expressing *ZmoSHC1*, good squalene conversion was found in presence of homofarnesol (Fig. 5.10). Using 10 mM of squalene as unique substrate, a low rate of 0.3 % was observed (Table

5.3). The conversion of 5 mM squalene was strongly increased to 4.1 % by addition of 5 mM of homofarnesol using cells expressing *ZmoSHC1* in a density of  $OD_{600} = 10$ . Increasing the cell density to  $OD_{600} = 80$ , the biotransformation of squalene was also higher in presence of homofarnesol. Remarkably, squalene conversion was higher with cells of lower cell density (4.1 % with  $OD_{600} = 10$  vs 0.9 % with  $OD_{600} = 80$ ; Fig. 5.10).

**Table 5.3: Substrate conversion using cells expressing *ZmoSHC1*. The results are shown as percentages of the product GC peak areas in relation to the sum of all GC peak areas.**

substrate	cells expressing <i>ZmoSHC1</i> $OD_{600} = 80$		cells expressing <i>ZmoSHC1</i> $OD_{600} = 10$		partially purified <i>ZmoSHC1</i> 0.1 mg/mL	
	homo-farnesol conversion	squalene conversion	homo-farnesol conversion	squalene conversion	homo-farnesol conversion	squalene conversion
5 mM homofarnesol + 5 mM squalene	71.1 ± 1.4	0.9 ± 0.3	38.4 ± 0.4	4.1 ± 0.2	17.5 ± 0.6	2.9 ± 0.5
10 mM homofarnesol	50.3 ± 6.6	-	22.9 ± 6.8	-	9.5 ± 0.6	-
10 mM squalene	-	0.5 ± 0.2	-	0.3 ± 0.2	-	0.2 ± 0.04

Similar results were observed using 0.1 mg/mL of partially purified *ZmoSHC1* (see 9.9.2 d). In the presence of both 5 mM of squalene and homofarnesol, the activity of *ZmoSHC1* towards squalene was highly increased (2.9 %) in comparison to its activity when no homofarnesol was added (0.2 %; 10 mM of squalene, see Table 5.3).

Good homofarnesol conversion was observed with cells of a high density (71.1 %) in presence of both 5 mM of homofarnesol and squalene. In contrast to this, by just adding 10 mM of homofarnesol, a much lower rate of 50.3 % had been observed. Similar results were obtained with cells of lower density and partially purified cyclase.

Different observations were made for biotransformations carried out with *AacSHC* as biocatalyst. As shown in Fig. 5.10, in all of the three setups (whole cells  $OD_{600} = 80$ , whole cells  $OD_{600} = 10$  and 0.1 mg/mL partially purified SHC) both squalene and homofarnesol were converted and the squalene conversion was enhanced over that of homofarnesol.

However, the different substrate concentrations of 5 and 10 mM in the approaches have to be considered. In order to obtain representative results for the inhibiting effects of the

substrates, several additional experiments were performed using partially purified SHCs (see 9.9.2 d). The conversions of 2 mM squalene or 2 mM homofarnesol using 0.1 mg/mL partially purified *ZmoSHC1* or *AacSHC* under presence of additional 2 mM of homofarnesol, squalene or ambroxan were determined. The results are shown in Table 5.4 and Table 5.5.

**Table 5.4: Conversion of 2 mM squalene using 0.1 mg/mL partially purified *ZmoSHC1* or *AacSHC*; shown as percentage of the product concentration in respect to the total concentration of both substrates and products calculated with ISTD1 calibration.**

substrate	enzyme	
	<i>ZmoSHC1</i>	<i>AacSHC</i>
2 mM squalene	1.0 ± 0.3	98.4 ± 0.3
2 mM squalene + 2 mM homofarnesol	4.2 ± 0.5	39.0 ± 1.4
2 mM squalene + 2 mM ambroxan	1.1 ± 0.2	44.1 ± 0.4
2 mM squalene + 2 mM homofarnesol + 2 mM ambroxan	3.1 ± 0.5	12.5 ± 1.0

Using *AacSHC* as biocatalyst, 2 mM of squalene as single substrate was converted almost completely. The conversion rate was strongly decreased in the presence of homofarnesol. The addition of ambroxan did not show significant influences on the activity of *AacSHC* towards squalene. However, when both homofarnesol and ambroxan were added to the system, the conversion rate of squalene decreased significantly (Table 5.4).

**Table 5.5: Conversion of 2 mM homofarnesol using 0.1 mg/mL partially purified *ZmoSHC1* or *AacSHC*; shown as percentage of the product concentration in respect to the total concentration of both substrates and products calculated with ISTD1 calibration.**

substrate	enzyme	
	<i>ZmoSHC1</i>	<i>AacSHC</i>
2 mM homofarnesol	41.4 ± 1.8	2.0 ± 0.2
2 mM homofarnesol + 2 mM squalene	30.1 ± 1.0	1.6 ± 0.1
2 mM homofarnesol + 2 mM ambroxan	15.8 ± 1.8	n.d.
2 mM homofarnesol + 2 mM squalene + 2 mM ambroxan	5.7 ± 0.6	n.d.

The same approach was performed for analyzing the influence of squalene and ambroxan on homofarnesol conversion (Table 5.5). For biotransformations using 0.1 mg/mL partially purified *ZmoSHC1*, the following observations were made: Addition of both squalene and / or ambroxan caused a decrease in homofarnesol conversion. The inhibiting effect of

ambroxan was stronger than that of squalene. The lowest conversion was observed when both ambroxan and squalene were added.

For *AacSHC* the observations were different. The addition of squalene did not influence the activity of *AacSHC* towards homofarnesol. The presence of ambroxan caused a complete loss of the activity of *AacSHC* towards homofarnesol.

The results suggested that there are inhibitory effects of ambroxan on the enzymatic activity of *ZmoSHC1* towards homofarnesol. In order to define inhibiting effects of the product ambroxan on the homofarnesol conversion, one additional experiment was carried out. Biotransformations of 0.1 – 10 mM of homofarnesol were performed with 0.1 mg/mL partially purified *ZmoSHC1* (see 9.9.2 d). The results are displayed in Fig. 5.11 A, showing percentages of substrate and product GC peak areas achieved after 20 h of incubation. Using substrate starting concentrations of 0.1, 0.5 and 1.0 mM, high rates were observed (81.0 %, 82.8 % and 78.4 %). An increase of the substrate starting concentration led to a continuous decrease of conversion from 60.7 % starting with 2 mM substrate concentration, over 41.7 %, 29.3 % and 20.9 % with 4, 6 and 8 mM of homofarnesol substrate concentration to the lowest rate of 17.1 % (10 mM of substrate). Another visualization of the results is given in Fig. 5.11 B, where the absolute GC peak areas of homofarnesol and ambroxan are displayed as a function of the starting concentrations of homofarnesol. Using 0.1 mg/mL of partially purified *ZmoSHC1* and substrate concentrations of more than 6 mM in the beginning of the biotransformations did not result in higher end concentrations of the product ambroxan.

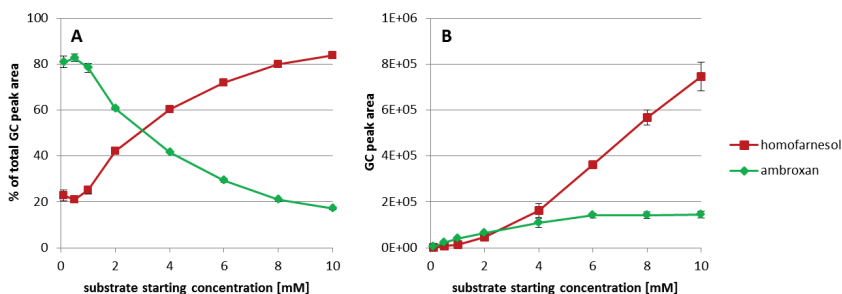


**Fig. 5.11:** Conversion of 0.1 - 10 mM of homofarnesol using 0.1 mg/mL of partially purified *ZmoSHC1* in 20 h. The values represent A) the percentages of the GC peak areas / B) the GC peak areas of the substrate homofarnesol (red) and the product ambroxan (green).

### 5.1.2.5 Internal standard experiments

For quantitative determination of the substrates and products, the use of an internal standard is the method of choice when calibration with an external standard is not possible or an instrument's response is varying from one run to the next for certain reasons. It should also be mentioned that there are deviations that are almost impossible to avoid during sample preparation, for example differences in substrate addition or product extraction. In order to develop an assay for the use of an internal standard, we tested the influence of 1-decanol to the enzymatic activity of the SHCs *ZmoSHC1* and *AacSHC*.

As an internal standard, 1-decanol was selected because its chemical and physical properties are similar to homofarnesol, it is cheap and easy to achieve and no cyclization reaction is expected. In order to test the influence of 1-decanol on the enzymatic activity of *ZmoSHC1*, homofarnesol was used as a substrate; for *AacSHC*, squalene was the substrate of choice. At the beginning of biotransformation using partially purified SHCs (0.1 mg/mL, 5 mM substrate), 5 mM of 1-decanol (ISTD1) was added to the reaction mixture (see 9.9.2 e). The conversion rates were determined and compared to assays performed in the absence of 1-decanol (Fig. 5.12).

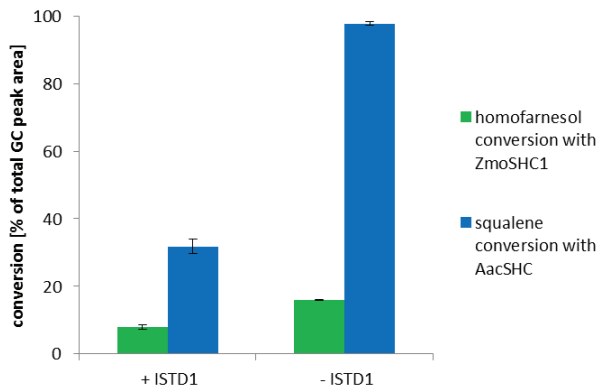


**Fig. 5.12:** Conversion of 5 mM homofarnesol using 0.1 mg/mL partially purified *ZmoSHC1* (green bars) / 5 mM squalene using 0.1 mg/mL of partially purified *AacSHC* (blue bars) with 5 mM ISTD1 1-decanol added prior to incubation (+ISTD, left side) / without ISTD1-addition (-ISTD, right side). The values are shown as percentage of total GC peak areas.

As shown in Fig. 5.12, the conversions were strongly affected when 1-decanol was added to the systems. Homofarnesol biotransformation catalyzed by partially purified *ZmoSHC1* was

determined as 8.0 % under presence of 1-decanol whereas a rate of 15.9 % was found without addition of the internal standard. The biotransformation of squalene catalyzed by *AacSHC* was influenced even stronger, as the rates were found as 31.8 % with internal standard and 97.8 % without 1-decanol.

#### 5.1.2.6 pH Studies

While the optimal pH for growth of the bacterial strain *Alicyclobacillus acidocaldarius* had been reported to be at pH 3, the best pH for squalene biotransformation with *AacSHC* was determined as pH 6 according to the intracellular conditions of the bacteria.<sup>114,267,268</sup> In order to test the influence of the pH on the activities of *ZmoSHC1*, *ZmoSHC2* and *AacSHC* towards the model substrates citronellal, homofarnesol and squalene, biotransformations of 10 mM of the substrates were carried out using 0.1 mg/mL partially purified *ZmoSHC1*, *ZmoSHC2* and *AacSHC* at pH 4.5, pH 5.0 and pH 6.0 (see 9.9.2 f).

**Table 5.6: Conversion of 10 mM of the model substrates at different pH values using 0.1 mg/mL of partially purified *ZmoSHC1*, *ZmoSHC2* and *AacSHC*. The results are given as percentages of total GC peak area.**

		(S)-citronellal	homofarnesol	squalene
<i>ZmoSHC1</i>	pH 4.5	0.5 ± 0.1	4.7 ± 0.6	< 0.1
	pH 5.0	0.3 ± 0.1	12.4 ± 4.8	0.1 ± 0.0
	pH 6.0	0.4 ± 0.1	9.5 ± 1.2	0.2 ± 0.1
<i>ZmoSHC2</i>	pH 4.5	n.d.	n.d.	< 0.1
	pH 5.0	n.d.	n.d.	0.7 ± 0.3
	pH 6.0	n.d.	n.d.	1.8 ± 1.0
<i>AacSHC</i>	pH 4.5	n.d.	n.d.	57.6 ± 9.9
	pH 5.0	n.d.	n.d.	69.9 ± 14.8
	pH 6.0	n.d.	n.d.	79.0 ± 9.4

As shown in Table 5.6, differences in the conversion rates were observed at varying pHs. The biotransformation of citronellal using *ZmoSHC1* was found to be similar for all of the three tested values. The best conversion of homofarnesol with *ZmoSHC1* was found to be at pH 5.0. Squalene was converted best at pH 6.0, as expected. The subsequent reactions were carried out at pH 6.0. However, citronellal biotransformations were performed at pH 4.5 due to the increased reduction rate of citronellal to citronellol at higher pH values (Fig. 5.13, Fig.

5.14). In order to avoid this side reaction, the pH of choice for the citronellal conversions was 4.5.

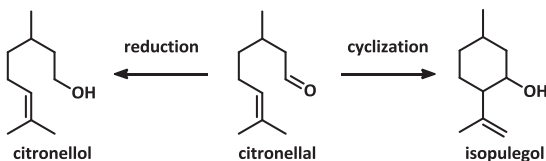


Fig. 5.13: Conversion of citronellal to citronellol or isopulegol.

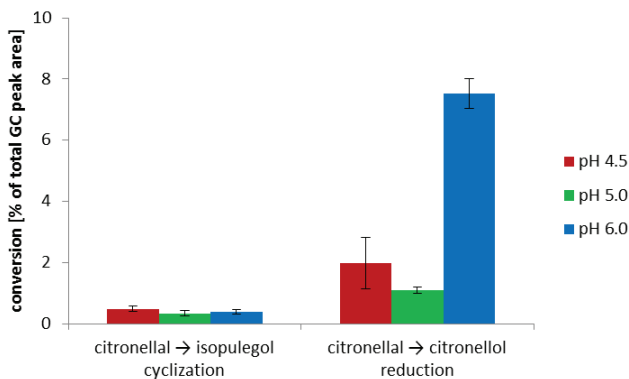


Fig. 5.14: Conversion of citronellal using 0.1 mg/mL partially purified *ZmoSHC1*. The biotransformations were performed at pH 4.5 (red bars) / pH 5.0 (green bars) / pH 6.0 (blue bars). The formation of the desired product isopulegol is shown on the left (values after subtraction of the values of the negative control), the formation of the side product citronellol is displayed on the right side. The values are shown as percentage of total GC peak areas.

## 5.2 Substrate specificity of SHCs

In order to explore the substrate specificity of the SHCs, several linear terpenoids varying in carbon chain lengths and functional groups were tested as substrates for *ZmoSHC1*, *ZmoSHC2* and *AacSHC*. When conversion was observed by new occurring peaks in GC analyses, large scale biotransformations were carried out; the products were isolated and characterized as described in 9.9 and 9.10. A short overview is given in Table 5.7.



**Table 5.7: Overview of the substrates tested with SHCs sorted by their functional groups. Positive conversion with SHCs is signed as green ✓ and no conversion is marked as red X.**

substrate	functionality	no. of C-atoms	conversion	
geraniol	alcohols	10	X	
homofarnesol		16	✓	
bishomofarnesol		17	✓	
linalool		tertiary	10	X
nerolidol			15	✓
geranylacetone	ketones	13	✓	
pseudoionone		13	X	
farnesylacetone		18	✓	
geranic acid	carboxylic acids	10	X	
homofarnesoic acid		16	✓	
bishomofarnesoic acid		17	✓	
citronellal	aldehydes	10	✓	
citral		10	X	
bishomofarnesal		17	✓	

### 5.2.1 Alcohols

The primary alcohols geraniol ( $C_{10}$ ), homofarnesol ( $C_{16}$ ) and bishomofarnesol ( $C_{17}$ ) were tested as substrates (Fig. 5.15). Geraniol did not show conversion with the SHCs under the standard conditions (9.9.2). Homofarnesol was converted to ambroxan with *Zmo*SHC1 and *Aac*SHC as biocatalysts. The product was identified by comparison with authentic standard. Bishomofarnesol was converted into two products by *Zmo*SHC1, seen as new occurring peaks in both GC-FID and GC-MS chromatograms in comparison to negative controls. For the major cyclization product, the literature MS data corresponds nicely with (±)-ambroxide and (±)-9-*epi*-ambroxide (Fig. 5.15).<sup>235</sup>

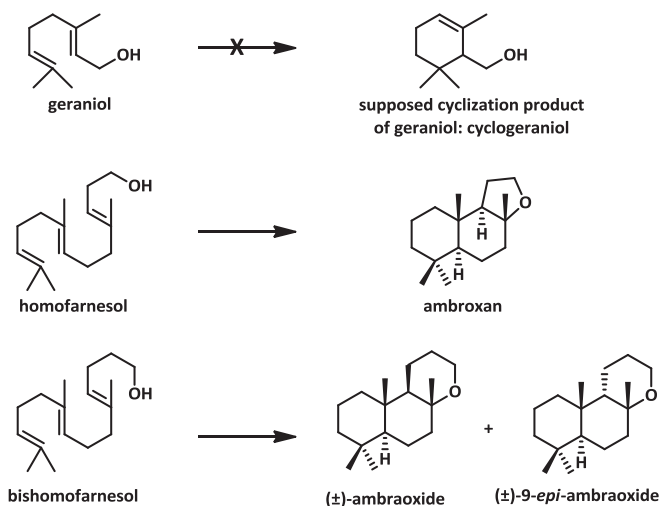


Fig. 5.15: Alcohols as substrates: geraniol did not show conversion into the suggested cyclization product cyclogeraniol; homofarnesol was converted to ambroxan by *ZmoSHC1* and *AacSHC*; bishomofarnesol was converted into two new products by *ZmoSHC1*, for which GC-MS analysis suggested to be ( $\pm$ )-ambroxide and ( $\pm$ )-9-*epi*-ambroxide.

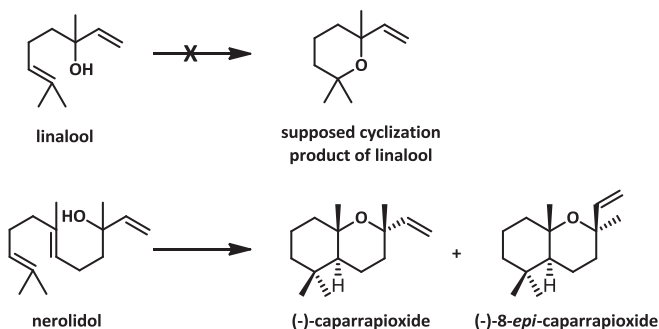


Fig. 5.16: Tertiary alcohols as substrates: nerolidol was converted to (-)-caparrapioxide and (-)-8-*epi*-caparrapioxide. Linalool did not show any product formation.

The tertiary alcohols linalool ( $C_{10}$ ) and nerolidol ( $C_{15}$ ) were tested as substrates (Fig. 5.16). While linalool was not cyclized by any of the SHCs, nerolidol conversion into two products could be shown with *ZmoSHC1* and *AacSHC*. After preparative biotransformation of nerolidol using partially purified *ZmoSHC1*, the products (-)-caparrapioxide and (-)-8-*epi*-caparrapioxide were successfully isolated (Fig. 5.16). The separation of both products was

achieved with preparative HPLC, leading to small amounts of the isomers that could be analyzed, as described in 9.9.4 and 9.10.3. The products were confirmed by NMR (1D and 2D) and MS (9.10).<sup>178,218</sup>

The cyclization reaction is stereoselective yielding (-)-caparrapioxide and (-)-8-*epi*-caparrapioxide from racemic nerolidol (Fig. 5.17).

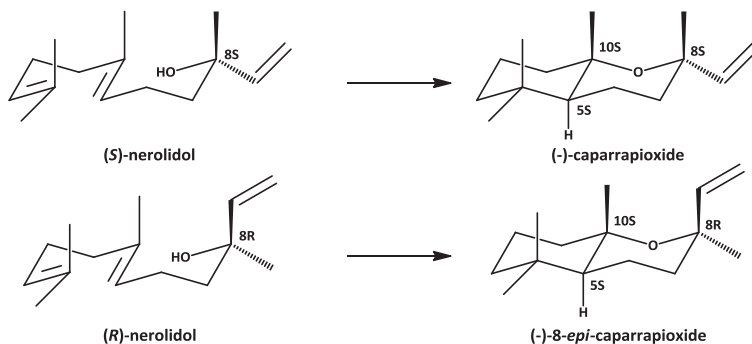


Fig. 5.17: Cyclization of (*S*)- or (*R*)-nerolidol catalyzed by SHCs forming the cyclic products (-)-caparrapioxide or (-)-8-*epi*-caparrapioxide.

## 5.2.2 Ketones

The ketones geranylacetone (C<sub>13</sub>), pseudoionone (C<sub>13</sub>) and farnesylacetone (C<sub>18</sub>) were tested as substrates (Fig. 5.18). Geranylacetone was cyclized to a bicyclic product containing a hexahydrochromene by *Zmo*SHC1 and *Aac*SHC. Pseudoionone was not converted under the given conditions. Farnesylacetone showed low but significant conversion to one product, sclareoloxide. The corresponding cyclic products were isolated and characterized (9.9.4 and 9.10.3).

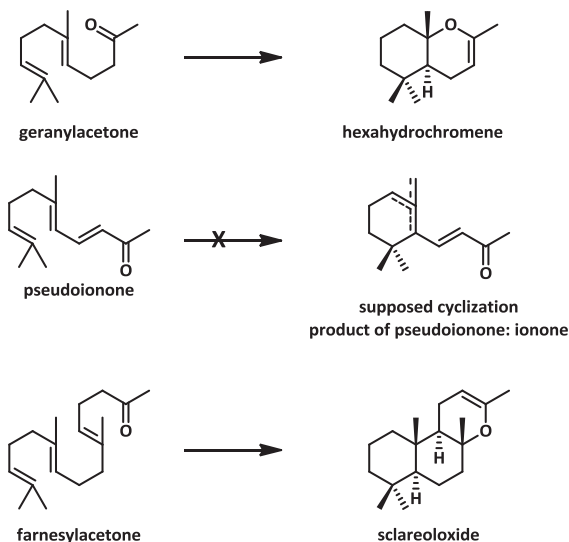


Fig. 5.18: Ketones as substrates: farnesylacetone was converted to sclareoloxide and geranylacetone to hexahydrochromene. Pseudoionone was not accepted as a substrate.

### 5.2.3 Carboxylic acids

Three carboxylic acids were tested as substrates, namely geranic acid ( $C_{10}$ ), homofarnesoic acid ( $C_{16}$ ) and bishomofarnesoic acid ( $C_{17}$ ) (Fig. 5.19). Geranic acid did not show conversion with the SHCs. Biotransformation of homofarnesoic acid was shown using *ZmoSHC1* and *AacSHC* as biocatalysts, leading to one single product identified with GC-FID and GC-MS. After preparative biotransformation of homofarnesoic acid using partially purified *ZmoSHC1*, the product sclareolide was successfully isolated and the structure was confirmed by NMR (1D and 2D), MS and IR (9.9.4 and 9.10.3).<sup>269</sup>

Bishomofarnesoic acid showed three new peaks in the GC chromatogram after conversion with *ZmoSHC1*. The mass spectra were compared to literature data. The major cyclization product is in good agreement with the literature MS spectra of ( $\pm$ )-ambreinolide and ( $\pm$ )-10-*epi*-ambreinolide.<sup>235</sup> The MS data of the minor product show some of the characteristic peaks of the comparison data for ( $\pm$ )-10-*epi*-ambreinolide (Fig. 5.19). The third product does not show any correspondence to literature data.

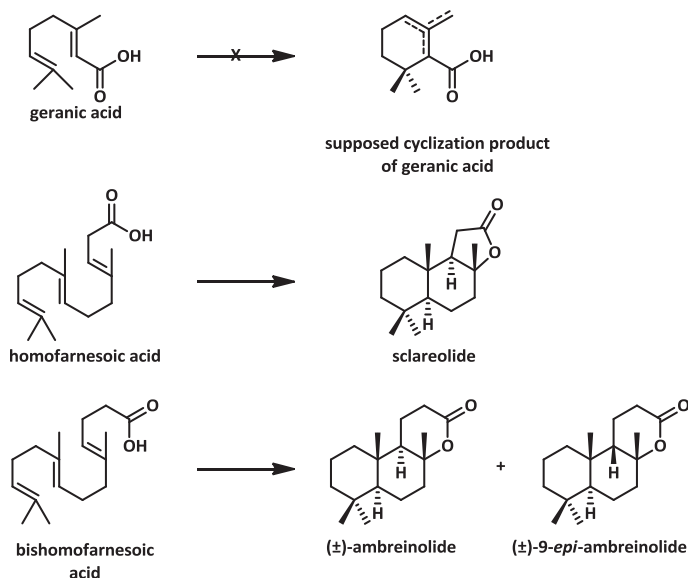


Fig. 5.19: Carboxylic acids tested as substrates: geranic acid did not show a conversion with SHCs, homofarnesoic acid was converted to sclareolide, bishomofarnesoic acid was converted into two products which are supposed to be (±)-ambreinolide and (±)-9-*epi*-ambreinolide.

### 5.2.4 Aldehydes

Three aldehydes were tested as substrates: (*S*)-citronellal ( $C_{10}$ ), *cis*-citral ( $C_{10}$ ) and bishomofarnesal ( $C_{17}$ ).<sup>238</sup> Incubation of (*S*)-citronellal led to the cyclic (-)-isopulegol. Due to acid-catalyzed autocyclization, which also occurred using the described parameters, the resulting isopulegol production in negative controls was subtracted. *Cis*-citral was not accepted as substrate (Fig. 5.20).

Biotransformations of the  $C_{17}$  aldehyde bishomofarnesal with *Zmo*SHC1 showed occurrence of two new peaks in comparison to the negative control. In order to characterize the product, all of the remaining substrate was converted using partially purified *Zmo*SHC1. Unfortunately, after extraction, silica gel column purification and preparative HPLC, the product could not be isolated in the necessary purity. No literature MS spectra of the expected cyclic product were found for comparison and the resulting amount of product was too small for any other purification steps and further characterization.

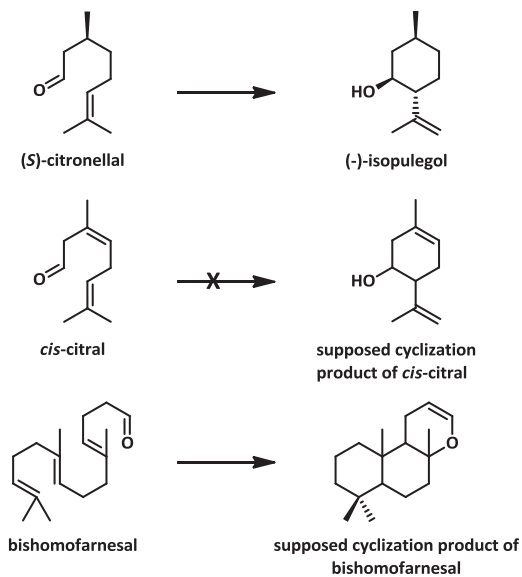


Fig. 5.20: Cyclization of the aldehydes (S)-citronellal to isopulegol and bishomofarnesol to the supposed cyclization product.

### 5.3 Comparison of the substrate specificities of *ZmoSHC1*, *ZmoSHC2* and *AacSHC*

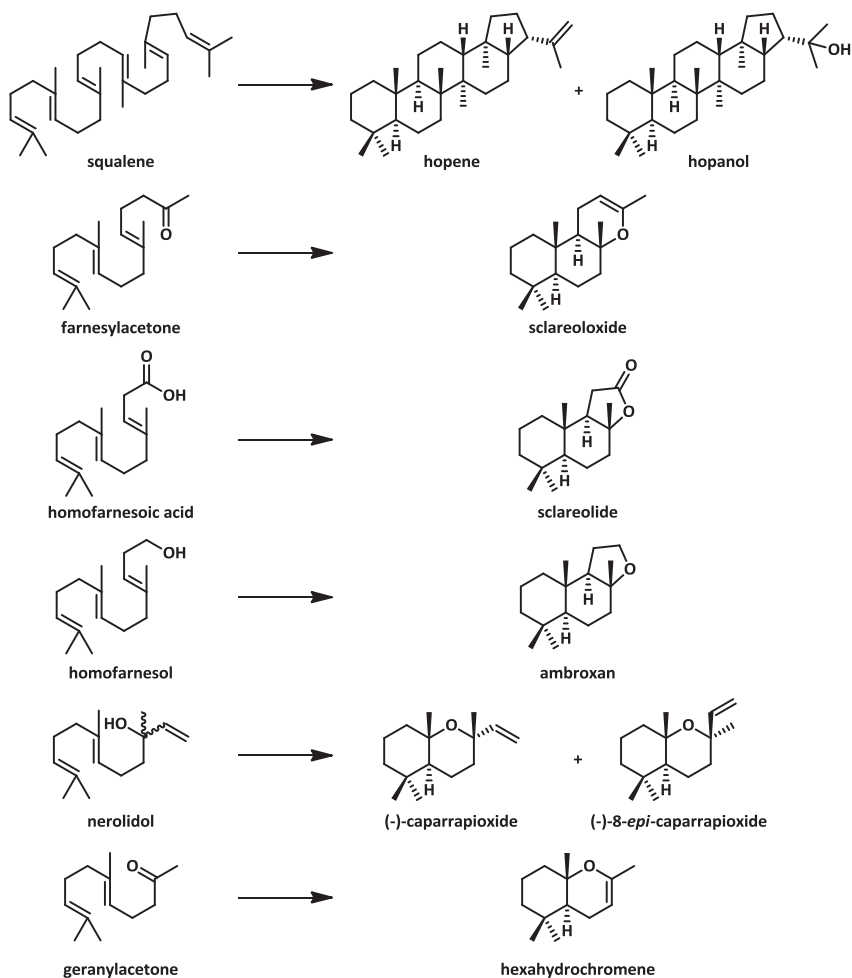


Fig. 5.21: Cyclization reactions catalyzed by SHCs: squalene to hopene and hopanol; farnesylacetone to sclareoloxide; homofarnesoic acid to scclareolide; homofarnesol to ambroxan; nerolidol to (-)-caparrapioxide and (-)-8-*epi*-caparrapioxide; geranylacetone to hexahydrochromene.

The activities of the SHCs *ZmoSHC1*, *ZmoSHC2* and *AacSHC* towards the novel substrates farnesylacetone, homofarnesoic acid, nerolidol and geranylacetone were determined and compared to the conversion rates obtained with the model substrates homofarnesol and squalene. An overview of all the catalyzed cyclization reactions is shown in Fig. 5.21.

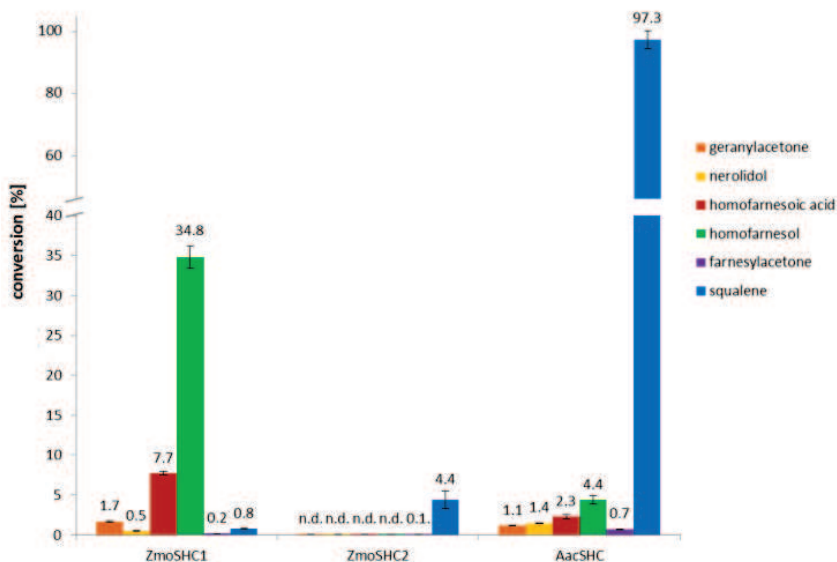


Fig. 5.22: Conversion rates of the substrates geranylacetone (orange), nerolidol (yellow), homofarnesoic acid (red), homofarnesol (green), farnesylacetone (purple), squalene (blue) using 0.35 mg/mL partially purified *ZmoSHC1* / *ZmoSHC2* / *AacSHC*. The values are shown as percentage of the product concentration in respect to the total concentration of both substrates and products calculated with ISTD1 calibration.

In order to compare the biotransformations of the different substrates catalyzed by the cyclases *ZmoSHC1*, *ZmoSHC2* and *AacSHC*, conversions were performed using 0.35 mg/mL partially purified SHCs and 10 mM substrate starting concentrations. The biotransformations were carried out for 20 h (see 9.9.2 a). The rates were determined with the effective carbon number concept (ECN) as described in 9.10.6. Using this concept of quantification, the concentrations of both substrates and products could be defined. The conversions were determined by calculating the percentage of the product concentration in respect to the total concentration of both substrates and products (Fig. 5.22 and Table 5.8).



**Table 5.8: Conversion of the different substrates (10 mM) after 20 h using 0.35 mg/mL partially purified SHCs, shown as percentage of the product concentration in respect to the total concentration of both substrates and products calculated with ISTD1 calibration; <sup>a</sup>ratio homopene:hopanol; <sup>b</sup>ratio (-)-caparrapioxide:(-)-8-*epi*-caparrapioxide.**

substrate	<i>Zmo</i> SHC1	<i>Zmo</i> SHC2	<i>Aac</i> SHC
squalene	0.8 ± 0.1 (2.6) <sup>a</sup>	4.4 ± 1.1 (3.3) <sup>a</sup>	97.3 ± 2.9 (6.3) <sup>a</sup>
farnesylacetone	0.2 ± 0.0	0.1 ± 0.0	0.7 ± 0.1
homofarnesol	34.8 ± 1.4	n.d.	4.4 ± 0.5
homofarnesoic acid	7.7 ± 0.2	n.d.	2.3 ± 0.3
nerolidol	0.5 ± 0.0 (3.4) <sup>b</sup>	n.d.	1.4 ± 0.1 (1.8) <sup>b</sup>
geranylacetone	1.7 ± 0.1	n.d.	1.1 ± 0.1

Homofarnesoic acid was accepted as substrate by *Zmo*SHC1 and *Aac*SHC and cyclized to the tricyclic lactone sclareolide. The conversion of homofarnesoic acid with *Zmo*SHC1 (7.7 %) was about 7-fold higher than the biotransformation of squalene (0.8 %). Homofarnesol was converted even better with both *Zmo*SHC1 and *Aac*SHC, displaying more than 6-fold higher conversion with *Zmo*SHC1 and 3-fold higher conversion using *Aac*SHC as biocatalyst in comparison to biotransformations of homofarnesoic acid.

**Table 5.9: Conversion of nerolidol to (-)-caparrapioxide and (-)-8-*epi*-caparrapioxide; shown as percentage of the product concentration in respect to the total concentration of both substrates and products calculated with ISTD1 calibration.**

	total conversion [%]	(-)-caparrapioxide [%]	(-)-8- <i>epi</i> -caparrapioxide [%]	ratio
<i>Zmo</i> SHC1	0.5 ± 0.0	0.4 ± 0.0	0.1 ± 0.0	3.4
<i>Zmo</i> SHC2	n.d.	n.d.	n.d.	-
<i>Aac</i> SHC	1.4 ± 0.1	0.9 ± 0.1	0.5 ± 0.0	1.8

The total conversion of nerolidol with *Zmo*SHC1 and *Aac*SHC was found to be 0.5 % and 1.4 %. (-)-caparrapioxide was the main product for biotransformation with both enzymes, the ratio between (-)-caparrapioxide and (-)-8-*epi*-caparrapioxide was determined to be 3.4 and 1.8 for *Zmo*SHC1 and *Aac*SHC, respectively (Table 5.9). Using *Zmo*SHC2 as biocatalyst, nerolidol was not accepted as a substrate.

The ketone farnesylacetone was converted by all of the three tested SHCs in low rates (0.2 % with *Zmo*SHC1, 0.1 % with *Zmo*SHC2 and 0.7 % with *Aac*SHC), representing the first substrate

besides squalene which was cyclized by *ZmoSHC2*. Geranylacetone was converted with *ZmoSHC1* (1.7 %) and *AacSHC* (1.1 %) into the corresponding cyclic enol ether.

### 5.3.1 Enhanced conversions

In order to increase the yield of the ambroxan and isopulegol formed from homofarnesol and citronellal using *ZmoSHC1* as biocatalyst, the cell density of cells expressing *ZmoSHC1* was increased to  $OD_{600} = 80$  and the substrates were incubated for 20 h (see 9.9.2 a). The results shown increased rates of homofarnesol (50.3 %) and (*S*)-citronellal (16.4 %) besides low squalene conversion (0.5 %, Table 5.10).

**Table 5.10: Biotransformations with cells expressing *ZmoSHC1*, carried out for 20 h using a cell density of  $OD_{600} = 80$ . The results are given as percentage of the product peaks in relation to the total GC peak areas.**

substrate	conversion [% of total GC peak area]
( <i>S</i> )-citronellal	16.4 ± 2.2
homofarnesol	50.3 ± 6.6
squalene	0.5 ± 0.2

Furthermore, the conversion rates of the new, unnatural substrates were found to be quite low under the present conditions. In order to test whether these rates could be increased, the biotransformations were repeated using an enhanced enzyme concentration of 4 mg/mL (see 9.9.2 g). The results obtained with partially purified *ZmoSHC1* are shown in Table 5.11.

The biotransformation rates could be increased when a higher concentration of enzyme was used for the biotransformations. The best increase of conversion could be achieved for farnesylacetone and geranylacetone showing a 13- and 14-fold higher rate than observed formerly using 0.35 mg/mL enzyme. Squalene was converted 5-fold better and homofarnesoic acid 3-fold. Lowest increase was displayed for homofarnesol and nerolidol, as these substrates were just converted twice more than shown before. The results are displayed in Fig. 5.23.

**Table 5.11: Conversion of the substrates (10 mM, 20 h) using 4 mg/mL partially purified *ZmoSHC1*. The results are shown as percentage of the product concentration in respect to the total concentration of both substrates and products calculated with ISTD1 calibration; <sup>a</sup>ratio hopene:hopanol; <sup>b</sup>ratio (-)-caparrapioxide:(-)-8-*epi*-caparrapioxide.**

substrate	conversion [%]
squalene	4.1 ± 0.4 (9.2) <sup>a</sup>
farnesylacetone	2.5 ± 0.2
homofarnesoic acid	22.9 ± 3.2
homofarnesol	65.6 ± 0.8
nerolidol	0.9 ± 0.1 (2.7) <sup>b</sup>
geranylacetone	23.0 ± 0.6

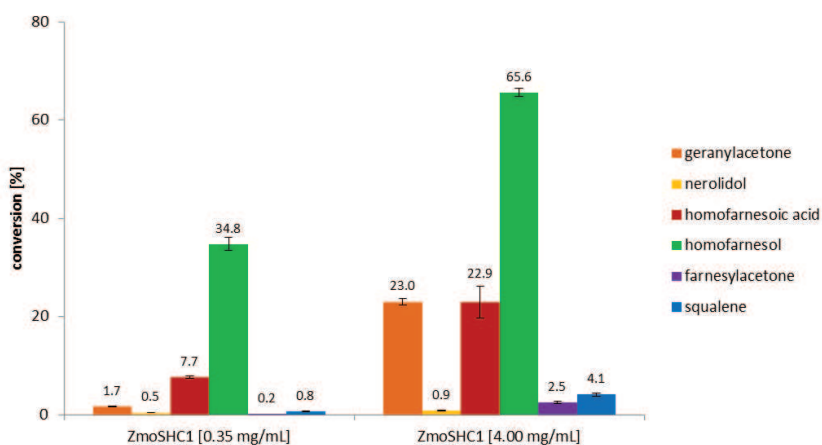


**Fig. 5.23: Conversion of the substrates using 0.35 mg/mL or 4.00 mg/mL partially purified *ZmoSHC1*. The values are shown as percentage of the product concentration in respect to the total concentration of both substrates and products calculated with ISTD1 calibration.**

### 5.3.2 Limits of substrate specificity

After description of the reactions catalyzed by the SHCs, there also have to be mentioned the substrates that were not cyclized.

All of these substrates, namely geraniol, linalool, pseudoionone, geranic acid and citral, consist of chain lengths of 13 or less carbon atoms and were expected to yield monocyclic products. In theory, the substrates geraniol and geranic acid were expected to be converted

to one or several of the products shown in Fig. 5.24, and linalool should be cyclized to a heterocyclic compound. However, no conversion could be determined under the given conditions. Also the C<sub>10</sub> aldehyde *cis*-citral and the C<sub>13</sub> ketone pseudoionone were not converted.

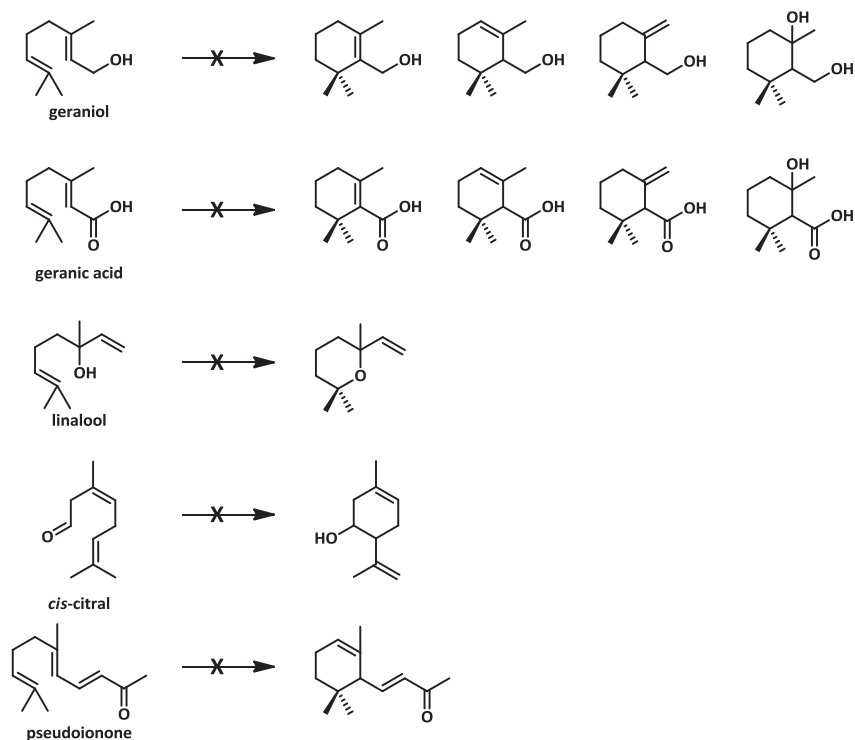


Fig. 5.24: Not SHC-catalyzed cyclization reactions of the C<sub>10</sub> substrates geraniol, geranic acid, linalool and *cis*-citral and the C<sub>13</sub> substrate pseudoionone.

## 5.4 Directed mutagenesis

### 5.4.1 Selection of spots for single mutants and screening

The single mutants *ZmoSHC1\_F486Y* and *AacSHC\_Y420C* were created (for details see 9.6 and 0) by side-directed mutagenesis of the genes encoding for *ZmoSHC1* and *AacSHC*. Functional expression and partial purification was successful. Their activities towards the

substrates was determined and could be compared to the activity of the wildtype SHCs. The results are shown in Table 5.12.

**Table 5.12: Conversion of the different substrates (10 mM) after 20 h using 0.35 mg/mL partially purified SHCs, shown as percentage of the concentrations of both substrates and products calculated with ISTD1 calibration; <sup>a</sup>ratio hopene:hopanol; <sup>b</sup>ratio (-)-caparrapioide:(-)-8-*epi*-caparrapioide.**

substrate	<i>Zmo</i> SHC1	<i>Zmo</i> SHC1_F486Y	<i>Aac</i> SHC_Y420C	<i>Aac</i> SHC
squalene	0.8 ± 0.1 (2.6) <sup>a</sup>	0.8 ± 0.2 (3.1) <sup>a</sup>	6.3 ± 0.5 (5.1) <sup>a</sup>	97.3 ± 2.9 (6.3) <sup>a</sup>
homofarnesol	34.8 ± 1.4	23.9 ± 0.1	n.d.	4.4 ± 0.5
homofarnesoic acid	7.7 ± 0.22	10.2 ± 1.5	1.0 ± 0.3	2.3 ± 0.3
nerolidol	0.5 ± 0.0 (3.4) <sup>b</sup>	1.3 ± 0.0 (2.1) <sup>b</sup>	n.d.	1.4 ± 0.8 (1.8) <sup>b</sup>
geranylacetone	1.7 ± 0.1	7.5 ± 0.2	n.d.	1.1 ± 0.1
farnesylacetone	0.2 ± 0.0	0.3 ± 0.2	< 0.1	0.7 ± 0.1

#### 5.4.2 Creation and screening of the loop deletion mutant

The *Zmo*SHC1\_Loop mutant was expressed and partially purified (for details see 9.6). The substrates which had shown activity with the wildtype *Zmo*SHC1 were screened. The loop deletion mutant was expressed in active form, as the conversion of all of the substrates was detected. The results are shown in Table 5.13.

**Table 5.13: Conversion of the different substrates after 20 h using 0.35 mg/mL partially purified SHCs, shown as percentage of the concentrations of both substrates and products calculated with ISTD1 calibration; <sup>a</sup>ratio hopene:hopanol; <sup>b</sup>ratio (-)-caparrapioide:(-)-8-*epi*-caparrapioide.**

substrate	<i>Zmo</i> SHC1	<i>Zmo</i> SHC1_Loop	<i>Aac</i> SHC
squalene	0.8 ± 0.1 (2.6) <sup>a</sup>	0.3 ± 0.0 (1.9) <sup>a</sup>	97.3 ± 2.9 (6.3) <sup>a</sup>
homofarnesol	34.8 ± 1.4	13.0 ± 1.0	4.4 ± 0.5
homofarnesoic acid	7.7 ± 0.2	12.5 ± 1.0	2.3 ± 0.3
nerolidol	0.5 ± 0.0 (3.4) <sup>b</sup>	0.2 ± 0.0 (1.9) <sup>b</sup>	1.4 ± 0.8 (1.8) <sup>b</sup>
geranylacetone	1.7 ± 0.08	0.7 ± 0.1	1.1 ± 0.1
farnesylacetone	0.2 ± 0.0	1.6 ± 0.1	0.7 ± 0.1

## 6 Discussion

### 6.1 Squalene-hopene cyclases: cloning, expression, enzyme preparation and biotransformations

The cloning of the SHCs into the expression strain and the functional expression of the enzymes could be confirmed by biotransformation experiments with whole cells. First conversion experiments were carried out with three model substrates containing different carbon chain lengths and functional groups: squalene, homofarnesol and (S)-citronellal.

#### 6.1.1 Biotransformations with whole cells

Using a low cell density of  $OD_{600} = 10$  and a long incubation time of 20 h (shown in Fig. 6.1 A), almost full conversion of squalene was obtained with *AacSHC*, while both *ZmoSHC1* and *ZmoSHC2* catalyzed the cyclization of the natural substrate squalene in much lower rates. In contrast to this, with an 8-fold higher cell density of  $OD_{600} = 80$  and a 4-fold shorter incubation time of 5 h (Fig. 6.1 B) there was almost no squalene conversion detected with all of the three enzymes. This presents a confirmation for works previously reporting that *AacSHC* expressed in *E. coli* showed activity towards squalene using the membrane fraction of the cells but not applied as whole cell biocatalysts. As *E. coli* does not synthesize squalene it was assumed that the membranes are not permeable for this substrate.<sup>60,89</sup>

A completely different observation was made for the biotransformations with the smallest substrate, (S)-citronellal. This substrate was accepted by *ZmoSHC1* and *AacSHC*, but the rates differed depending on the setup. In contrast to squalene, a much better citronellal conversion was observed using a higher cell density of  $OD_{600} = 80$  and a shorter incubation time of 5 h.

Remarkably, high homofarnesol conversions were obtained using cells expressing *ZmoSHC1* in both setups, showing that *ZmoSHC1* is much more capable to convert the  $C_{16}$  alcohol homofarnesol than the natural substrate squalene, yielding in much higher biotransformation rates. In addition to this, the activity towards citronellal was shown to be considerably higher than towards squalene in both systems.

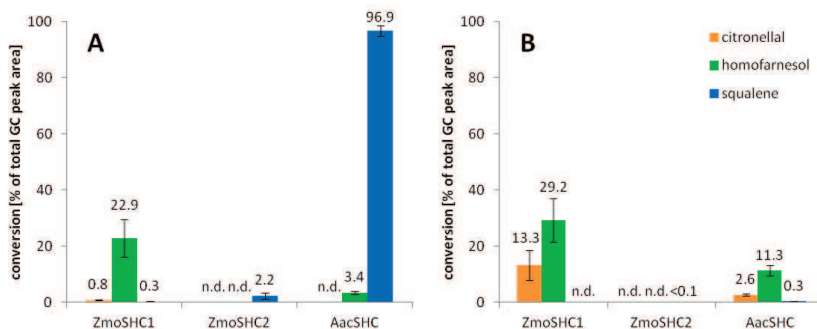


**Fig. 6.1:** Biotransformations with cells expressing *ZmoSHC1*, *ZmoSHC2* and *AacSHC*. The biotransformations were carried out A) for 20 h using a cell density of  $OD_{600} = 10$  and B) for 5 h using a cell density of  $OD_{600} = 80$ . The results are given as percentage of the product peaks in relation to the total GC peak areas. Conversions of (*S*)-citronellal are shown as orange, homofarnesol as green and squalene as blue bars, respectively.

The results obtained from these whole cell experiments demonstrated the ability of the SHCs to catalyze the cyclization of unnatural substrates. The use of whole cells as biocatalysts provides several advantages, especially the easy and fast handling makes this procedure very attractive, and the experiments are useful for a fast estimation of the SHCs' capabilities to catalyze the cyclization of different substrates. However, there were also several drawbacks using this system. As shown in Fig. 5.2, the expressions between different SHCs varied regarding their content of enzyme and, thus, the biotransformations did not result in reproducible biotransformation data, even for different expressions of the same enzyme.

In addition to this, the different properties of the substrates in these systems have to be considered. The permeability of the *E. coli* cell membranes differs between the substrates. The *E. coli* cells are not permeable for squalene and conversion was only observed after long incubation times when cell lysis and the resulting access of the substrate to the membrane-bound enzymes is possible. However, it is difficult to estimate when the cell lysis starts during the incubation, since there are several influencing parameters, such as (i) the cell density, (ii) the treatment of the cells during preparation like freezing and thawing, or (iii) the type and concentration of detergent added to the system. Especially (iii) is expected to have a strong influence. The present detergent can affect the cell lysis and the solubilization of the SHCs from the membranes. It can also have a strong effect on the access of the

substrates to the enzyme since the emulsification of the different substrates depends on the present surfactant.

In contrast to the observations made with squalene, the smaller substrates, such as citronellal, can pass *E. coli* cell membranes and obtain a better access to the enzyme resulting in higher conversion rates. Thus, the biotransformation rates obtained from these experiments represent the biocatalytic activities of the different SHCs but are strongly influenced by other parameters, such as expression, enzyme content and accessibility of the substrates to the enzyme.

A reproducible system was generated enabling the comparison of both the conversion of different substrates with the same enzyme and the different enzymes' activities towards the same substrate.

### 6.1.2 Biotransformations with partially purified SHCs

Considering the results obtained from biotransformation experiments using whole cells expressing SHCs as biocatalysts, a protocol for biotransformations with partially purified SHCs was elaborated. The obtained fractions of partially purified SHCs had constant protein concentrations of 3.5 to 6.0 mg/mL and a SHC content of 90-95 % of the total protein.

As shown in Fig. 6.6, the experiments with the three model substrates, using 0.1 mg/mL SHCs, led to similar patterns as seen for whole cell biotransformations using the setup A ( $OD_{600} = 10$ , 20 h, Fig. 6.1 A). This coincides with the observations made before: *ZmoSHC1* typically prefers other substrates rather than its natural substrate squalene. As also already seen before, again *ZmoSHC2* is simply converting squalene at a low rate.

The advantage of using partially purified SHCs for biotransformations in comparison to whole cell biocatalysis is the comparability of both different enzymes and substrates. As the cyclases are solubilized from the membranes, the differences in permeability for the substrates cannot influence the conversion rates any longer. Thus, the results obtained from these experiments enabled a better comparison of the substrate activities. In addition, the rates obtained from these biotransformations with the three model substrates were reproducible.



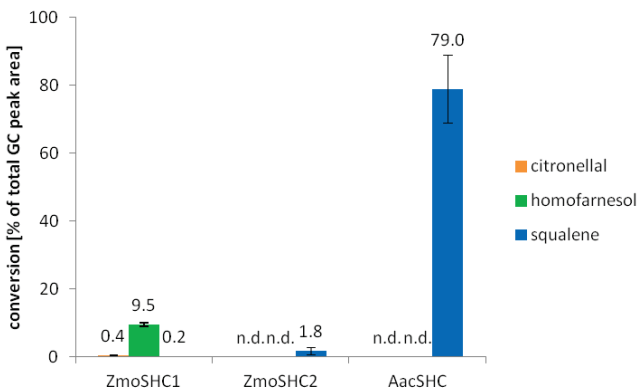


**Fig. 6.2:** Biotransformations of 10 mM of substrate with 0.1 mg/mL partially purified *ZmoSHC1*, *ZmoSHC2* and *AacSHC* carried out for 20 h. The results are given as percentage of the product peaks in relation to the total GC peak areas. Conversions of (*S*)-citronellal are shown as yellow, homofarnesol as green and squalene as blue bars, respectively.

Unfortunately, a loss of enzyme during partial purification has been determined (Fig. 5.3, Fig. 5.4). Another drawback is the permanent incorporation of detergent in the enzyme solution, as it had been shown that detergents influence the enzymatic activity of the biocatalyst towards different substrates.<sup>147,148</sup> It also has to be considered that the interactions of detergent molecules and substrates of varying hydrophobicity are different and the emulsions of the hydrophobic substrates in the aqueous system are unequal. Thus, the accessibilities of the substrates to the enzymes' active sites are influenced.

### 6.1.3 Stability experiments

Experiments regarding the biocatalytic stability revealed that *ZmoSHC1*, used as whole cell biocatalyst, exhibit a good stability at 30°C incubation temperature over four days (Fig. 5.6). Higher temperatures caused a loss of activity. The activity of partially purified *ZmoSHC1* showed highest activity combined with good stability at 30°C and 37°C (Fig. 5.7). Whereas the whole cell system was not active at all at 42°C, the partially purified *ZmoSHC1* displayed a good activity in the first 24 h of the experiment. However, the activity decreased significantly with longer pre-incubation at 42°C. For this reasoning, biotransformations were performed at 30°C using *ZmoSHC1* as biocatalyst either in a whole cell system or as partially purified cyclase.

Additional experiments carried out at 30°C with partially purified *Zmo*SHC1 and with cells expressing *Zmo*SHC1 demonstrated activity towards homofarnesol conversion over 96 h. However, low activity was observed in the first 12 h of the experiments.

The low conversion without pre-incubation using partially purified *Zmo*SHC1 could be due to the hydrophobicity of homofarnesol. The required emulgation in the aqueous system could be improved with increased pre-incubation time of the enzyme and the detergent at 30°C and, thus, the substrate's access to the enzyme is improved. Here it has to be considered, if different conditions could improve the conversion rates right from the beginning of the experiments. The selection of an appropriate detergent of the right concentration could be crucial to enhance the formation of the desired product. Thus, the careful selection of the surfactant should be studied in more detail.

In addition to these discussed explanations, the reason for the low activity of the whole cell biotransformation setup without any or just 12 h of pre-incubation could be traced to the permeability of the *E. coli* cell membrane. As already mentioned in the previous chapters, the *E. coli* cell membrane is not permeable for squalene, and thus, the biotransformation of squalene with cells expressing *Aac*SHC could only be observed after several hours of incubation, due to the cell lysis leading to access for squalene to the enzyme. Using homofarnesol as a substrate in the whole cell biotransformations, conversion was observed after shorter time periods and it was assumed that homofarnesol was able to pass the cell membrane. However, in direct comparison, this conclusion has to be corrected, as the results shown in Fig. 5.8 exhibit an enhanced homofarnesol conversion after a longer pre-incubation time and expected cell lysis. Thus, it is assumed that homofarnesol can pass the cell membrane but its access to the active site and the conversion is facilitated when cell lysis has started.

In another experiment, different densities of cells expressing *Zmo*SHC1 were used and the conversion of homofarnesol during a period of one to five days was determined. The highest activity was observed after 24 h. With longer incubation time, the activity decreased. However, here it has to be considered that after a certain time the substrate concentration was lower than in the beginning of the experiment and, thus, the conversion rates can decrease. One should also take into account the fact that the product ambroxan could have inhibiting effects on the cyclase. The analysis of this possible inhibition was carried out and the discussion will follow in the next chapters.

### 6.1.4 Substrate and product inhibition

The biotransformation rates when both squalene and homofarnesol were added to cells expressing *ZmoSHC1* and *AacSHC* or partially purified SHCs were tested, showing that the activity of *ZmoSHC1* towards squalene was increased when homofarnesol was added to the system (Fig. 6.3). An explanation for these enhanced squalene conversions could be due to the amphiphilic properties of homofarnesol. As it contains both a non-polar carbon chain and a polar hydroxyl-group, homofarnesol could act as co-surfactant and improve the emulsification of the hydrophobic squalene. Regarding the two setups using cells of a different density, it was remarkable that the conversion of squalene was enhanced with cells of lower cell density (Fig. 5.10). This can be explained by differences in cell lysis enabling the access of squalene to the active site of *ZmoSHC1* as previously discussed. Ambroxan addition did not affect the activity of *ZmoSHC1* towards squalene.

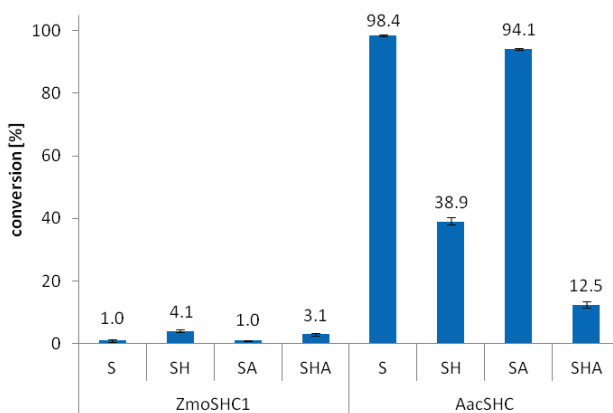


**Fig. 6.3: Conversion of squalene using 0.1 mg/mL of partially purified *ZmoSHC1* / *AacSHC* and the following substrates: S: 2 mM squalene, SH: 2 mM squalene + 2 mM homofarnesol, SA: 2 mM squalene + 2 mM ambroxan, SHA: 2 mM squalene + 2 mM homofarnesol + 2 mM ambroxan; the results are shown as percentage of product GC peak area of the sum of GC peak areas of both substrates and products.**

The activity of *ZmoSHC1* towards homofarnesol was decreased when squalene or especially ambroxan were present in the system (Fig. 6.4).

Therefore, the inhibiting effect of the product ambroxan formed from homofarnesol was investigated in more detail. Different homofarnesol concentrations were incubated with

0.1 mg/mL partially purified *ZmoSHC1* and the conversions were determined. Low concentrations of homofarnesol (0.1-1 mM) were converted almost completely (Fig. 5.11 A). However, when ambroxan reached a certain concentration, no more product was formed (Fig. 5.11 B). That means that increasing substrate concentrations yielded in lower conversion rates. The results accompany the observations made before: Ambroxan is inhibiting the activity of *ZmoSHC1* when it reaches a certain product concentration.

Taking these results into account, the biotransformation protocol was changed to an increased enzyme concentration of 0.35 mg/mL instead of 0.1 mg/mL for later experiments (see 5.3 and 5.4). Using this enhanced ratio of enzyme to substrate, the inhibiting concentration of ambroxan was not reached during the biotransformation time and, importantly, there was still conversion detected with the less active enzyme-substrate combinations. Using this enzyme concentration, comparable conversion rates for all of the tested substrates were generated.

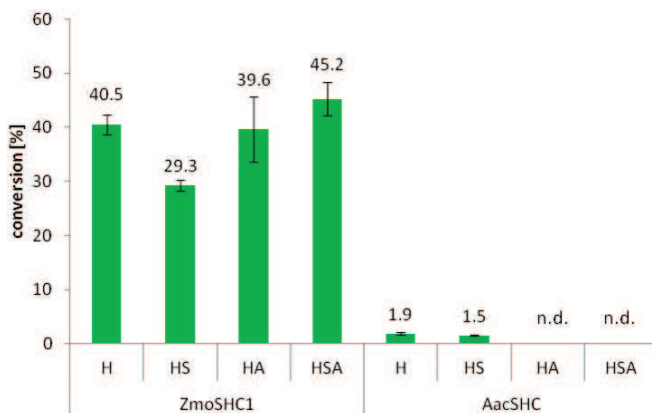


**Fig. 6.4:** Conversion of homofarnesol using 0.1 mg/mL of partially purified *ZmoSHC1* / *AacSHC* and the following substrates: H: 2 mM homofarnesol, HS: 2 mM squalene + 2 mM homofarnesol, HA: 2 mM homofarnesol + 2 mM ambroxan, HSA: 2 mM squalene + 2 mM homofarnesol + 2 mM ambroxan; the results are shown as percentage of product GC peak area of the sum of GC peak areas of both substrates and products. For approaches with ambroxan addition, the concentration of the additional ambroxan was subtracted. n.d.: no conversion detected.

Different results were obtained from biotransformations carried out with *AacSHC* as biocatalyst. The activity of *AacSHC* towards squalene was strongly decreased when

homofarnesol was added to the system (Fig. 6.3). Addition of ambroxan did not influence squalene conversion catalyzed by *AacSHC*.

While the addition of squalene had no influence on homofarnesol conversion, the activity of *AacSHC* towards homofarnesol was completely lost when ambroxan was added to the system (Fig. 6.4). This result goes along with observations made by Neumann *et al.* in 1986, in which they already reported that ambroxan showed inhibitory effects on the homofarnesol cyclization catalyzed by *AacSHC*.<sup>16</sup>

However, there are certain facts that have to be discussed in the context with these observations, revealing that not only the presence of additional products or substrates influences the activity of an enzyme. The solubility and emulsion of the substrates is different and has to be considered, as the experiments were carried out in aqueous environment. As already mentioned above, the reason for enhanced squalene conversions under presence of homofarnesol could be the improved emulsion of squalene providing an enhanced access of the non-polar substrate to the enzyme in the aqueous environment. In addition to this, also the other components could influence micelle formation, emulsification and therefore access and conversion. It also has to be considered, that the detergent present in the reaction mixture could affect the conversions. In the discussed experiments, 0.2 % of Triton X-100 was present in all samples. Both the concentration of the surfactant and the detergent itself can be beneficial or not for the different reactions. Consequently, additional experiments have to be carried out in the future in order to obtain a better understanding of the surfactant's effects on the different biotransformations and to generate optimal conditions for each substrate.

### 6.1.5 Internal standard experiments

It was shown that the addition of 1-decanol prior to biotransformation affects the conversion rates significantly and cannot be used in this way. Adding 1-decanol to homofarnesol conversion assays using partially purified *ZmoSHC1* as biocatalyst caused a decrease of conversion from 15.9 % to 8.0 % and squalene conversion catalyzed by partially purified *AacSHC* was reduced from 97.8 % to 31.8 %. Based on these results it was assumed that 1-decanol shows remarkable inhibiting effects on both *ZmoSHC1* and *AacSHC*. Consequently, it was decided to use the internal standard just as an extraction standard by adding a certain amount of 1-decanol to the samples after incubation but prior to extraction

and analysis. Using the internal standard in this way, quantification of substrates and products was possible.

### 6.1.6 pH Studies

Testing the activity of partially purified *ZmoSHC1*, *ZmoSHC2* and *AacSHC* towards the three model substrates squalene, homofarnesol and (*S*)-citronellal at pH 4.5, 5.0 and 6.0, the best conversion of homofarnesol and squalene was observed at pH 6.0 (Table 5.6). Strongly reduced conversion could be detected at pH 4.5. In contrast to this, the conversion of (*S*)-citronellal, which was only observed using partially purified *ZmoSHC1* under the given conditions, was comparably low with all of the three pH values. However, at pH 5.0 and 6.0, reduction of (*S*)-citronellal to citronellol was observed (Fig. 5.14). It is suggested that alcohol dehydrogenases from the *E. coli* expression strain are active at higher pH values, thus reducing the aldehyde to the alcohol product.

Taking these results into account, the subsequent reactions were carried out at pH 6.0. However, citronellal biotransformations were performed at pH 4.5 due to the increased reduction rate of citronellal to citronellol at higher pH values.

## 6.2 Substrate specificity of SHCs

Previous studies indicated that the SHCs bear the potential to convert various truncated squalene analogs to cyclic products. This high catalytic flexibility was furthermore emphasized by conversion of homofarnesol with *AacSHC*, where the ene-functionality relevant for termination of the cyclization reaction was replaced by a hydroxy-group forming a cyclic ether as product.. Therefore, it was decided to explore this diversity by testing new substrates which contain different carbon chain lengths and provide different functional groups serving as new nucleophiles (Fig. 6.5). Other decisive arguments that were taken into account were the possible applications of the generated products and the availability of the substrates.

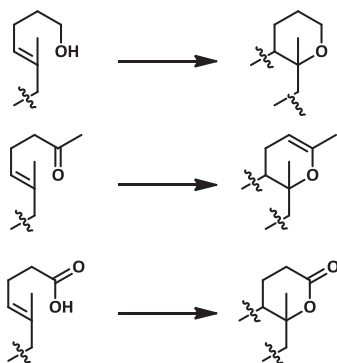


Fig. 6.5: Functional groups selected for replacement of the ene-functionality of the substrates taking part in the termination step of the cyclization reactions.

Outgoing from the results obtained by Neumann *et al.*, where homofarnesol cyclization to ambroxan was performed with AacSHC, the substrates were expected to be cyclized analogously. The suggested mechanism includes protonation of a C=C double bond by the catalytic aspartate in the active site, stereospecific cyclization forming a final carbocation and a termination step integrating an oxygen containing group in the last cycle of the formed product. This mechanism is displayed in Fig. 6.6.

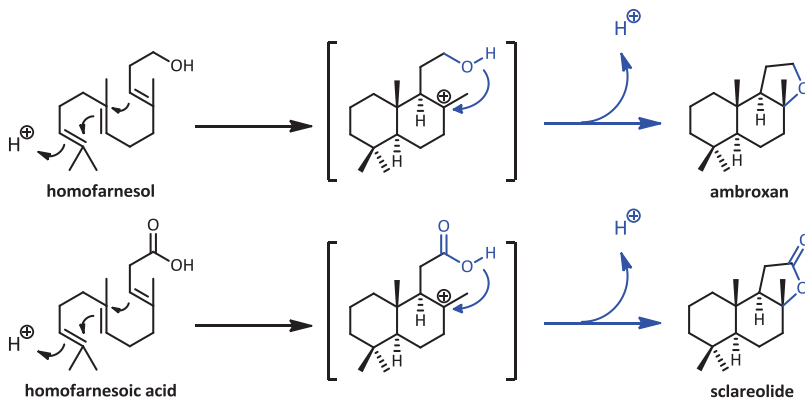


Fig. 6.6: Suggested mechanism for the cyclizations of homofarnesol and homofarnesoic acid to ambroxan and sclareolide using SHCs. After initial protonation of the C=C-double bond, the stereospecific cyclization of the linear substrates occurs forming a final carbocation. The positive charge is quenched by intramolecular nucleophilic attack of the alcohol- / carboxy-group.

Taking these considerations into account, several substrates were selected, tested and the activities of *ZmoSHC1*, *ZmoSHC2* and *AacSHC* towards them were compared to the activities of these enzymes towards their natural substrate squalene. Terpenoids containing 10 to 18 carbon atoms and different functional groups such as hydroxy-, carboxy-, keto- and carbonyl-groups were selected as new substrates, since they were promising precursors for formation of cyclic products with new properties.

### **6.3 Comparison of the substrate specificity of *ZmoSHC1*, *ZmoSHC2* and *AacSHC***

Under the given conditions, both partially purified *ZmoSHC1* and *AacSHC* exhibited activity towards all of the mentioned substrates, namely geranylacetone, nerolidol, homofarnesoic acid, homofarnesol and farnesylacetone as well as towards the natural substrate squalene (Fig. 5.22, Table 5.8). In contrast to this, *ZmoSHC2* showed activity just towards squalene and very low activity towards farnesylacetone.

Regarding the conversion rates obtained for *ZmoSHC1* and *AacSHC*, there are remarkable differences to be discussed in detail. While *AacSHC* showed the highest activity towards the natural substrate squalene, which was converted almost completely under the given reaction conditions, much lower rates were detected for all of the other substrates, which were converted in rates of less than 5 %. This behavior was expected, as the cyclization of squalene is the natural reaction catalyzed by the SHCs and catalysis of all of the other substrates can be traced to the enzyme's flexibility towards other substrates. In contrast to this, *ZmoSHC1* exhibited a completely different activity pattern. While conversion of squalene was determined as 0.8 %, the C<sub>16</sub> alcohol homofarnesol was converted best with 34.8 %, which is more than 40-fold higher than the conversion of squalene. Also the corresponding homofarnesoic acid was converted much better than squalene, exhibiting an almost 10-fold higher conversion rate of 7.7 %. Geranylacetone was converted about twice as well as squalene. Just the tertiary alcohol nerolidol and the C<sub>18</sub> ketone farnesylacetone were converted in lower rates of less than 1 %, respectively.

These results are visualized in Fig. 5.22, showing the "activity patterns" of the SHCs towards the different substrates. Comparing the relative biotransformation rates, the difference



between *ZmoSHC1*, *ZmoSHC2* and *AacSHC* substrate specificity is even more obvious, as shown in Fig. 6.7.

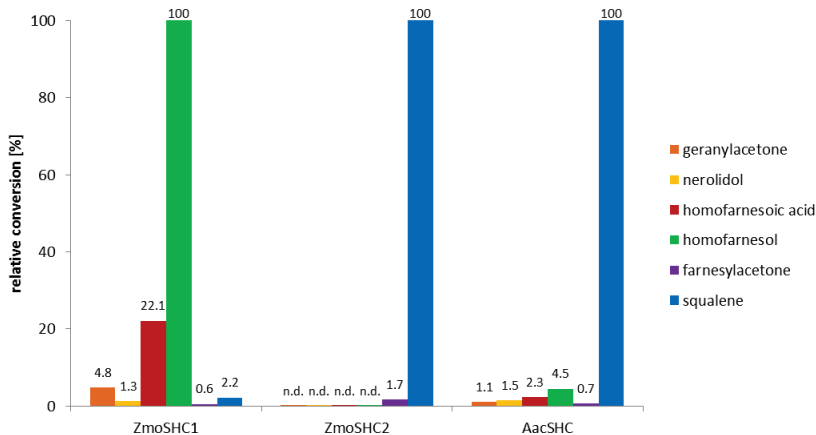


**Fig. 6.7: Conversion rates in relation to the preferred substrate (homofarnesol for *ZmoSHC1* and squalene for *ZmoSHC2* and *AacSHC*).**

From these results the question arises, why *ZmoSHC1* exhibits such a different substrate activity pattern compared to the other SHCs and why the activity of this enzyme towards its natural substrate squalene is so low. As *Zymomonas mobilis* is known to be one of the best hopanoid producing bacteria found in nature, we have to reflect how these hopanoids are generated and if *ZmoSHC1* is involved in the hopanoid biosynthesis or if this enzyme is responsible for the catalysis of other reactions. It also has to be considered which reactions could be catalyzed in nature by this enzyme as well as if there are other substrates towards which *ZmoSHC1* shows an even higher activity than towards homofarnesol.

One explanation for differences in the activity towards different substrates can be found looking at the genetic surroundings of *ZmoSHC1* and *ZmoSHC2* genes which are completely different (Fig. 6.8).<sup>270</sup> While the gene encoding for *ZmoSHC2* shows several genes with connection to the hopanoid biosynthesis in its proximity, the *ZmoSHC1* gene does not have any neighboring genes related to the squalene metabolism. The genetic surrounding of *AacSHC* is similar to that from *ZmoSHC2* as there are various genes encoding for enzymes connected to the hopanoid metabolism.

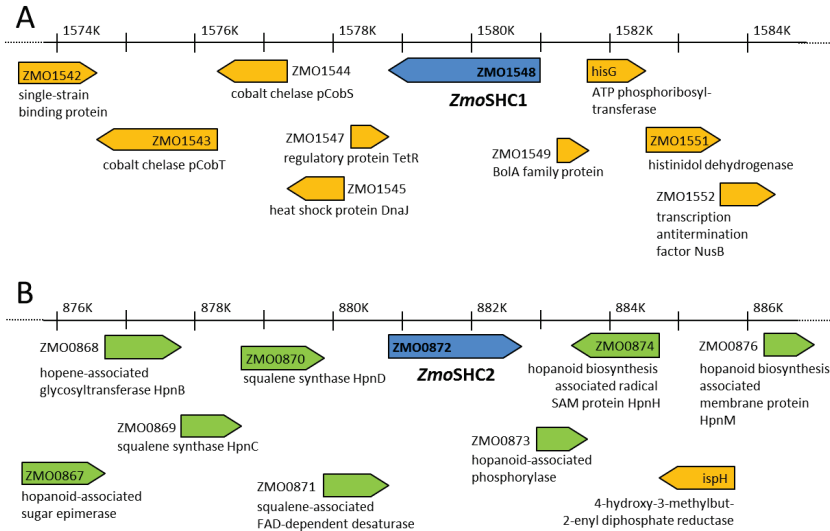


**Fig. 6.8: Genomic regions surrounding of *ZmoSHC1* (A) and *ZmoSHC2* (B) (blue): genes associated to the hopene metabolism are coloured in green, genes not associated to the hopene metabolism in yellow.**

These observations shown in Fig. 6.8 emphasize the hypothesis that *ZmoSHC1* is most probably not a squalene-hopene cyclase, rather an enzyme catalyzing the cyclization of other terpenoids. However, in comparison to *AacSHC*, *ZmoSHC2* exhibited a very low activity towards squalene. This is surprising, since *ZmoSHC2* in difference to *ZmoSHC1* was almost exclusively showing conversion with squalene besides a low conversion with farnesylacetone. Also the genetic surrounding of this enzyme unveils a hopanoid-biosynthesis connected genetic neighborhood, similar to the gene encoding for *AacSHC*. The low activity can probably be explained as the conditions for expression, partial purification and substrate conversion were optimized for *ZmoSHC1* and *AacSHC* but not for *ZmoSHC2*, where the standard conditions of *ZmoSHC1* handling were assumed. In conclusion, the genetic surrounding of *ZmoSHC1* indicates that it might be not a real squalene-hopene cyclase and it could be assumed that *ZmoSHC1* belongs to another group of isoprenoid cyclases.

Besides the different genetic surroundings of *ZmoSHC1* and the other two SHCs there is another evident difference to mention regarding the hydrophobicity of the accepted

substrates. The highest activity of *AacSHC* and *ZmoSHC2* was shown with squalene, the most hydrophobic substrate. In contrast to this, *ZmoSHC1* displayed higher activity towards the conversion of other, less hydrophobic substrates. Thus, another approach to explain the differences between *ZmoSHC1* and *AacSHC* could be found by considering the differences in polarity of the substrates. The partition coefficients ( $\log P$ ) were determined (9.10.5) and give comparable information about the hydrophobicities of the substrates (Table 6.1).<sup>271–273</sup>

**Table 6.1: Overview of the substrates used for biotransformations, the corresponding  $\log P$  values, the number of carbon atoms of the substrates and the conversion rates with *ZmoSHC1* and *AacSHC*. The values given for conversions are shown as percentage of the product concentration in respect to the total concentration of both substrates and products calculated with ISTD1 calibration.**

substrate	$\log P$	carbon chain length	conversion [%] with	
			<i>ZmoSHC1</i>	<i>AacSHC</i>
squalene	$10.60 \pm 2.34$	30	$0.8 \pm 0.1$	$97.3 \pm 2.9$
farnesylacetone	$5.58 \pm 1.04$	18	$0.2 \pm 0.0$	$0.7 \pm 0.1$
homofarnesol	$5.01 \pm 1.02$	16	$34.8 \pm 1.4$	$4.4 \pm 0.5$
homofarnesoic acid	$4.91 \pm 1.02$	16	$7.7 \pm 0.2$	$2.3 \pm 0.3$
nerolidol	$4.67 \pm 0.57$	15	$0.5 \pm 0.0$	$1.4 \pm 0.1$
geranylacetone	$4.00 \pm 0.53$	13	$1.7 \pm 0.1$	$1.1 \pm 0.1$

In previous works dealing with the crystal structure of *AacSHC* and the positions of crucial amino acids in the active site it was confirmed that the entrance to active cavity is hydrophobic.<sup>58</sup> Thus, it is not surprising that the most hydrophobic substrate, squalene, is the one which is converted best by *AacSHC*. The  $\log P$  values displayed in Table 6.1 show that the gap between the polarities of the most hydrophobic substrate, squalene, and the less hydrophobic one, geranylacetone, is large and the  $\log P$  values correlate with the conversion rates determined for *AacSHC*. This is visualized in Fig. 6.9 (red areas). That means that the more polar the substrate the less conversion with *AacSHC* could be observed. One exception constitutes farnesylacetone which was converted much worse than homofarnesol. *ZmoSHC1* however exhibits a different behavior (Fig. 6.9, blue areas). With *ZmoSHC1* as biocatalyst, no correlation between partition coefficients and activities can be found. This significant difference again indicates that *ZmoSHC1* could constitute an enzyme catalyzing a different reaction in nature and that it is not in charge of the biosynthesis of the hydrophobic membrane constituents hopene and hopanol but for something else in its original host.

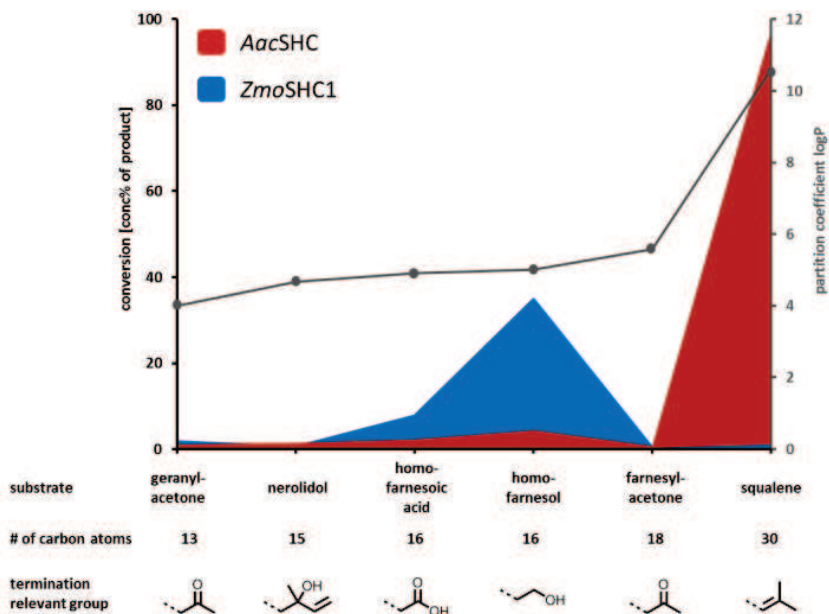


Fig. 6.9: Comparison of the enzymatic activities of ZmoSHC1 and AacSHC towards the different substrates arranged by substrate carbon chain lengths. The blue curve represents the conversion with ZmoSHC1, the red curve the conversion with AacSHC as enzyme. The areas refer to the left y-axis, showing conversion rates. The gray line, referring to the right y-axis, is showing the log P values for the different substrates.

As already mentioned, in the active site of AacSHC there were 36 amino acids defined as being in direct contact with the substrate analog.<sup>10</sup> In order to find another explanation for the discussed differences in substrate activity, the corresponding amino acids in ZmoSHC1 and ZmoSHC2 were defined by multisequence alignment, as highlighted in Fig. 3.22. The amino acids are listed in Table 6.2. Comparing these residues in ZmoSHC1 and AacSHC, 30 of the 36 discussed positions hold the same amino acids, while just six positions show differences. In contrast, comparison of ZmoSHC1 with ZmoSHC2 and AacSHC with ZmoSHC2 reveals 23 corresponding amino acids besides 13 non-matching residues. However, it is difficult to explain the different substrate activities of ZmoSHC1 and AacSHC observing the high correspondence of the crucial amino acids. Three of the six differing amino acids are quite similar regarding their polarities (ZmoSHC1\_V88 vs AacSHC\_L36, ZmoSHC1\_M227 vs AacSHC\_V174, ZmoSHC1\_T369 vs AacSHC\_S307). Subsequently, there are just three amino

acid residues in the active sites of *ZmoSHC1* and *AacSHC* which could offer an explanation, namely the residues E429, F486 and S506 (for *ZmoSHC1*; corresponding Q366, Y420 and V440 for *AacSHC* numbering). In order to explore the influence of at least one of these positions, the couple *ZmoSHC1\_F486* vs *AacSHC\_Y420* was selected for mutational analysis (see 5.4.1).

**Table 6.2: Amino acid residues in the active sites of *ZmoSHC1*, *ZmoSHC2* and *AacSHC*; the amino acids of *AacSHC* have shown to be in direct interaction with the substrate analog azasqualene in the crystallized enzyme; the corresponding amino acids of *ZmoSHC1* and *ZmoSHC2* were associated by sequence alignment. Very hydrophobic amino acids are marked in blue, hydrophobic amino acids in green, neutral amino acids in orange and hydrophilic amino acids in red.<sup>10,274</sup>**

<i>ZmoSHC1</i>		<i>ZmoSHC2</i>		<i>AacSHC</i>		<i>ZmoSHC1</i>		<i>ZmoSHC2</i>		<i>AacSHC</i>	
aa	pos	aa	pos	aa	pos	aa	pos	aa	pos	aa	pos
V	88	L	43	L	36	D	439	D	392	D	376
M	94	I	49	M	42	D	440	D	393	D	377
R	180	N	135	R	127	A	485	A	437	A	419
F	182	F	137	F	129	F	486	F	438	Y	420
W	222	W	177	W	169	F	500	F	452	F	434
A	223	A	178	A	170	C	501	A	453	C	435
T	226	V	181	T	173	F	503	H	455	F	437
M	227	L	182	V	174	E	505	A	457	E	439
G	319	G	268	G	259	S	506	L	458	V	440
I	321	I	270	I	261	V	514	V	466	V	448
Q	322	Y	271	Q	262	W	555	W	507	W	489
P	323	P	272	P	263	Y	561	Y	513	Y	495
A	368	P	321	A	306	G	667	G	619	G	600
T	369	C	322	S	307	F	668	F	620	F	601
W	374	W	327	W	312	F	698	F	624	F	605
F	428	F	381	F	365	L	700	L	626	L	607
E	429	Q	382	Q	366	Y	702	Y	628	Y	609
D	437	D	390	D	374	Y	705	Y	631	Y	612

Concerning the distribution of hydrophobic and hydrophilic amino acids among the 36 relevant positions in the active sites of the three SHCs there is no significant difference. The polarity tendencies of the amino acids was classified into the four groups very hydrophobic, hydrophobic, neutral and hydrophilic according to literature data and highlighted in different colors in Table 6.2.<sup>274</sup> However, also the overall differences in the polarities of the amino

acids in the relevant positions are too small to generate a theory which explains the different properties of the SHCs.

It is surprising that the 36 amino acids which were defined to be very important for the catalysis of the squalene cyclization show so few differences between *Aac*SHC and *Zmo*SHC1. However, it has to be considered, that these amino acids in *Zmo*SHC1 were just defined by multisequence alignment. Since the crystal structure of *Zmo*SHC1 remains unknown, it is also possible that the mentioned relevant residues are positioned in a different manner than in *Aac*SHC. Thus, the active cavity of *Zmo*SHC1 could exhibit a completely different surrounding for the substrate. In conclusion, without knowledge of the three-dimensional structure of *Zmo*SHC1 it is very difficult to explain its remarkable shift in substrate specificity towards the unnatural substrate homofarnesol.

### 6.3.1 Enhanced conversions

Homofarnesol was converted to ambroxan, and this reaction is interesting as the product ambroxan is a valuable flavor compound. Furthermore, the cyclization of citronellal to isopulegol is remarkable, as this product can be reduced to the smelling compound menthol.

In order to increase the conversion rates forming these products, the density of cells expressing *Zmo*SHC1 was increased. The rates could be enhanced up to 16.4 % for isopulegol formation from (*S*)-citronellal and 50.3 % for the conversion of homofarnesol to the corresponding cyclic product ambroxan. However, squalene conversion remained low under these conditions, displaying the low activity of *Zmo*SHC1 again. Another important fact for the low activity is the supposed low access of squalene to the active cavity of *Zmo*SHC1, as this substrate cannot pass the *E. coli* cell membrane.

Furthermore, also the novel reactions shown in the expanded substrate spectrum catalyzed by the SHCs are of economic interest. The products sclareolide, sclareoloxide, hexahydrochromene and caparrapioxide are important intermediates in synthesis of fragrances or other valuable compounds.

Using a higher concentration of partially purified *Zmo*SHC1 of 4 mg/mL instead of 0.35 mg/mL exhibited higher conversion rates with all of the substrates. However, it has to be taken into account that the increase of conversion differed between the substrates (Fig. 5.23). Highest increase of conversion was shown for geranylacetone, which was increased

14-fold. In contrast to this, the lowest enhancement (2-fold) was shown for the conversion of nerolidol.

These differences can be traced back to different detergent concentrations used in these experiments. The biotransformations with 0.35 mg/mL of enzyme were carried out under presence of 0.2 % of Triton X-100, since the solutions of partially purified SHCs were diluted prior to application. In contrast to this, the partially purified *ZmoSHC1* used for the enhanced conversion was not diluted and contained 1 % Triton X-100. It is supposed that different amounts of tensides could influence the conversions, as the emulsion of enzyme and substrates are influenced and, thus, the access of the substrates to the active site of the enzyme can differ.

In conclusion, *ZmoSHC1* is a not efficient catalyst for the cyclization of squalene to hopene and hopanol, but a much more effective catalyst for ambroxan formation from homofarnesol.

### 6.3.2 Limits of substrate specificity

Several substrates were expected to be cyclized by the SHCs but did not show any biotransformation product under the applied reaction conditions (Table 5.7). Remarkably, substrates of shorter chain lengths were not converted, like linalool, geraniol or geranic acid, while larger homologs were accepted as substrates. These observations go along with the assumption made by Hoshino and coworkers, who reported that substrates of short C-chain lengths cannot be accepted as substrates by the triterpene cyclases.<sup>17</sup> The SHCs' missing abilities to catalyze the cyclizations of these C<sub>10</sub> substrates can have the following reasons: (i) The substrates are more hydrophilic than the substrates which were shown to be accepted and, thus, it is possible that they cannot enter the hydrophobic active cavity. (ii) They might enter the channel to the active site but get bound to another position and do not reach the catalytic Brønsted acid. (iii) It is possible that the substrates reach the catalytic aspartate but cannot be stabilized in a conformation enabling the cyclization reaction due to their small size. Modeling experiments with *AacSHC* and selection of positions for directed mutagenesis could enable the conversion of small substrates. However, this remains difficult for *ZmoSHC1*, as the crystal structure is unknown and definition of amino acid residues for mutagenesis is not possible.

Another observation was the inactivity of the SHCs towards cyclization of pseudoionone or citral, while the substrates geranylacetone and citronellal, which just differ by the absence of a C=C-double bond, were accepted. The explanation for this could be found right in the presence of this additional C=C-double bond which prevents an active conformation of the substrate and, thus, biotransformation is not possible (Fig. 6.10).

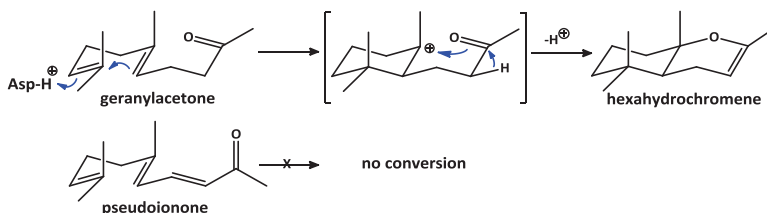


**Fig. 6.10: Suggested mechanism for geranylacetone cyclization. Pseudoionone cannot adopt a conformation enabling the cyclization.**

Citronellal represents the only monoterpene which was accepted and cyclized. However, this substrate differs from the other mentioned substrates by the presence of an aldehyde group replacing the ene-functionality at the initiation site of the substrate. A reason for catalysis of this reaction can be the fact that protonation of the C=O double is facilitated in comparison to C=C protonation. It is also possible that citronellal is activated by water addition and cyclization is facilitated, as shown in Fig. 6.11.

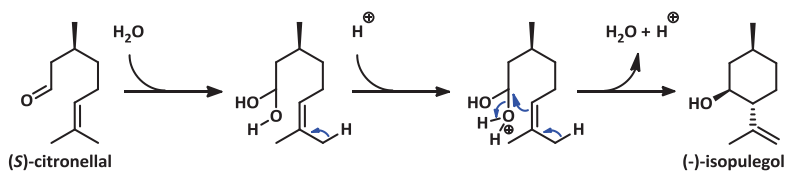


**Fig. 6.11: Supposed cyclization of citronellal after water addition.**

## 6.4 Directed mutagenesis

### 6.4.1 Selection of spots for single mutants and screening

Mutations of single amino acids can be crucial for changing the properties of an enzyme, its substrate acceptance and activity. Several positions were expected to have an influence on the substrate specificity of the SHCs. In scope of the present work, mutational analysis was



performed for position F486 (referring to the numbering for *ZmoSHC1*), which was shown to be a highly conserved residue.<sup>10,275</sup> In 96 % of 325 aligned SHC sequences phenylalanine was conserved. In contrast to this, *AacSHC* represents one of the SHCs not harboring phenylalanine but tyrosine at this position (Y420). In order to investigate the influence of this position on the specificity and activity of the cyclases, two mutants were tested. For *ZmoSHC1*, the phenylalanine residue was changed to tyrosine, expecting to increase the conversion of squalene. For *AacSHC*, the corresponding tyrosine was replaced by a cysteine residue, as previous works by Siedenburg *et al.* had indicated that a cysteine residue at this position could shift the substrate activity towards shorter chain substrates.<sup>275,276</sup>

In comparison to the wildtype, the single mutant of *ZmoSHC1*, *ZmoSHC1\_F486Y*, showed several differences regarding its activity towards the different substrates. It was expected that the conversion rates would match the rates observed for *AacSHC*, as the amino acid F486 has been replaced for a tyrosine, which corresponds to the amino acid at this position in *AacSHC* (Y420). Regarding the biotransformation of squalene, where an increase was expected, no difference in comparison to *ZmoSHC1* wildtype could be observed for the mutant. The conversions of homofarnesoic acid and geranylacetone were increased. For farnesylacetone a slight enhancement of activity was detected for the mutant in comparison to the wildtype. Homofarnesol and nerolidol conversion showed the expected behavior: The rate for homofarnesol biotransformation diminished about 1.5-fold from 34.8 % (wildtype *ZmoSHC1*) to 23.9 % (mutant *ZmoSHC1\_F486Y*), and the nerolidol conversion was increased about 3-fold (Table 5.12, Fig. 6.12).

For the mutation Y420C in *AacSHC*, it was presumed that the enzymatic activity towards the larger substrates would decrease and the activity towards smaller substrates would rise. Testing the mutant under the same conditions as the wildtype and comparing the activities with each other, the following observations were made: The activities towards squalene, farnesylacetone and homofarnesoic acid were reduced with the mutation. The other substrates, homofarnesol, nerolidol and geranylacetone, did not show conversion with the mutant at all. From these results it can be concluded that the position Y420 of *AacSHC* is very important for the catalysis of squalene cyclization. Also for all of the other substrates, a lower conversion was observed with the *AacSHC\_Y420C* mutant in comparison to the wildtype. Y420 is crucial for the activity of *AacSHC* towards all of the substrates.

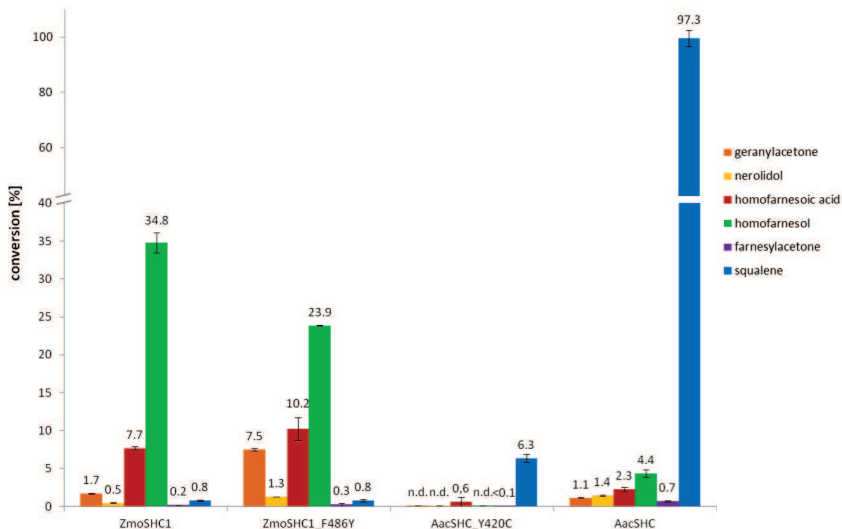


**Fig. 6.12:** Conversion rates of geranylacetone (orange), nerolidol (yellow), homofarnesic acid (red), homofarnesol (green), farnesylacetone (purple) and squalene (blue), using partially purified *ZmoSHC1*, *ZmoSHC1\_F486Y*, *AacSHC\_Y420C* and *AacSHC*. The values are shown as percentage of the concentrations of both substrates and products calculated with ISTD1 calibration.

In contrast to this, mutations of the corresponding F486 of *ZmoSHC1* did not exhibit such a strong impact on the activity of this SHC. The mutations lead to differences in substrate activities compared to the wildtype SHC but did not change the activities in such a high rate as observed for Y420 in *AacSHC*. Remarkably, the conversion of two of the substrates, geranylacetone and homofarnesic acid, were significantly increased with *ZmoSHC1\_F486Y*. This observation indicates that with few mutations the activity pattern of *ZmoSHC1* can be shifted. Thus, the potential for usage of *ZmoSHC1* for catalysis of complex reactions and formation of attractive products could be enlarged by usage of appropriate mutants.

## 6.4.2 Creation and screening of the loop deletion mutant

A sequence alignment of *ZmoSHC1*, *ZmoSHC2* and *AacSHC* has shown that there is one significant difference (Fig. 3.22). In contrast to *AacSHC* and *ZmoSHC2*, the amino acid sequence of *ZmoSHC1* shows an insertion at the C-terminal end of the sequence. This insertion (“loop”) contains 26 amino acids. Modeling of the crystal structure of *ZmoSHC1*

(Fig. 3.23, done by A. Steudle and B. Juhl, bioinformatics group, ITB) revealed that this insertion possibly could be positioned right at the entrance of the substrate channel. As it was already discussed that *ZmoSHC1* and *AacSHC* show a high similarity regarding the amino acids in the active site, these results triggered the question if the insertion could be the reason for the decreased activity of *ZmoSHC1* towards squalene, as it is possible that the bulkier substrate is just hindered in its access to the active site. In order to test this hypothesis, a loop deletion mutant of *ZmoSHC1*, *ZmoSHC1\_Loop*, was created and tested. The conversion rates of the loop deletion mutant in comparison to the wildtype SHCs are displayed in Fig. 6.13.

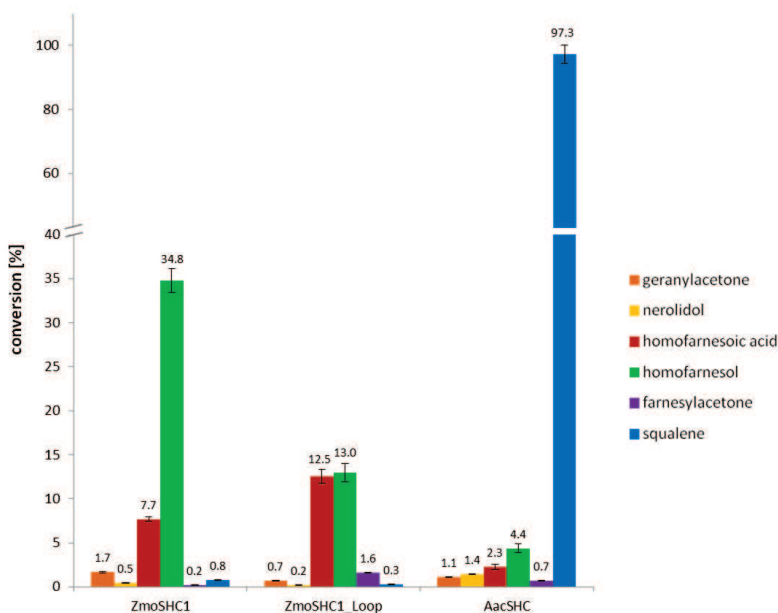


**Fig. 6.13:** Conversion rates of geranylacetone (orange), nerolidol (yellow), homofarnesoic acid (red), homofarnesol (green), farnesylacetone (purple) and squalene (blue), using partially purified *ZmoSHC1*, *ZmoSHC1\_Loop* and *AacSHC*. The values are shown as percentage of the concentrations of both substrates and products calculated with ISTD1 calibration.

The activity towards squalene was decreased with deletion of the loop. This indicates that the loop does not hinder access of squalene to the active site and that there must be some other reasons for the low activity of *ZmoSHC1* towards squalene cyclization. For homofarnesol, nerolidol and geranylacetone, a decrease of activity was observed.

Interestingly, the conversion rates of farnesylacetone and homofarnesoic acid were significantly increased for the loop deletion mutant in comparison to the wildtype enzyme. Considering these observations, it is clear that the loop indeed has an influence on the substrate specificity of *ZmoSHC1* and that a deletion of the loop causes shifts regarding the substrate activities.

## 7 Conclusion

The aim of the present work was the investigation of SHCs which catalyze cyclization reactions of new, unnatural substrates. The studied substrates provide different carbon chain lengths and functional groups which are the decisive molecular parameters for the final nucleophilic attack terminating the cyclization procedure. The novel squalene-hopene cyclase *ZmoSHC1* was characterized and found to be a promising biocatalyst for the cyclization of varying substrates and the stereospecific formation of bi- and triheterocyclic products was observed. All of the products exhibit beneficial properties, as being fragrances or intermediates in the synthesis of pharmaceuticals for example.

*ZmoSHC1*'s activity towards these novel substrates was determined and compared to the well investigated *AacSHC* and *ZmoSHC2*, revealing a completely different activity pattern. While *AacSHC* and *ZmoSHC2* showed highest conversion of the natural substrate squalene, *ZmoSHC1* was found to be much more active towards the cyclization of the C<sub>16</sub> alcohol homofarnesol to the flavor compound ambroxan. Besides formation of this valuable tricyclic ether which is used in the perfume industry, the cyclic lactone sclareolide was formed from homofarnesoic acid as well as two enol ethers from the ketones geranylacetone and farnesylacetone and the ether caparrapioxide from nerolidol.

In addition to the description and discussion of these findings, approaches for an explanation of the substrate specificity and the differences between these enzymes were made. The biocatalytic potential of SHCs general and *ZmoSHC1* in particular was clarified leading to new ideas for their application as well as for the understanding of this attractive class of triterpene cyclases.

## 8 Outlook

The characterization of the SHCs revealed a flexible substrate spectrum and special biocatalytic properties of *ZmoSHC1*, as this enzyme was shown to be much more potent to catalyze the cyclization of other substrates than squalene.

It has to be questioned whether the function of *ZmoSHC1* in nature is the catalysis of hopene and hopanol formation from squalene, or if this enzyme catalyzes another reaction. One approach to discover the natural reaction is to screen further substrates of varying carbon chain lengths containing not yet investigated functional groups. As new nucleophiles, nitrogen- or sulfur-containing functional groups could be studied. By enhancement of the substrate spectrum, more information about the promiscuity of the SHCs and the possible catalysis of completely different reaction types can be gained.

Further mutational analysis could elucidate the functionality of the “loop”. Interestingly, the deletion mutant showed differences regarding the activities towards the different substrates compared to the wildtype and, thus, the mutant could serve for catalysis of other cyclization reactions. Another interesting mutant could be created with the insertion of the loop into *AacSHC* or *ZmoSHC2*, or with the deletion of the N-terminal residue of *ZmoSHC1* or by exchange of other positions discussed as crucial for squalene conversion. Moreover, it could be helpful to screen other SHCs. The loop-containing SHCs from strains with two SHCs are promising examples for further investigations.

The conversion rates for some of the new substrates were low. An enhancement of these rates could be achieved by optimization of the biotransformation conditions. One very important fact is the selection of a suitable surfactant. Possibly, for each substrate another surfactant of a distinct concentration can provide the optimal conditions for a good conversion.

Several substrates were not accepted by the SHCs. Random and site-directed mutagenesis could change the structure of the active cavity and enable the conversion of these substrates. The mutants could be selected by bioinformatic methods like docking experiments. The solving of the crystal structure of *ZmoSHC1* is indispensable for a entire

understanding of the reaction mechanisms and the selection of important amino acid residues for mutagenesis.

In summary, there remains plenty of work to do on the understanding of the SHCs. In my opinion, it is worth investigating on these fascinating enzymes that could one day be applied as versatile biocatalysts for highly complex reactions.

## 9 Materials and methods

### 9.1 Instruments

agarose gel	Mini Sub Cell GT (Bio Rad)
bioreactor	42 L bioreactor, (Bioengineering AG, Wald, Switzerland)
cell homogenisator	APV 1000 (APV GmbH, Unna, Germany)
centrifuges	centrifuge RC 6 Plus / 5C Plus, Sorvall, Thermo Scientific, Langenselbold, Germany; Rotors: SLA-3000 (Sorvall), SS-34 (Sorvall), Fiberlite F21-8x50y (Piramoone) centrifuge 5418 R (Eppendorf) centrifuge 5810 R (Eppendorf); Rotor: A-4-62.
GC columns	5 % phenyl / 95 % dimethylpolysiloxane phase columns DB-5 / DB-5 MS (30 m, 0.25 mM, 0.25 $\mu$ m, agilent technologies) FS-Supreme 5 / FS-Supreme 5 HT (30 m, 0.25 mM, 0.25 $\mu$ m, CS-Chromatographie)
GC-FID	GC-2010 Plus (Shimadzu), AOC-20i auto injector (Shimadzu)
GC-MS	GCMS-QP 2010 (Shimadzu), AOC-5000 auto injector (CTC Analytics)
HPLC	Knauer HPLC coupled with RI detector K2400 (Knauer)
HPLC column	preparative normal-phase silica column, Eurospher 100 Si (100 Å pore size, 350 m <sup>2</sup> / g surface area, Vertex)
HREIMS	MAT 95 (Finnigan)
IR spectra	Vector 22 FT-IR spektrometer in ATR modus (Bruker)
NMR	Avance 500 spectrometer (Bruker)
photo station	Quantum ST4 (Vilber Loumat)
power supply	Power Pac 300 (Bio Rad)



rotary evaporator	Laborota 400 efficient (Heidolph)
SDS-PAGE	SE 250 (Hoefler)
shaking incubator	Multitron HT (Infors AG, Bottmanningen, Switzerland)
thermomixer	Thermomixer comfort (Eppendorf)
ultrasonifier	Sonifier 250, duty cycle 35 %, output control 4 (Branson)

## 9.2 Software

alignment	Multisequence Alignments: MAFFT, version 6, CLUSTAL format alignment by MAFFT, version v6.935b (CBRC – Computational Biology Research Centre; AIST – Advanced Industrial Science and Technology, Japan) <sup>277–281</sup>  For the calculation of global sequence identities: LALIGN-software; BLOSUM 50, penalty settings of 14 for opening and 4 for extending a gap (EMBnet) <sup>153,282</sup>
Chemdraw	ChemDraw Ultra, version 11.0.1 (Cambridge Soft)
Clonemanager	Clone Manager 7, version 7.03 (Si Ed Central)
densitometric analysis	ImageJ software, version 1.44p (Wayne Rasband)
GC-FID	LabSolutions, GCsolution, version 2.30.00 (Shimadzu)
GC-MS	LabSolutions, GCMSsolution, version 2.50 (Shimadzu)
HPLC	EUROCHROM 2000 for Windows, version 3.05 (Knauer)
literature	Mendeley Desktop, version 1.6 (Mendeley Ltd)
MS Office	Microsoft Office Professional Plus 2010, version 14.0.6123.5001 (Microsoft)
NMR Evalutaion	TOPSPIN, version 3.0 pl 2 (Bruker BioSpin GmbH)
photo station	Quantum ST4, version 15.12 (Vilber Lourmat)
phylogenetic tree	Dendroscope, version 3.3.2 (Daniel H. Huson)

Pymol                                      The PyMOL Molecular Graphics System, version 1.2r1 (DeLano Scientific LLC)

### **9.3      Consumables**

Eppendorf tubes                      0.5 / 1.5 / 2.0 mL (Eppendorf)  
GC consumables                      glass vials (1.7 mL), caps and inserts (300 µL) (WICOM)  
Greiner tubes                          15 / 50 mL (Greiner)  
Microtiter plates                      96-well DeepWell™ plates (nunc)

### **9.4      Chemicals**

The chemicals and solvents were purchased from Sigma-Aldrich. Homofarnesol and homofarnesoic acid were provided by BASF SE. Bishomofarnesol, bishomofarnesoic acid and bishomofarnesal were provided by Michael Pohl (ITB, 2012).<sup>238</sup> All products were identified with GC-MS or GC-FID analysis by using reference material. The systematic nomenclature of the substrates, products and other compounds relevant in this work is shown in Table 9.1.

**Table 9.1: Systematic nomenclature of substrates, products and other compounds used in this work.**

compound	systematic nomenclature
(±)-ambraoxide	(4 <i>α</i> R,6 <i>α</i> S,10 <i>α</i> S,10 <i>β</i> R)-4 <i>α</i> ,7,7,10 <i>α</i> -tetramethyldodecahydro-1 <i>H</i> -benzo[f]chromene
(±)- <i>epi</i> -ambraoxide	(4 <i>α</i> R,6 <i>α</i> S,10 <i>α</i> R,10 <i>β</i> R)-4 <i>α</i> ,7,7,10 <i>α</i> -tetramethyldodecahydro-1 <i>H</i> -benzo[f]chromene
(±)-9- <i>epi</i> -ambraoxide	(4 <i>α</i> R,6 <i>α</i> S,10 <i>α</i> S,10 <i>β</i> S)-4 <i>α</i> ,7,7,10 <i>α</i> -tetramethyldodecahydro-1 <i>H</i> -benzo[f]chromene
(±)-ambreinolide	(4 <i>α</i> R,6 <i>α</i> S,10 <i>α</i> S,10 <i>β</i> R)-4 <i>α</i> ,7,7,10 <i>α</i> -tetramethyldecahydro-1 <i>H</i> -benzo[f]chromen-3(2 <i>H</i> )-one
(±)-9- <i>epi</i> -ambreinolide	(4 <i>α</i> R,6 <i>α</i> S,10 <i>α</i> S,10 <i>β</i> S)-4 <i>α</i> ,7,7,10 <i>α</i> -tetramethyldecahydro-1 <i>H</i> -benzo[f]chromen-3(2 <i>H</i> )-one
(±)-10- <i>epi</i> -ambreinolide	(4 <i>α</i> R,6 <i>α</i> S,10 <i>α</i> R,10 <i>β</i> R)-4 <i>α</i> ,7,7,10 <i>α</i> -tetramethyldecahydro-1 <i>H</i> -benzo[f]chromen-3(2 <i>H</i> )-one
ambroxan	(3 <i>α</i> R,5 <i>α</i> S,9 <i>α</i> S,9 <i>β</i> R)-3 <i>α</i> ,6,6,9 <i>α</i> -tetramethyl-dodecahydronaphto[2,1- <i>β</i> ]furan
(-)-8- <i>epi</i> -caparrapioxide	(2 <i>R</i> ,8 <i>α</i> S)-2,5,5,8 <i>α</i> -tetramethyl-2-vinyloctahydro-2 <i>H</i> -chromene
(-)-caparrapioxide	(2 <i>S</i> ,8 <i>α</i> S)-2,5,5,8 <i>α</i> -tetramethyl-2-vinyloctahydro-2 <i>H</i> -chromene
<i>cis</i> -citral	( <i>Z</i> )-3,7-dimethylocta-3,6-dienal
farnesylacetone	(5 <i>E</i> ,9 <i>E</i> )-6,10,14-trimethylpentadeca-5,9,13-trien-2-one
geranic acid	( <i>E</i> )-3,7-dimethylocta-2,6-dienoic acid
geraniol	( <i>E</i> )-3,7-dimethylocta-2,6-dien-1-ol
geranylacetone	( <i>E</i> )-6,10-dimethylundeca-5,9-dien-2-one
hexahydrochromene	2,5,5,8 <i>α</i> -tetramethyl-4 <i>α</i> ,5,6,7,8,8 <i>α</i> -hexahydro-4 <i>H</i> -chromene
homofarnesoic acid	(3 <i>E</i> ,7 <i>E</i> )-4,8,12-trimethyltrideca-3,7,11-trienoic acid
homofarnesol	(3 <i>E</i> ,7 <i>E</i> )-4,8,12-trimethyltrideca-3,7,11-trien-1-ol, > 90 % <i>E,E</i> -homofarnesol
hopanol	hopan-22-ol
hopene	hop-22(29)-ene
linalool	3,7-dimethylocta-1,6-dien-3-ol
nerolidol	( <i>E</i> )-3,7,11-trimethyldodeca-1,6,10-trien-3-ol
pseudoionone	(3 <i>E</i> ,5 <i>E</i> )-6,10-dimethylundeca-3,5,9-trien-2-one
sclareolide	(3 <i>α</i> R,9 <i>β</i> S)-3 <i>α</i> ,6,6,9 <i>α</i> -tetramethyldecahydronaptho[2,1- <i>β</i> ]furan-2(3 <i>α</i> H)-one
sclareoloxide	3,4 <i>α</i> ,7,7,10 <i>α</i> -pentamethyl-4 <i>α</i> ,5,6,6 <i>α</i> ,7,8,9,10,10 <i>a</i> ,10 <i>b</i> -decahydro-1 <i>H</i> -benzo[f]chromene
squalene	(6 <i>E</i> ,10 <i>E</i> ,14 <i>E</i> ,18 <i>E</i> )-2,6,10,15,19,23-hexamethyltetracos-2,6,10,14,18,22-hexaene

## 9.5 Media, buffers and Kits

### Media

LB agar: 10 g tryptone, 5 g yeast extract, 5 g NaCl, 16 g agar-agar, ad 1000 mL (dH<sub>2</sub>O).

LB medium: 10 g tryptone, 5 g yeast extract, 5 g NaCl, ad 1000 mL (dH<sub>2</sub>O).

TB medium: 10 g tryptone, 24 g yeast extract, 4 mL glycerol, ad 900 mL (dH<sub>2</sub>O); addition of 100 mL 10 × TB phosphate buffer after autoclaving.

### Buffers

cell disruption buffer 1: 0.2 M sodium citrate, 0.1 M EDTA, pH 6.0 (dH<sub>2</sub>O).

cell disruption buffer 2: 0.2 M Tris/HCl, 0.5 M EDTA, pH 8.0 (dH<sub>2</sub>O).

cell washing buffer: 0.1 M sodium phosphate, pH 7.

DNA—sample buffer: 2 g sucrose, 10 mg Orange G, ad 5 mL (ddH<sub>2</sub>O).

SDS—sample buffer: 2 mL 1 M Tris/HCl (pH 6.8), 405.7 mg MgCl<sub>2</sub>\*6 H<sub>2</sub>O, 1 mL glycerol, 0.8 g SDS, 2 mg bromphenolblue, 30.85 mg dithiothreitol, ad 20 mL (ddH<sub>2</sub>O).

solubilization buffer 1: 0.05 M sodium citrate, 0.01 M MgCl<sub>2</sub>, 1 % Triton X-100, pH 6.0 (dH<sub>2</sub>O).

solubilization buffer 2: 0.05 M Tris/HCl, 0.01 M MgCl<sub>2</sub>, 1 % Triton X-100, pH 8.0 (dH<sub>2</sub>O).

10 × TB phosphate buffer: 0.17 M KH<sub>2</sub>PO<sub>4</sub>, 0.72 M K<sub>2</sub>HPO<sub>4</sub>, pH = 7.0.

### Kits

Bradford: Bradford Ultra® (Expedeon, UK-Harston).

gel extraction: QIAquick® Gel Extraction Kit (Qiagen).

plasmid isolation: Zippy™ Plasmid Miniprep Kit (Zymo-Research).

### Others

agarose gel staining: GelRed™ (Biotium).

DNA marker: 1 kb DNA Ladder (Fermentas).

IPTG stock solution (1 M): 476,6 mg isopropyl-β-D-thiogalactopyranoside, ad 2 mL (ddH<sub>2</sub>O).

PMSF-solution (0.1 M): 17.42 mg in isopropanol, ad 1 mL (ddH<sub>2</sub>O).

protein marker: PageRuler™ Unstained Protein Ladder (Fermentas).

## 9.6 Molecular biological devices

### Organisms and plasmids

expression plasmid: pET22-b(+) (Novagen).

strain for enzyme expression: *Escherichia coli* (*E. coli*) BL21(DE3) (Novagen).

strain for plasmid amplification: *Escherichia coli* (*E. coli*) DH5α (Clontech).

### Wildtype enzymes

AacSHC: Squalene-hopene cyclase from *Alicyclobacillus acidocaldarius* (P33247.4) was derived from S. Hammer (ITB, Uni Stuttgart) as *E. coli* BL21(DE3)\_pET22b(+)\_AacSHC.

ZmoSHC1: Squalene-hopene cyclase 1 from *Zymomonas mobilis* (YP\_163283.1) was derived from M. Breuer (BASF SE) as *E. coli* LU15568\_pDHE\_ZmoSHC1 and could be amplified and subcloned into the expression vector pET-22b(+) from Novagen by using the restriction sites *Bam*HI and *Nde*I (Fermentas; Buffer: 10 × Tango buffer).<sup>283</sup>

ZmoSHC2: Squalene-hopene cyclase 2 from *Zymomonas mobilis* (AAF12829.1) was derived from G. Siedenburg (IMB, Uni Stuttgart) as *E. coli* BL21(DE3)\_pET16b\_ZmoSHC2 and could be amplified and subcloned into the expression vector pET-22b(+) from Novagen by using the restriction sites *Bam*HI and *Nde*I (Fermentas; Buffer: 10 × Tango buffer).<sup>283</sup>

All genes were confirmed by sequencing (GATC-Biotech AG, Konstanz).

### Mutant enzymes

ZmoSHC1 Loop: The loop deletion mutant was created using the QuikChange® protocol from the *PfuUltra* II Fusion HS DNA Polymerase Kit (Stratagene, Agilent Technologies). The primer were chosen as follows:

#1 5' – CGG CAC CGG ATT CCC CCG GGC GTT TAT GCT GC – 3'

#2 3' – GCA GCA TAA ACG CCC GGG GGA ATC CGG TGC CG – 5'

ZmoSHC1\_F486Y: The mutant was derived from S. Racolta (ITB, Uni Stuttgart) as *E. coli* BL21(DE3)\_pET22b(+)\_ZmoSHC1\_F486Y.

AacSHC Y420C: The mutant was derived from S. Hammer (ITB, Uni Stuttgart) as *E. coli* BL21(DE3)\_pET22b(+)\_ZmoSHC1\_F486Y.

All genes were confirmed by sequencing (GATC-Biotech AG, Konstanz).

### Other enzymes

restriction enzymes: *Bam*HI, *Nde*I (Fermentas), used with Tango-Buffer (Fermentas).

## 9.7 Cell culture and enzyme expression

For plasmid maintenance, protein expression and biotransformations with cells, the *E. coli* strain BL21(DE3) was used and 100 µg/mL ampicillin was added to all growth media.

### a) Enzyme expression

Precultures of the strains were grown overnight in 5 mL LB medium at 37°C with shaking at 180 rpm. These precultures were used to inoculate three independent 200 mL TB cultures in 2 L Erlenmeyer flasks (without baffles) with an optical density of  $OD_{600} = 0.05$  and the cultures were incubated as described above. When an  $OD_{600} = 0.5$  was reached, SHC expression was induced by the addition of IPTG in a final concentration of 0.2 mM. 4 h after induction, the three cultures were mixed, the cells were harvested by centrifugation at  $13,670 \times g$  for 20 min at 4°C, pooled and washed twice with cell ashing buffer (9.5). After the final washing step the cells were aliquoted and stored at -20°C until further usage for biotransformations (see 9.9.1) or partial purification (see 9.8.1). For controlling of successful expressions of the enzymes, aliquots were routinely analyzed by SDS-PAGE using standard protocols.<sup>284</sup>

### b) Fermentation

Precultures of the strains were grown overnight in 5 mL LB medium at 37°C with shaking at 180 rpm. These precultures were used to inoculate three 400 mL TB cultures in 2 L Erlenmeyer flasks (without baffles) with an optical density of  $OD_{600} = 0.05$  and the cultures were incubated as described above. When an  $OD_{600} = 0.7$  was reached, the cultures were subsequently used to seed a 42 L bioreactor containing 25 L buffered complex medium (25 L containing 550 g tryptone, 275 g yeast extract, 125 g NaCl, 1.875 g  $CaCl_2 \cdot 2 H_2O$ , 500 g glycerol (87 %), 354 g  $Na_2HPO_4$ , 83 g  $KH_2PO_4$ , 200 g  $(NH_4)_2SO_4$ , 41 g  $NH_4Cl$ , 50 g

MgSO<sub>4</sub>\*7 H<sub>2</sub>O, 15 mL Antifoam 204 (Sigma, Taufkirchen, Germany). The fermentation temperature was 30°C, the pH was maintained at 7 using NH<sub>4</sub>OH (28 %) and H<sub>2</sub>PO<sub>4</sub> (10 %). The airflow was kept at 15 L/min and the stirrer speed was adjusted to 550 rpm. 8 h after inoculation, the glycerol feeding (1500 g glycerol + 100 g (NH<sub>4</sub>)<sub>2</sub>HPO<sub>4</sub> in 200 mL water) was started. Cyclase expression was induced 16 h after inoculation with IPTG (final concentration 0.1 mM) when cell density reached OD<sub>600</sub> = 38.6. The expression was maintained for at least 4 h. Subsequently, the cells were harvested by centrifugation at 13,500 × g for 20 min at 4°C. The obtained wet cell weight was 1.4 kg. The cells were stored overnight at 4°C. The following procedures are described in 9.8.1 b).

## 9.8 Protein biochemical methods

### 9.8.1 Partial purification of the membrane bound protein fraction

#### a) Standard protocol for partial purification

For the partial purification of the SHCs, thawed cells (OD<sub>600</sub> = 100) were resuspended in cell disruption buffer 1 (9.5). The cells were disrupted by ultrasonic treatment for six times one minute on ice, with cooling on ice for at least one minute in between the sonification steps. The cell debris was collected by centrifugation at 38,000 × g for 60 min at 4°C; the supernatant was discarded. The cell debris was resuspended in 1/5 of the volume used for cell disruption in solubilization buffer 1 (9.5) and incubated for 1 h gently mixing at 4°C, in order to solubilize the membrane-bound proteins from the membranes with the detergent (1 % Triton X-100). Afterwards, the mixture was centrifuged (conditions see above) and the supernatant was used for the biotransformations (partially purified enzyme).

#### b) Protocol for partial purification after fermentation

The obtained wet cell weight of total 1.4 kg was resuspended in 3.6 L cell disruption buffer 2 (9.5) and after addition of 32 mL PMSF solution, cells were disrupted by homogenization at 900 bar. The cell debris was collected by centrifugation at 13,500 × g for 60 min and resuspended in 3 L solubilization buffer 2. After a final centrifugation step at 13,500 × g for 60 min, the cell debris was discarded and the supernatant was stored at -18°C.

### 9.8.2 Protein determination

The protein expression was confirmed by standard SDS-PAGE methods using a 12.5 % polyacrylamide SDS-Gel.<sup>284</sup> The total protein concentration was determined using the Bradford Ultra assay. The quantification was performed in two different dilutions in triplicate using bovine serum albumin containing 0.1 % Triton X-100 as a standard. The percentage of SHC within the total protein mixture was determined densitometrically from SDS-gels. The optical measurements were performed by a digital photo station and densitometric analysis of the gels was performed using the ImageJ software.

## 9.9 Biotransformations

All experiments were performed technical triplicates. As negative control, cells / membrane protein fraction of *E. coli* BL21(DE3) carrying the empty pET-22b(+) vector were used. If not further mentioned, the final biotransformation conditions were: 10 mM substrate, 0.05 M sodium citrate, 0.002 M MgCl<sub>2</sub>, 0.2 % Triton X-100, pH 6.0; for biotransformations of (S)-citronellal pH 4.5. The substrates were added as 100 mM emulsion in solubilization buffer after mixing thoroughly. The biotransformations were carried out at 30°C for conversions with *ZmoSHC1* and *ZmoSHC2* and at 60°C for conversions with *AacSHC*, respectively, with shaking at 1,200 rpm in an Eppendorf Thermomixer. The reactions were carried out in 2 mL Eppendorf reaction tubes.

### 9.9.1 Biotransformations with whole cells

#### a) Standard protocol for biotransformations with whole cells

Cells expressing *ZmoSHC1*, *ZmoSHC2* and *AacSHC* (9.7 a) were resuspended and diluted to OD<sub>600</sub> = 10 / 80 and the final conditions as described above. The biotransformations were carried out for 5 or 20 h. The biotransformations were carried out for 5 or 20 h.

#### b) Protocol for stability experiments with whole cells at different temperatures

Cells expressing *ZmoSHC1* (9.7 a) were resuspended and diluted to OD<sub>600</sub> = 5 and the following final conditions: 10 mM substrate, 0.05 M Tris/HCl, 0.1 M sodium citrate, 0.01 M MgCl<sub>2</sub>, 1 % Triton X-100, pH 4.5. The biotransformations were carried out for 12 / 24 / 48 / 72 / 96 / 120 h at 30 / 37 / 42°C with shaking at 180 rpm in a shaking incubator.



**c) Protocol for stability experiments with whole cells at 30 C**

Cells expressing *ZmoSHC1* (9.7 a) were resuspended and diluted to  $OD_{600} = 80$  and the final conditions mentioned above but without addition of the substrate. After 0 / 12 / 24 / 48 / 72 / 96 / 120 h of pre-incubation at 30°C with shaking at 1,200 rpm in an Eppendorf Thermomixer, the substrate homofarnesol was added to a final concentration of 10 mM and incubated further for 5 h under the same conditions.

**d) Protocol for stability experiments with whole cells of different cell densities**

Cells expressing *ZmoSHC1* (9.7 a) were resuspended and diluted to  $OD_{600} = 30 / 20 / 10 / 5 / 1$  and the final conditions mentioned above. The biotransformations were carried out for 24 / 48 / 72 / 96 / 120 h.

**e) Protocol for inhibition experiments with whole cells**

Cells expressing *ZmoSHC1* and *AacSHC* (9.7 a) were resuspended and diluted to  $OD_{600} = 10 / 80$  and the final conditions mentioned above but with both 5 mM of squalene and 5 mM homofarnesol as substrates. The biotransformations were carried out for 20 h.

**9.9.2 Biotransformations with partially purified SHC****a) Protocol for biotransformations with partially purified SHC**

Partially purified SHCs (9.8.1 a) were diluted to a protein concentration of 0.1 / 0.35 mg/mL and the final conditions mentioned above. The biotransformations were carried out for 20 h

**b) Protocol for stability experiments with partially purified *ZmoSHC1* at different temperatures**

Partially purified *ZmoSHC1* (9.8.1 b) was diluted to a protein concentration of >1 mg/mL and the following final conditions: 0.05 M Tris/HCl, 0.1 M sodium citrate, 0.01 M  $MgCl_2$ , 1 % Triton X-100, pH 4.5. After 0 / 12 / 24 / 48 / 72 / 96 / 120 h of pre-incubation at 30°C with shaking at 1,200 rpm in an Eppendorf Thermomixer, the substrate homofarnesol was added to a final concentration of 10 mM and incubated further for 5 h under the same conditions. As negative control, solubilization buffer 2 instead of partially purified enzyme was used.

**c) Protocol for stability experiments with partially purified *Zmo*SHC1 at 30°C**

Partially purified *Zmo*SHC1 (9.8.1 a) was diluted to a protein concentration of 0.1 mg/mL and the final conditions mentioned above but without addition of the substrate. After 0 / 12 / 24 / 48 / 72 / 96 / 120 h of pre-incubation at 30°C with shaking at 1,200 rpm in an Eppendorf Thermomixer, the substrate homofarnesol was added to a final concentration of 10 mM and incubated further for 5 h under the same conditions.

**d) Protocol for inhibition experiments with partially purified SHCs**

Partially purified SHCs (9.8.1 a) were diluted to a protein concentration of 0.1 mg/mL and the final conditions mentioned above but with (i) 5 mM of squalene and 5 mM of homofarnesol or with (ii) 20 mM of squalene /homofarnesol / ambroxan or (iii) 0.1 / 0.05 / 1 / 2 / 4 / 6 / 8 / 10m M of homofarnesol as substrates. The biotransformations were carried out for 20 h.

**e) Protocol internal standard experiments with partially purified SHCs**

Partially purified SHCs (9.8.1 a) were diluted to a protein concentration of 0.1 mg/mL and the final conditions mentioned above but with 5 mM of squalene /homofarnesol and 5 mM of 1-decanol as substrates. The biotransformations were carried out for 20 h.

**f) Protocol pH experiments with partially purified SHCs**

Partially purified SHCs (9.8.1 a) were diluted to a protein concentration of 0.1 mg/mL and the final conditions mentioned above but with pH 6.0 / 5.0 / 4.5. The biotransformations were carried out for 20 h.

**g) Protocol enhanced conversions with partially purified SHCs**

900 µL of partially purified *Zmo*SHC1 (9.8.1 a), containing a final protein concentration of 4.4 mg/mL was mixed with 100 µL substrate emulsion (100 mM in solubilization buffer 1) (final conditions: protein concentration 4 mg/mL, 1 % Triton X-100, 10 mM substrate). The biotransformations were carried out for 20 h.

**9.9.3 Sample preparation**

After incubation, 20 µL of internal standard 1 (1 M 1-decanol in solubilization buffer 2, ISTD1) was added to the samples and mixed thoroughly. Subsequently, 750 µL of *n*-heptane

was added. After mixing and centrifugation at  $20,800 \times g$  for 60 min at room temperature (Eppendorf, Centrifuge 5417R), the organic phases were transferred into glass GC-Vials. The extraction procedure was performed two times leading to a final volume of 1.5 mL. The analysis was performed by gas chromatography coupled with a flame ionization detector (GC-FID).

#### 9.9.4 Preparative biotransformations and product isolation

To obtain the products hopene, hopanol, sclareolide, sclareoloxide, (-)-caparrapioxide, (-)-8-*epi*-caparrapioxide and hexahydrochromene, a large scale incubation was conducted by using 100 mg – 1 g of the corresponding substrates squalene, homofarnesoic acid, farnesylacetone, nerolidol and geranylacetone, upscaling the total reaction and extraction volume as used for standard biotransformations. The biotransformations were performed with partially purified *ZmoSHC1* (derived as described in 9.8.1 b) at 30°C, 180 rpm for 70-144 h.

##### **Biotransformation of squalene to hopene and hopanol**

biotransformation: 1 g of substrate, 70 h, conversion: 97.8 % (88.9 % hopene, 8.9 % hopanol);

extraction: 2\*100 mL *n*-heptane;

purification: column chromatography, silica gel, petrolether:ethylacetate (10:1);

product: due to losses during isolation approx. 150 mg product hopene (white solid, 99 %) and 50 mg product hopanol (colourless oil);

TLC: silica gel: cyclohexane:ethylacetate (5:1),  $R_f(\text{squalene}) = 1.0$ ,  $R_f(\text{hopene}) = 0.9$ ,  $R_f(\text{hopanol}) = 0.5$ , stained with vanillin/sulfuric acid.

##### **Biotransformation of homofarnesoic acid to sclareolide**

biotransformation: 0.5 g of substrate, 120 h, conversion: 55 %;

extraction: 500 mL cyclohexane / ethylacetate;

purification: column chromatography, silica gel, cyclohexane: ethylacetate (20:1, 10:1, 0:100);

product: due to losses during isolation approx. 100 mg product sclareolide (white solid, 99 %);

TLC: silica gel: cyclohexane:ethylacetate (5:1),  $R_f$ (homofarnesoic acid) = 0.2,  $R_f$ (sclareolide) = 0.4, stained with vanillin/sulfuric acid.

#### **Biotransformation of farnesylacetone to sclareoloxide**

biotransformation: 2 g of substrate, 144 h, conversion 0.7 %;

extraction: 2\*100 mL *n*-heptane, 2\*100 mL ethylacetate;

purification: column chromatography, silica gel, cyclohexane:ethylacetate (20:1);

product: due to losses during isolation approx. 10 mg product sclareoloxide (yellow oil, 91 %);

TLC: silica gel: cyclohexane:ethylacetate (5:1),  $R_f$ (farnesylacetone) = 0.5,  $R_f$ (sclareoloxide) = 2.8, Stained with vanillin/sulfuric acid

#### **Biotransformation of nerolidol to (-)-caparrapioxide and (-)-8-*epi*-caparrapioxide**

biotransformation: 3 g of substrate, 144 h, conversion 2.5 % (1.9 % (-)-caparrapioxide / 0.6 % (-)-8-*epi*-caparrapioxide);

extraction: 2\*100 mL *n*-heptane, 2\*100 mL ethylacetate;

purification: column chromatography, silica gel, cyclohexane:ethylacetate (30:1);

product: due to losses during isolation approx. 30 mg products (pale yellow oil, 95 %, 73 % (-)-caparrapioxide / 22 % (-)-8-*epi*-caparrapioxide);

separation of the products: separation of (-)-caparrapioxide and (-)-8-*epi*-caparrapioxide: the products were separated with HPLC (Kramer HPLC with RI-detector K2400), column: Vertex Eurospher 100 Si (normal phase), 7 mL/min, petrolether:ethylacetate (30:1), fraction 1: 9.10 min-10.00 min ((-)-caparrapioxide, 91 %, approx. 10 mg), fraction 2: 10.00-10.50 min ((-)-8-*epi*-caparrapioxide, 87 %, approx. 8 mg);

TLC: silica gel: cyclohexane:ethylacetate (5:1),  $R_f$ (nerolidol) = 0.42,  $R_f$ (caparrapioxide) = 0.77, stained with vanillin/sulfuric acid, the products (-)-caparrapioxide and (-)-8-*epi*-caparrapioxide could not be separated using TLC.

## Biotransformation of geranylacetone to hexahydrochromene

biotransformation: 1 g of substrate, 70 h, conversion 70 %;

extraction: 500 mL cyclohexane/ethylacetate, 2\*100 mL ethylacetate;

purification: column chromatography: cyclohexane:ethylacetate (50:1, 20:1, 0:100);

product: due to losses during isolation approx. 20 mg product (yellow brown oil, 97 %);

TLC: silica gel: cyclohexane:ethylacetate (10:1),  $R_f(\text{substrate}) = 0.37$ ,  $R_f(\text{product}) = 0.74$ , stained with vanillin/sulfuric acid.

## 9.10 Analysis and evaluation

### 9.10.1 GC-FID

GC-FID analyses were performed using H<sub>2</sub> as a carrier gas (linear velocity 30 cm/sec). The injection temperature was set as 250°C and the detector temperature was set as 330°C. The temperature programs were as follows:

**Table 9.2: GC-FID parameters for squalene conversions showing the temperature program and the retention times of the different analysts.**

rate [°C/min]	final temp. [°C]	holding time [min]
-	120	3
60	310	16

retention times: ISTD1: 4.79 min, squalene: 9.57 min, hopene: 14.23 min, hopanol: 17.26 min

**Table 9.3: GC-FID parameters for homofarnesol conversions showing the temperature program and the retention times of the different analysts.**

rate [°C/min]	final temp. [°C]	holding time [min]
-	120	2
4	200	0
60	300	3

retention times: ISTD1: 6.46 min, ambroxan: 18.72 min, *cis*-homofarnesol: 19.13 min, *trans*-homofarnesol: 19.42 min

**Table 9.4: GC-FID parameters for conversions of homofarnesol and squalene showing the temperature program and the retention times of the different analysts.**

rate [°C/min]	final temp. [°C]	holding time [min]
-	120	2
4	200	0
60	320	14

retention times: ISTD1: 6.44 min, ambroxan: 18.56 min, *cis*-homofarnesol: 19.00 min, *trans*-homofarnesol: 19.26 min, squalene: 26.66 min, hopene: 30.36 min, hopanol: 32.44 min

**Table 9.5: GC-FID parameters for geranylacetone conversions showing the temperature program and the retention times of the different analysts.**

rate [°C/min]	final temp. [°C]	holding time [min]
-	120	0
5	200	0
50	300	5

retention times: ISTD1: 5.36 min, hexahydrochromene: 6.71 min, geranylacetone: 8.40 min

**Table 9.6: GC-FID parameters for farnesylacetone conversions showing the temperature program and the retention times of the different analysts.**

rate [°C/min]	final temp. [°C]	holding time [min]
-	200	0
10	220	0
5	250	0
50	300	3

retention times: ISTD1: 2.28 min, farnesylacetone: 4.42 / 4.61 / 4.80 min, sclareoloxide: 4.97 min

**Table 9.7: GC-FID parameters for nerolidol conversions showing the temperature program and the retention times of the different analysts.**

rate [°C/min]	final temp. [°C]	holding time [min]
-	100	2
10	300	2

retention times: ISTD1: 7.34 min, (-)-caparrapioxide: 10.03 min, (-)-8-*epi*-caparrapioxide: 10.20 min, *cis*-nerolidol: 10.85 min, *trans*-nerolidol: 11.22 min

**Table 9.8: GC-FID parameters for conversions of homofarnesoic acid, bishomofarnesol, bishomofarnesoic acid, bishomofarnesol, geraniol, geranic acid, farnesene, pseudoionone, beta-ionone and linalool showing the temperature program and the retention times of the different analysts.**

rate [°C/min]	final temp. [°C]	holding time [min]
-	100	0
15	300	5

retention times: ISTD1: 4.89 min, homofarnesoic acid: 9.46 min, sclareolide: 11.27 min, bishomofarnesol: 9.78 min, bishomofarnesol conversion product: 9.94 (major product) / 10.35 min, bishomofarnesoic acid: 10.01 min, bishomofarnesoic acid conversion product: 10.76 / 12.50 (major product) min, bishomofarnesol: 9.37 min, bishomofarnesol conversion product: 11.20 min, geraniol: 4.77 min, geranic acid: 4.83 / 4.89 / 4.99 / 5.11 / 5.33 (major product) min, farnesene: 6.43 (major product) / 7.18 min, pseudoionone: 6.85 / 7.07 / 7.48 (major product) min, beta-ionone: 6.78 min, linalool: 3.64 min

For GC-FID chromatograms see supporting information on CD-ROM.

## 9.10.2 GC-MS

GC-MS analyses were performed using He as a carrier gas (linear velocity 30 cm/sec). The injection temperature was set as 250°C and the detector temperature was set as 280°C. The MS detector was operating with 70 eV (EI ionisation) in full scan mode ranging from 40 m/z to 250 -420 m/z (depending on the molecular weight of the analysts). The temperature programs were as follows:

**Table 9.9: GC-MS parameters for squalene conversions showing the temperature program and the retention times of the different analysts.**

rate [°C/min]	final temp. [°C]	holding time [min]
-	120	0
20	320	20

retention times: squalene: 11.51 min, hopene: 15.87 min, hopanol: 18.36 min

**Table 9.10: GC-MS parameters for homofarnesol conversions showing the temperature program and the retention times of the different analysts.**

rate [°C/min]	final temp. [°C]	holding time [min]
-	120	3
20	205	0
3	225	0
15	320	8

retention times: *cis*-homofarnesol: 9.44 min, *trans*-homofarnesol: 9.56 min, ambroxan: 9.61 min

**Table 9.11: GC-MS parameters for homofarnesoic acid conversions showing the temperature program and the retention times of the different analysts.**

rate [°C/min]	final temp. [°C]	holding time [min]
-	100	2
10	300	2

retention times: homofarnesoic acid: 13.01 min, sclareolide: 15.70 min

**Table 9.12: GC-MS parameters for geranylacetone conversions showing the temperature program and the retention times of the different analysts.**

rate [°C/min]	final temp. [°C]	holding time [min]
-	100	2
10	300	2

retention times: hexahydrochromene: 9.07 min, geranylacetone: 10.29 min

**Table 9.13: GC-MS parameters for nerolidol conversions showing the temperature program and the retention times of the different analysts.**

rate [°C/min]	final temp. [°C]	holding time [min]
-	100	2
10	300	2

retention times: (-)-caparrapi oxide: 8.56 min, (-)-8-*epi*-caparrapi oxide: 8.90 min, *cis*-nerolidol: 9.91 min, *trans*-nerolidol: 10.29 min

For GC-MS chromatograms and spectra see supporting information on CD-ROM.



### 9.10.3 New products – characterization with NMR

The cyclic products of the conversions were characterized by comparison with authentic standards and standard nuclear magnetic resonance (NMR) methods after large scale conversion and isolation of the product using silica gel chromatography (9.9.4). The  $^1\text{H}$  and  $^{13}\text{C}$  NMR spectra were recorded on a Bruker Avance 500 spectrometer operating at 500.15 MHz. All spectra were recorded at room temperature in  $\text{CDCl}_3$ . Chemical shifts are expressed in parts per million (ppm,  $\delta$ ) and referenced to tetramethylsilane (TMS,  $\delta = 0$  ppm). The correct assignment of the chemical shifts was confirmed by application of two-dimensional correlation measurements, including correlation spectroscopy (COSY), heteronuclear single quantum coherence (HSQC), heteronuclear multiple bond coherence (HMBC), and nuclear Overhauser enhancement spectroscopy (NOESY). The numbering of the C-atoms is shown in Fig. 9.1. The product was characterized by  $^1\text{H}$ ,  $^{13}\text{C}$ , COSY, HSQC, HMBC and NOESY NMR. The H-atoms and C-atoms could be assigned by comparison with literature data.<sup>108</sup> The chemical shifts of  $^1\text{H}$  and  $^{13}\text{C}$  spectra are shown in Table 9.14, Table 9.15 and Table 9.16. The new bonds formed could be confirmed by HMBC signals. The three dimensional structures were confirmed with NOESY (Fig. 9.2 and Fig. 9.3).

For 2D and 3D NMR spectra see supporting information on CD-ROM.

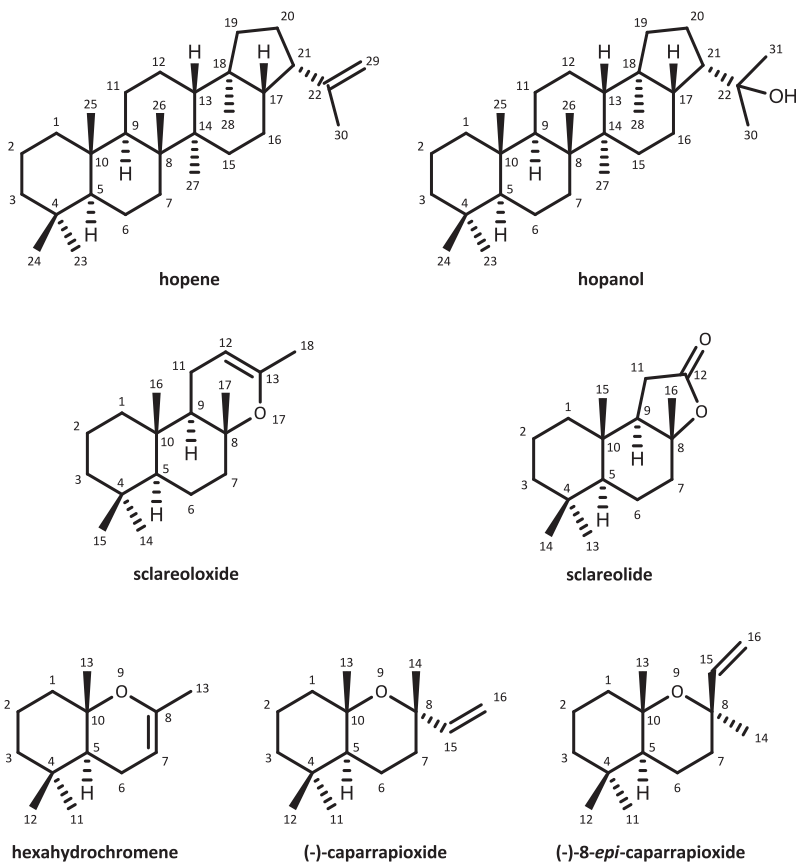


Fig. 9.1: Products characterized showing the numbering of the C-atoms.

**Table 9.14: Chemical shifts for  $^{13}\text{C}$  NMR expressed in parts per million (ppm,  $\delta$ ) and referenced to tetramethylsilane (TMS,  $\delta = 0$  ppm). The atom numbers are shown in Fig. 9.1.**

C-#	hopene	hopanol	scla-reolide	sclareol-oxide	(-)-caparrapi-oxide	(-)-8- <i>epi</i> -caparrapi-oxide	hexa-hydro-chromene
C-1	40.31	40.29	38.70	39.31	41.6*	41.7*	40.00
C-2	18.70	18.68	18.08	18.58	20.1	16.9	19.83
C-3	42.10	42.09	42.16	41.93	41.9*	41.5*	41.66
C-4	33.24	33.24	33.11	33.17	33.6	33.4	33.26
C-5	56.10	56.08	56.64	56.19	51.6	54.4	48.38
C-6	18.70	18.68	20.55	19.76	16.2	20.2	19.22
C-7	33.24	33.22	39.49	41.15	51.6	35.1	94.99
C-8	41.89	41.83	86.39	76.24	73.4	73.5	148.00
C-9	50.37	50.33	59.10	52.46	-	-	-
C-10	37.39	37.38	36.04	36.70	75.2	76.2	76.49
C-11	20.91	20.89	28.71	18.28	32.0	32.5	32.25
C-12	23.98	24.13	176.90	94.61	20.7	20.9	20.78
C-13	49.42	49.83	21.56	147.86	24.3	22.7	19.07
C-14	42.06	41.90	33.16	21.58	28.7	32.8	20.51
C-15	33.62	34.36	20.92	33.45	148.0	147.8	
C-16	21.66	21.95	15.06	15.03	110.2	109.5	
C-17	54.88	53.91		20.10			
C-18	44.78	44.08		20.47			
C-19	41.89	41.23					
C-20	27.38	26.60					
C-21	46.48	51.11					
C-22	148.76	73.94					
C-23	33.41	33.41					
C-24	21.59	21.59					
C-25	15.84	15.82					
C-26	16.69	17.02*					
C-27	16.75	16.71*					
C-28	16.07	16.14					
C-29	110.07	28.73					
C-30	25.02	30.85					

\* might be reversed

**Table 9.15: Chemical shifts for hopene and hopanol <sup>1</sup>H NMR expressed in parts per million (ppm,  $\delta$ ) and referenced to tetramethylsilane (TMS,  $\delta = 0$  ppm). The atom numbers are shown in Fig. 9.1.**

H-#	hopene	hopanol
H-1	1.65, 0.77	1.65, 0.74
H-2	1.54, 1.35	1.60, 1.41
H-3	1.33, 1.12	1.33, 1.12
H-4	-	-
H-5	0.69	0.72
H-6	1.49, 1.37	1.46, 1.33
H-7	1.48, 1.19	1.48, 1.23
H-8	-	-
H-9	1.25	1.25
H-10	-	-
H-11	1.54, 1.30	1.51, 1.30
H-12	1.46, 1.40 (e)	1.54, 1.38
H-13	1.33	1.38
H-14	-	-
H-15	1.38, 1.22	1.43, 1.22
H-16	1.62, 1.43	1.93, 1.57
H-17	1.35	1.35
H-18	-	-
H-19	1.60, 1.03	1.51, 0.93
H-20	1.84, 1.80	1.74, 1.47
H-21	2.67	2.22
H-22	-	-
H-23	0.84 (3H, s)	0.84 (3H, s)
H-24	0.79 (3H, s)	0.76 (3H, s)
H-25	0.81 (3H, s)	0.81 (3H, s)
H-26	0.96 (3H, s)	0.95 (6H, s)*
H-27	0.94 (3H, s)	0.95 (6H, s)*
H-28	0.72 (3H, s)	0.76 (3H, s)
H-29	4.78 (2H, s)	1.18 (3H, s)
H-30	1.75 (3H, s)	1.21 (3H, s)

\*methyl groups at C-26 and C-27 one signal

**Table 9.16: Chemical shifts for sclareolide, sclareoloxide, (-)-caparrapioxiide, (-)-8-epi-caparrapioxiide and hexahydrochromene  $^1\text{H}$  NMR expressed in parts per million (ppm,  $\delta$ ) and referenced to tetramethylsilane (TMS,  $\delta = 0$  ppm). The atom numbers are shown in Fig. 9.1.**

H-#	sclareoloxide	sclareolide	(-)-caparrapioxiide	(-)-8-epi-caparrapioxiide	hexahydrochromene
H-1	1.62*	1.43, 1.08	1.22 (a)**	1.65 (e), 1.30 (a)	1.82 (e), 1.46 (a)
H-2	1.78 (e), 1.42 (a)	1.64 (a), 1.48 (e)	1.52 (m, 2H)	1.55 (e), 1.44 (a)	1.58, 1.49
H-3	1.37 (a), 1.13 (e)	1.45 (e), 1.20 (a)	1.70 (a)***, 1.38 (e)***	1.36 (e), 1.23 (a)	1.40 (e), 1.26 (a)
H-5	0.97	1.05	1.36	1.25	1.44
H-6	1.70 (e), 1.29 (a)	1.88, 1.38	1.58 (e), 1.50 (a)	1.5 (m, 2H)	1.92 (e), 1.75 (a)
H-7	1.93 (e), 1.52 (a)	2.08 (e), 1.73 (a)	1.78 (e)	2.22 (a), 1.5 (e)	4.46
H-9	1.39	1.97			
H-11	1.82 (a), 1.58 (e)	2.41 (a), 2.23 (e)	0.86 (3H, s)	0.89 (3H, s)	0.91 (3H, s)
H-12	4.43	-	0.79 (3H, s)	0.73 (3H, s)	0.82 (3H, s)
H-13		0.84 (3H, s)	1.30 (3H, s)	1.22 (3H, s)	1.17 (3H, s)
H-14	0.81 (3H, s)	0.89 (3H, s)	1.28 (3H, s)	1.14 (3H, s)	1.69 (3H, s)
H-15	0.88 (3H, s)	0.91 (3H, s)	5.89 (dd, J = 17.23, J' = 10.49)	6.01 (dd, J = 17.71, J' = 10.73)	
H-16	0.81 (3H, s)	1.34 (3H, s)	5.15 (Z, d, J = 17.55), 4.92 (E, d, J = 10.83)	4.98 (Z, d, J = 18.16), 4.92 (E, d, J = 10.77)	
H-17	1.15 (3H, s)				
H-18	1.68 (3H, s)				

\*no HSQC for the second H-1 could be seen

\*\*H-1(e) below one of these

\*\*\* might be reversed

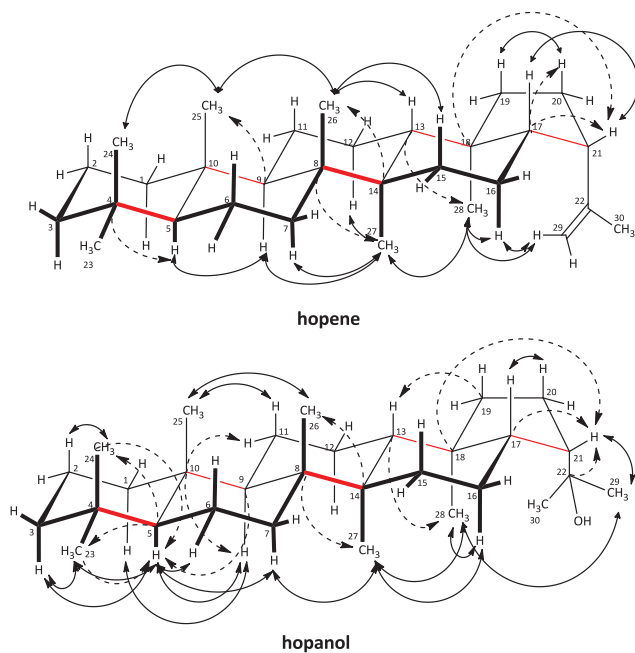


**Fig. 9.2: Products hopene and hopanol in chair conformation showing the HMBC signals as dashed and the NOESY signals as black arrows. The new formed carbon-carbon bonds are marked in red.**

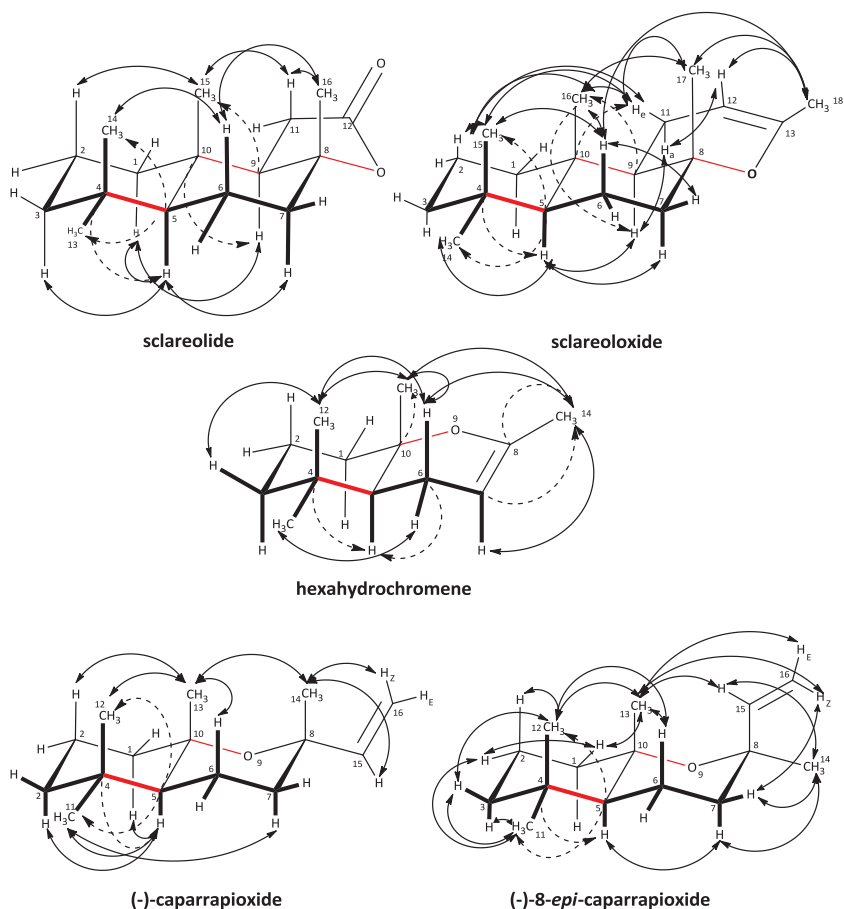


**Fig. 9.3:** New products sclareolide, sclareoloxide, hexahydrochromene, (-)-caparrapioxide and (-)-8-*epi*-caparrapioxide in chair conformation showing the HMBC signals as dashed and the NOESY signals as black arrows. The new formed carbon-carbon bonds are marked in red.

### 9.10.4 IR and HREIMS analyses

IR spectra were measured on a Bruker Vector 22 FT-IR spectrometer in an ATR mode. Mass spectra were measured using electron impact ionization on a Finnigan MAT 95. The values for HREIMS are as follows:

**hopene:** predicted as 410.3913 and determined as 410.3916.<sup>107</sup> Full MS spectrum:  $m/z$  (rel. int.) 410 [M] (75), 395 (14), 367 (5), 342 (9), 299 (13), 218 (19), 204 (18), 191 (100), 189 (78),

177 (10), 161 (14), 150 (13), 138 (17), 121 (19), 109 (27), 95 (34), 81 (29), 69 (26), 55 (16). 41 (10).

**hopanol:** predicted as 428.4018 and determined as 428.4016.<sup>285</sup> Full MS spectrum: m/z (rel. int.): 428 [M] (32), 410 (16), 395 (9), 370 (15), 355 (6), 231 (6), 207 (38), 191 (100), 177 (8), 163 (15), 149 (58), 137 (16), 113 (16), 109 (18), 95 (39), 81 (22), 69 (21), 59 (30), 43 (9).

**sclareoloxide:** predicted as 262.2297 and determined as 262.2297. Full MS spectrum: m/z (rel. int.): 262 [M] (3), 247 (1), 212 (3), 197 (3), 183 (7), 169 (10), 155 (10), 141 (8), 113 (14), 99 (17), 85 (52), 71 (69), 57 (100), 43 (49).

**(-)-caparrapioxiide:** predicted as 222.1984 and determined as 222.1981.<sup>219</sup> Full MS spectrum: m/z (rel. int.): 222 [M] (4), 207 (100), 189 (25), 177 (7), 152 (7), 137 (13), 124 (33), 109 (47), 95 (16), 81 (35), 69 (21), 55 (17), 43 (21).

**(-)-8-epi-caparrapioxiide:** predicted as 222.1984 and determined as 222.1982.<sup>219</sup> Full MS spectrum: m/z (rel. int.): 222 [M] (3), 207 (100), 189 (21), 177 (7), 152 (8), 137 (13), 124 (32), 109 (46), 95 (16), 81 (34), 69 (21), 55 (18), 43 (24).

**sclareolide:** predicted as 250.3807 and determined as 250.1930.<sup>286</sup> Full MS spectrum: m/z (rel. int.): 250 [M] (5), 235 (82), 206 (54), 191 (18), 177 (14), 163 (8), 150 (25), 137 (45), 136 (42), 123 (100), 109 (58), 95 (67), 82 (65), 81 (52), 69 (54), 67 (35), 55 (41), 43 (64)

**hexahydrochromene:** predicted as 194.1671 and determined as 194.1668. Full MS spectrum: m/z (rel. int.): 194 [M] (52), 179 (19), 161 (21), 151 (12), 136 (20), 123 (34), 109 (100), 95 (23), 81 (26), 71 (24), 55 (17), 43 (38).

For IR and HREIMS spectra see supporting information on CD-ROM.

### 9.10.5 Determination of log P values

The log P values of the substrates and products were determined using the online tool on the vcclab (virtual computational chemistry laboratory) homepage using the ALOGPS 2.1 program (Table 9.17).<sup>271-273</sup>



**Table 9.17: Log P values of the substrates and products determined with ALOGP 2.1.**

	log P
squalene	10.60 ± 2.34
hopene	9.21 ± 1.88
hopanol	8.18 ± 1.67
farnesylacetone	5.58 ± 1.04
sclareoloxide	5.26 ± 0.90
homofarnesol	5.01 ± 1.02
ambroxan	4.43 ± 0.75
homofarnesosoic acid	4.91 ± 1.02
sclareolide	4.05 ± 0.79
nerolidol	4.67 ± 0.57
caparrapioxide	4.24 ± 0.60
geranylacetone	4.00 ± 0.53
hexahydrochromene	3.85 ± 0.68

### 9.10.6 Quantification

The concentrations of the internal standards in the samples were determined with an external calibration curve. Using effective carbon number (ECN) values, the concentrations all of the substrates and products could be determined in reference to the internal standards. ISTD1 was used for correction of the loss of the analysts during extraction.

The concentrations of the internal standards in the samples were determined with an external calibration curve. Using an internal standard (1-decanol) and external calibration of this, the substrates and products were quantified by using relative response factors (RF). These RF values are calculated from the ECNs of the different compounds ( $ECN_x$ ) in relation to ECN of the internal standard ( $ECN_{ISTD}$ ) using the following equation (1).<sup>287</sup>

$$RF = \frac{ECN_x}{ECN_{ISTD}} \quad (1)$$

The concentration of the internal standard ( $C_{ISTD}$ ) was determined by external calibration and the concentrations of the analysts ( $c_x$ ) could be determined from the GC peak areas ( $area_{ISTD}$ ,  $area_x$ ) using the following equation (2).

$$c_x = \frac{c_{ISTD}}{RF} \times \frac{area_x}{area_{ISTD}} \quad (2)$$

The ECNs and RF values of the different compounds are given in Table 9.18.

**Table 9.18: Calculated effective carbon numbers (ECN) of the substrates and products and the relative response factors (RF) in relation to the internal standard 1-decanol.**

compound	ECN	RF
1-decanol	9.50	1.00
squalene	29.40	3.09
hopene	29.90	3.15
hopanol	29.75	3.13
homofarnesol	14.45	1.52
ambrox	15.00	1.58
homofarnesoic acid	14.70	1.55
homofarnesoic acid derivate TMSH	17.70	1.86
sclareolide	15.00	1.58
linalool	9.30	0.98
nerolidol	14.20	1.49
(-)-caparrapioxide	13.90	1.46
(-)-8- <i>epi</i> -caparrapioxide	13.90	1.46
geranylacetone	11.80	1.24
hexahydrochromene	11.90	1.25
pseudoionone	11.70	1.23
farnesylacetone	16.70	1.76
sclaroeloxide	16.90	1.78

## 10 Literature

1. Christianson, D. W. Structural biology and chemistry of the terpenoid cyclases. *Chemical Reviews* **106**, 3412–3442 (2006).
2. Christianson, D. W. Unearthing the roots of the terpenome. *Current Opinion in Chemical Biology* **12**, 141–150 (2008).
3. Waknine-Grinberg, J. H. *et al.* Artemisone effective against murine cerebral malaria. *Malaria Journal* **9**, 227 (2010).
4. Degenhardt, J., Köllner, T. G. & Gershenzon, J. Monoterpene and sesquiterpene synthases and the origin of terpene skeletal diversity in plants. *Phytochemistry* **70**, 1621–1637 (2009).
5. Sandler, A. *et al.* Paclitaxel-carboplatin alone or with bevacizumab for non-small-cell lung cancer. *The New England Journal of Medicine* **355**, 2542–2550 (2006).
6. Volkman, J. K. Sterols and other triterpenoids: source specificity and evolution of biosynthetic pathways. *Organic Geochemistry* **36**, 139–159 (2005).
7. Davis, E. M. & Croteau, R. Cyclization Enzymes in the Biosynthesis of Monoterpenes, Sesquiterpenes, and Diterpenes. *Topics in Current Chemistry* **209**, 53–95 (2000).
8. Siedenburg, G. & Jendrossek, D. Squalene-hopene cyclases. *Applied and Environmental Microbiology* **77**, 3905–3915 (2011).
9. Abe, I., Rohmer, M. & Prestwich, G. D. Enzymatic cyclization of squalene and oxidosqualene to sterols and triterpenes. *Chemical Reviews* **93**, 2189–2206 (1993).
10. Racolta, S., Juhl, P. B., Sirim, D. & Pleiss, J. The triterpene cyclase protein family: A systematic analysis. *Proteins* **80**, 2009–2019 (2012).
11. Wendt, K. U., Feil, C., Lenhart, A., Poralla, K. & Schulz, G. E. Crystallization and preliminary X-ray crystallographic analysis of squalene-hopene cyclase from *Alicyclobacillus acidocaldarius*. *Protein Science* **6**, 722–724 (1997).
12. Wendt, K. U., Lenhart, A. & Schulz, G. E. The Structure of the Membrane Protein Squalene-Hopene Cyclase at 2.0 Å resolution. *Structure* **286**, 175–187 (1999).
13. Hoshino, T. & Sato, T. Squalene-hopene cyclase: catalytic mechanism and substrate recognition. *Chemical Communications* **4**, 291–301 (2002).

14. Perzl, M. *et al.* Cloning of conserved genes from *Zymomonas mobilis* and *Bradyrhizobium japonicum* that function in the biosynthesis of hopanoid lipids. *Biochimica et Biophysica Acta* **1393**, 108–118 (1998).
15. Reipen, I. G., Poralla, K., Sahn, H. & Sprenger, G. A. *Zymomonas mobilis* squalene-hopene cyclase gene (*shc*): cloning, DNA sequence analysis and expression in *Escherichia coli*. *Microbiology* **141**, 155–161 (1995).
16. Neumann, S. & Simon, H. Purification, Partial Characterization and Substrate Specificity of a Squalene Cyclase from *Bacillus acidocaldarius*. *Biological Chemistry Hoppe-Seyler* **367**, 723–730 (1986).
17. Hoshino, T., Kumai, Y., Kudo, I., Nakano, S. & Ohashi, S. Enzymatic cyclization reactions of geraniol, farnesol and geranylgeraniol, and those of truncated squalene analogs having C20 and C25 by recombinant squalene cyclase. *Organic & Biomolecular Chemistry* **2**, 2650–2657 (2004).
18. Tanaka, H., Noma, H., Noguchi, H. & Abe, I. Enzymatic formation of pyrrole-containing novel cyclic polyprenoids by bacterial squalene:hopene cyclase. *Tetrahedron Letters* **47**, 3085–3089 (2006).
19. Tanaka, H., Noguchi, H. & Abe, I. Enzymatic formation of indole-containing unnatural cyclic polyprenoids by bacterial squalene:hopene cyclase. *Organic Letters* **7**, 5873–5876 (2005).
20. Schäfer, B. Ambrox®. *Chemie in unserer Zeit* **45**, 374–388 (2011).
21. Frija, L. M. T., Frade, R. F. M. & Afonso, C. A. M. Isolation, Chemical, and Biotransformation Routes of Labdane-type Diterpenes. *Chemical Reviews* **111**, 4418–4452 (2011).
22. Buckholz, L. J., Farbood, M. I., Kossiakkoff, N. & Scharpf, L. G. Use of sclareolide in augmenting or enhancing the organoleptic properties of foodstuffs. European Patent EP0420402 (1990).
23. Barrero, A. F., Alvarez-Manzaneda, E. J., Chahboun, R. & Coral Páiz, M. A new enantiospecific route toward monocarbocyclic terpenoids: Synthesis of (–)-caparrapi oxide. *Tetrahedron Letters* **39**, 9543–9544 (1998).
24. Ohloff, G., Giersch, W., Schulte-Elte, K. H. & Vial, C. Zur Stereochemie der Geruchswahrnehmung von 1-Dekalon-Derivaten und ihren oxaanalogen Verbindungen. *Helvetica Chimica Acta* **59**, 1140–1157 (1976).
25. Nasu, S. S. *et al.* Puupehenone-related metabolites from two Hawaiian sponges, *Hyrtios* spp. *The Journal of Organic Chemistry* **60**, 7290–7292 (1995).

26. Loya, S., Tal, R., Kashman, Y. & Hizi, A. Illimaquinone, a selective inhibitor of the RNase H activity of human immunodeficiency virus type 1 reverse transcriptase. *Antimicrobial Agents and Chemotherapy* **34**, 2009–2012 (1990).
27. Whitfield, F. B., Stanley, G. & Murray, K. E. Concerning the structures of edulan I and II. *Tetrahedron Letters* **14**, 95–98 (1973).
28. Stork, G. & Burgstahler, A. W. The Stereochemistry of Polyene Cyclization. *Journal of the American Chemical Society* **77**, 5068–5077 (1955).
29. Eschenmoser, A., Ruzicka, L., Jeger, O. & Arigoni, D. Zur Kenntnis der Triterpene. 190. Mitteilung. Eine stereochemische Interpretation der biogenetischen Isoprenregel bei den Triterpenen. *Helvetica Chimica Acta* **38**, 1890–1904 (1955).
30. Ruzicka, L., Stoll, M. & Schinz, H. Zur Kenntnis des Kohlenstoffringes II. Synthese der carbocyclischen Ketone vom Zehner- bis zum Achtzehnering. *Helvetica Chimica Acta* **9**, 249–264 (1926).
31. Ruzicka, L., Meyer, J. & Mingazzini, M. Hoehere Terpenverbindungen III. Ueber die Naphtalinkohlenwasserstoffe Cadalin und Eudalin, zwei aromatische Grundkoerper der Sesquiterpenreihe. *Helvetica Chimica Acta* **5**, 345–368 (1922).
32. Ourisson, G. The general role of terpenes and their global significance. *Pure and Applied Chemistry* **62**, 1401–1404 (1990).
33. Hargittai, I. Guy Ourisson (1926–2006). *Structural Chemistry* **18**, 415–416 (2007).
34. Rodríguez-Concepción, M. & Boronat, A. Elucidation of the methylerythritol phosphate pathway for isoprenoid biosynthesis in bacteria and plastids. A metabolic milestone achieved through genomics. *Plant Physiology* **130**, 1079–89 (2002).
35. Croteau, R., Kutchan, T. M. & Lewis, N. G. *Biochemistry and Molecular Biology of Plants - Chapter 24: Natural products (secondary metabolites)*. 1250–1268 (2000).
36. Martin, V. J. J., Pitera, D. J., Withers, S. T., Newman, J. D. & Keasling, J. D. Engineering a mevalonate pathway in *Escherichia coli* for production of terpenoids. *Nature Biotechnology* **21**, 796–802 (2003).
37. Dictionary of Natural Products. <http://dnp.chemnetbase.com> (2012).
38. Gershenzon, J. & Dudareva, N. The function of terpene natural products in the natural world. *Nature Chemical Biology* **3**, 408–414 (2007).
39. Ourisson, G. & Nakatani, Y. The terpenoid theory of the origin of cellular life: the evolution of terpenoids to cholesterol. *Chemistry & Biology* **1**, 11–23 (1994).

40. Sangwan, N. S., Farooqi, A. H. A., Shabih, F. & Sangwan, R. S. Regulation of essential oil production in plants. *Plant Growth Regulation* **34**, 3–21
41. Lichtenthaler, H. K. The 1-deoxy-D-xylulose-5-phosphate pathway of isoprenoid biosynthesis in plants. *Annual Review of Plant Physiology and Plant Molecular Biology* **50**, 47–65 (1999).
42. Flesch, G. & Rohmer, M. Prokaryotic hopanoids: the biosynthesis of the bacteriohopane skeleton. Formation of isoprenic units from two distinct acetate pools and a novel type of carbon/carbon linkage between a triterpene and d-ribose. *European Journal of Biochemistry* **175**, 405–411 (1988).
43. Sahm, H., Rohmer, M., Bringer-Meyer, S., Sprenger, G. a & Welle, R. Biochemistry and physiology of hopanoids in bacteria. *Advances in Microbial Physiology* **35**, 247–273 (1993).
44. Harrewijn, P., Oosten, A. M. V. & Piron, P. G. M. *Natural Terpenoids As Messengers: A Multidisciplinary Study of Their Production, Biological Functions, and Practical Applications*. (2001).
45. Rohmer, M., Knani, M., Simonin, P., Sutter, B. & Sahm, H. Isoprenoid biosynthesis in bacteria: a novel pathway for the early steps leading to isopentenyl diphosphate. *The Biochemical Journal* **295**, 517–524 (1993).
46. Wendt, K. U. & Schulz, G. E. Isoprenoid biosynthesis: manifold chemistry catalyzed by similar enzymes. *Structure* **6**, 127–133 (1998).
47. Poulter, C. D. & Rilling, H. C. The prenyl transfer reaction. Enzymic and mechanistic studies of the 1'-4 coupling reaction in the terpene biosynthetic pathway. *Accounts of Chemical Research* **11**, 307–313 (1978).
48. Gao, Y., Honzatko, R. B. & Peters, R. J. Terpene synthase structures: a so far incomplete view of complex catalysis. *Natural Product Reports* **29**, 1153–1175 (2012).
49. Wallach, O. Zur Kenntniss der Terpene und der ätherischen Oele; Fünfte Abhandlung. *Justus Liebig's Annalen der Chemie* **239**, 1–54 (1887).
50. Ruzicka, L. & Capato, E. Hoehere Terpenverbindungen XXIV. Ringbildungen bei Sesquiterpenen. Totalsynthese des Bisabolens und eines Hexahydro-cadalins. *Helvetica Chimica Acta* **8**, 259–274 (1925).
51. Ruzicka, L. The isoprene rule and the biogenesis of terpenic compounds. *Experientia* **9**, 357–367 (1953).

52. Eschenmoser, A. & Arigoni, D. Revisited after 50 Years: The "Stereochemical Interpretation of the Biogenetic Isoprene Rule for the Triterpenes." *Helvetica Chimica Acta* **88**, 3011–3050 (2005).
53. Corey, E. J. & Russey, W. E. Metabolic Fate of 10,11-Dihydrosqualene in Sterol-Producing Rat Liver Homogenate. *Journal of the American Chemical Society* **80**, 4751–4752 (1966).
54. Corey, E. J., Ortiz de Montellano, P. R., Lin, K. & Dean, P. D. G. 2,3-Iminosqualene, a Potent Inhibitor of the Enzymatic Cyclization of 2,3-Oxidosqualene to Sterols. *Journal of the American Chemical Society* **89**, 2797–2798 (1967).
55. Corey, E. J. & Gross, S. K. Formation of Sterols by the Action of 2,3-Oxidosqualene-Sterol Cyclase on the Factitious Substrates 2,3 : 22,23-Dioxidosqualene and 2,3-Oxido-22,23-dihydrosqualene. *Journal of the American Chemical Society* **89**, 4561–4562 (1967).
56. Corey, E. J. *et al.* Studies on the Substrate Binding Segments and Catalytic Action of Lanosterol Synthase . Affinity Labeling with Carbocations Derived from Mechanism-Based Analogs of 2 , 3-Oxidosqualene and Site-Directed Mutagenesis Probes. *Journal of the American Chemical Society* **119**, 1289–1296 (1997).
57. Corey, E. J. & Cheng, H. Conversion of a C20 2,3-Oxidosqualene Analog to Tricyclic Structures with a Five-Membered C-Ring by Lanosterol Synthase. Further Evidence For a C-Ring Expansion Step in Sterol Biosynthesis. *Science* **37**, 2709–2712 (1996).
58. Wendt, K., Schulz, G., Corey, E. & Liu, D. Enzyme Mechanisms for Polycyclic Triterpene Formation. *Angewandte Chemie (International ed. in English)* **39**, 2812–2833 (2000).
59. Corey, E. J., Virgil, S. C. & Sarshar, S. New mechanistic and stereochemical insights on the biosynthesis of sterols from 2,3-oxidosqualene. *Journal of the American Chemical Society* **113**, 8171–8172 (1991).
60. Siedenburg, G. & Jendrossek, D. Squalene-hopene cyclases. *Applied and Environmental Microbiology* **77**, 3905–3915 (2011).
61. Dougherty, D. A. Cation- $\pi$  Interactions in Chemistry and Biology: A New View of Benzene, Phe, Tyr, and Trp. *Science* **271**, 163–168 (1996).
62. Croteau, R. Biosynthesis and catabolism of monoterpenoids. *Chemical Reviews* **87**, 929–954 (1987).
63. Hyatt, D. C. *et al.* Structure of limonene synthase, a simple model for terpenoid cyclase catalysis. *Proceedings of the National Academy of Sciences of the United States of America* **104**, 5360–5365 (2007).

64. Yoon, C., Kang, S.-H., Jang, S.-A., Kim, Y.-J. & Kim, G.-H. Repellent Efficacy of Caraway and Grapefruit Oils for *Sitophilus oryzae* (Coleoptera: Curculionidae). *Journal of Asia-Pacific Entomology* **10**, 263–267 (2007).
65. Tarshis, L. C. Regulation of product chain length by isoprenyl diphosphate synthases. *Proceedings of the National Academy of Sciences* **93**, 15018–15023 (1996).
66. Kellogg, B. A. & Poulter, C. D. Chain elongation in the isoprenoid biosynthetic pathway. *Current Opinion in Chemical Biology* **1**, 570–578 (1997).
67. Cane, D. E. Enzymic formation of sesquiterpenes. *Chemical Reviews* **90**, 1089–1103 (1990).
68. Rynkiewicz, M. J., Cane, D. E. & Christianson, D. W. Structure of trichodiene synthase from *Fusarium sporotrichioides* provides mechanistic inferences on the terpene cyclization cascade. *Proceedings of the National Academy of Sciences of the United States of America* **98**, 13543–13548 (2001).
69. Cane, D. E., Shim, J. H., Xue, Q., Fitzsimons, B. C. & Hohn, T. M. Trichodiene Synthase. Identification of Active Site Residues by Site-Directed Mutagenesis. *Biochemistry* **34**, 2480–2488 (1995).
70. Back, K. & Chappell, J. Identifying functional domains within terpene cyclases using a domain-swapping strategy. *Proceedings of the National Academy of Sciences* **93**, 6841–6845 (1996).
71. Starks, C. M. Structural Basis for Cyclic Terpene Biosynthesis by Tobacco 5-Epi-Aristolochene Synthase. *Science* **277**, 1815–1820 (1997).
72. Isoe, S., Katsumura, S. & Sakan, T. The Synthesis of Damascenone and beta-Damascone and the possible mechanism of their formation from carotenoids. *Helvetica Chimica Acta* **56**, 1514–1516 (1973).
73. Schäfer, B. *Naturstoffe der chemischen Industrie (German Edition)*. (Spektrum Akademischer Verlag: 2006).
74. Daniel, D. M. *Medicinal Plants: Chemistry and Properties*. (2006).
75. Witschel, M. C. & Bestmann, H. J. Synthese der Pestwurzinhaltstoffe (+)-Petasin und (+)-Isopetasin. *Tetrahedron Letters* **36**, 3325–3328 (1995).
76. Alireza, M. Antimicrobial activity and chemical composition of essential oils of chamomile from Neyshabur, Iran. *Journal of Medicinal Plants Research* **6**, 820–824 (2012).
77. Owlia, P., Rasooli, I. & Saderi, H. Antistreptococcal and Antioxidant Activity of Essential Oil from *Matricaria chamomilla* L. *Research Journal of Biological Sciences* **2**, 155–160 (2007).



78. Bowden, B., Coll, J. & Tapiolas, D. Studies of Australian soft corals. XXX. A novel trisnorsesquiterpene from a *Cespitularia* species and the isolation of guaiazulene from a small blue *Alcyonium* species. *Australian Journal of Chemistry* **36**, 211–214 (1983).
79. Jaspers, N. G. . *et al.* Anti-tumour compounds illudin S and Irofulven induce DNA lesions ignored by global repair and exclusively processed by transcription- and replication-coupled repair pathways. *DNA Repair* **1**, 1027–1038 (2002).
80. Bohlmann, J. & Keeling, C. I. Terpenoid biomaterials. *The Plant Journal: For Cell and Molecular Biology* **54**, 656–669 (2008).
81. Ro, D.-K. *et al.* Production of the antimalarial drug precursor artemisinic acid in engineered yeast. *Nature* **440**, 940–943 (2006).
82. Bollinger, P., Sigg, H. P. & Weber, H. P. Structure of ovalicin. *Helvetica Chimica Acta* **56**, 819–830 (1973).
83. Fernandes, E. S. *et al.* Anti-inflammatory effects of compounds alpha-humulene and (-)-trans-caryophyllene isolated from the essential oil of *Cordia verbenacea*. *European Journal of Pharmacology* **569**, 228–236 (2007).
84. Amaro-Luis, J. M., Ramírez, I., Delgado-Méndez, P. & Jorge, Z. D. Eudesmane Derivatives from *Verbesina turbacensis*. *Journal of the Brazilian Chemical Society* **13**, 352–357 (2002).
85. Bohlmann, J., Meyer-Gauen, G. & Croteau, R. Inaugural Article: Plant terpenoid synthases: Molecular biology and phylogenetic analysis. *Proceedings of the National Academy of Sciences* **95**, 4126–4133 (1998).
86. Toyomasu, T. *et al.* Cloning of a Full-length cDNA Encoding ent-Kaurene Synthase from *Gibberella fujikuroi*: Functional Analysis of a Bifunctional Diterpene Cyclase. *Bioscience, Biotechnology, and Biochemistry* **64**, 660–664 (2000).
87. Moesta, P. & West, C. A. Casbene synthetase: Regulation of phytoalexin biosynthesis in *Ricinus communis* L. seedlings. *Archives of Biochemistry and Biophysics* **238**, 325–333 (1985).
88. Mau, C. Cloning of Casbene Synthase cDNA: Evidence for Conserved Structural Features Among Terpenoid Cyclases in Plants. *Proceedings of the National Academy of Sciences* **91**, 8497–8501 (1994).
89. Ochs, D., Kaletta, C., Entian, K.-D., Beck-Sickinger, A. & Poralla, K. Cloning, Expression, and Sequencing of Squalene-Hopene Cyclase, a Key Enzyme in Triterpenoid Metabolism. *Microbiology* **174**, 298–302 (1992).

90. Cyr, A., Wilderman, P. R., Determan, M. & Peters, R. J. A modular approach for facile biosynthesis of labdane-related diterpenes. *Journal of the American Chemical Society* **129**, 6684–6685 (2007).
91. Geuns, J. Stevioside. *Phytochemistry* **64**, 913–921 (2003).
92. Nozoe, S., Morisaki, M., Tsuda, K. & Okuda, S. Biogenesis of ophiobolins. The origin of the oxygen atoms in the ophiobolins. *Tetrahedron Letters* **8**, 3365–3368 (1967).
93. Canonica, L. *et al.* The biosynthesis-of ophiobolins. *Tetrahedron Letters* **8**, 3371–3376 (1967).
94. Nozoe, S., Morisaki, M., Okuda, S. & Tsuda, K. Biosynthesis of ophiobolins from the doubly labeled mevalonate. *Tetrahedron Letters* **9**, 2347–2349 (1968).
95. Au, T. K., Chick, W. S. H. & Leung, P. C. The biology of ophiobolins. *Life Sciences* **67**, 733–742 (2000).
96. Nozoe, S. *et al.* The Structure of Ophiobolin, a C25 Terpenoid Having a Novel Skeleton. *Journal of the American Chemical Society* **87**, 4968–4970 (1965).
97. Sugawara, F. Phytotoxins from the Pathogenic Fungi *Drechslera maydis* and *Drechslera sorghicola*. *Proceedings of the National Academy of Sciences* **84**, 3081–3085 (1987).
98. Sugawara, F. *et al.* Some new phytotoxic ophiobolins produced by *Drechslera oryzae*. *The Journal of Organic Chemistry* **53**, 2170–2172 (1988).
99. Reddy, L. H. & Couvreur, P. Squalene: A natural triterpene for use in disease management and therapy. *Advanced Drug Delivery Reviews* **61**, 1412–1426 (2009).
100. Singh, S. B. *et al.* Structure and conformation of ophiobolin K and 6- epiophiobolin K from *Aspergillus ustus* as a nematocidal agent. *Tetrahedron* **47**, 6931–6938 (1991).
101. Appendino, G. *et al.* Genepolide, a sesterpene gamma-lactone with a novel carbon skeleton from mountain wormwood (*Artemisia umbelliformis*). *Journal of Natural Products* **72**, 340–344 (2009).
102. Cimino, G., De Stefano, S., Minale, L. & Fattorusso, E. Ircinin-1 and -2, linear sesterterpenes from the marine sponge *Ircinia oros*. *Tetrahedron* **28**, 333–341 (1972).
103. Liu, Y. *et al.* New Cytotoxic Sesterterpenes from the Sponge *Sarcotragus* Species. *Journal of Natural Products* **64**, 1301–1304 (2001).
104. Rowland, S. J. *et al.* Effects of temperature on polyunsaturation in cytostatic lipids of *Haslea ostrearia*. *Phytochemistry* **56**, 597–602 (2001).

105. Ruzicka, L. Proceedings of the Chemical Society. *Proceedings of the Chemical Society* 341 (1959).
106. Jäger, S., Trojan, H., Kopp, T., Laszczyk, M. N. & Scheffler, A. Pentacyclic triterpene distribution in various plants - rich sources for a new group of multi-potent plant extracts. *Molecules (Basel, Switzerland)* **14**, 2016–2031 (2009).
107. Ageta, H. & Arai, Y. Fern constituents: pentacyclic triterpenoids isolated from *Polypodium niponicum* and *P. formosanum*. *Phytochemistry* **22**, 1801–1808 (1983).
108. Ageta, H., Shiojima, K., Suzuki, H. & Nakamura, S. NMR Spectra of Triterpenoids. I. Conformation of the Side Chain of Hopane and Isohopane, and Their Derivatives. *Chemical & Pharmaceutical Bulletin* **41**, 1939–1943 (1993).
109. Shiojima, K., Sasaki, Y. & Ageta, H. Fern Constituents : Triterpenoids Isolated from the Leaves of *Adiantum pedatum*. 23-Hydroxyfernene, Glaucanol A and Filicenoic Acid. *Chemical & Pharmaceutical Bulletin* **41**, 268–271 (1993).
110. Shiojima, K. *et al.* Mass spectra of pentacyclic triterpenoids. *Chemical & Pharmaceutical Bulletin* **40**, 1683–1690 (1992).
111. Nes, W. D. & Heftmann, E. A Comparison of Triterpenoids with Steroids as Membrane Components. *Journal of Natural Products* **44**, 377–400 (1981).
112. Heftmann, E. Functions of sterols in plants. *Lipids* **6**, 128–133 (1971).
113. Taylor, R. F. Bacterial triterpenoids. *Microbiological Reviews* **48**, 181–198 (1984).
114. Poralla, K. Effect of temperature and pH on the hopanoid content of *Bacillus acidocaldarius*. *FEMS Microbiology Letters* **23**, 253–256 (1984).
115. Rohmer, M., Bouvier, P. & Ourisson, G. Molecular evolution of biomembranes: structural equivalents and phylogenetic precursors of sterols. *Proceedings of the National Academy of Sciences of the United States of America* **76**, 847–851 (1979).
116. Nes, W. R. Role of sterols in membranes. *Lipids* **9**, 596–612 (1974).
117. Ourisson, G., Rohmer, M. & Poralla, K. Prokaryotic Hopanoids and other Polyterpenoid Sterol Surrogates. *Annual Review of Microbiology* **41**, 301–333 (1987).
118. Rohmer, M., Bouvier-Nave, P. & Ourisson, G. Distribution of Hopanoid Triterpenes in Prokaryotes. *Microbiology* **130**, 1137–1150 (1984).
119. Ourisson, G., Chimie, I. D., Pasteur, U. L. & Neurochimie, C. D. The evolution of terpenes to sterols. *Pure and Applied Chemistry* **61**, 345–348 (1989).

120. Ourisson, G., Albrecht, P. & Rohmer, M. Predictive microbial biochemistry — from molecular fossils to procaryotic membranes. *Trends in Biochemical Sciences* **7**, 236–239 (1982).
121. Sato, T. & Hoshino, T. Catalytic Function of the Residues of Phenylalanine and Tyrosine Conserved in Squalene-Hopene Cyclases. *Bioscience, Biotechnology, and Biochemistry* **65**, 2233–2242 (2001).
122. Raymond, J. & Blankenship, R. E. Biosynthetic pathways, gene replacement and the antiquity of life. *Geobiology* **2**, 199–203 (2004).
123. Pearson, A., Budin, M. & Brocks, J. J. Phylogenetic and biochemical evidence for sterol synthesis in the bacterium Gemmata obscuriglobus. *Proceedings of the National Academy of Sciences of the United States of America* **100**, 15352–15357 (2003).
124. Volkman, J. K. Sterols in microorganisms. *Applied Microbiology and Biotechnology* **60**, 495–506 (2003).
125. Tippelt, a, Jahnke, L. & Poralla, K. Squalene-hopene cyclase from *Methylococcus capsulatus* (Bath): a bacterium producing hopanoids and steroids. *Biochimica et Biophysica Acta* **1391**, 223–232 (1998).
126. Lamb, D. C. *et al.* Lanosterol biosynthesis in the prokaryote *Methylococcus capsulatus*: insight into the evolution of sterol biosynthesis. *Molecular Biology and Evolution* **24**, 1714–1721 (2007).
127. Nakano, C., Motegi, A., Sato, T., Onodera, M. & Hoshino, T. Sterol Biosynthesis by a Prokaryote: First in Vitro Identification of the Genes Encoding Squalene Epoxidase and Lanosterol Synthase from *Methylococcus capsulatus*. *Bioscience, Biotechnology, and Biochemistry* **71**, 2543–2550 (2007).
128. Rohmer, M., Bisseret, P. & Neunlist, S. The hopanoids, prokaryotic triterpenoids and precursors of ubiquitous molecular fossils. *Biological Markers in Sediments and Petroleum* 1–17 (1992).
129. Behrens, A., Schaeffer, P., Bernasconi, S. & Albrecht, P. 17(E)-13 $\alpha$ (H)-Malabarica-14(27),17,21-triene, an unexpected tricyclic hydrocarbon in sediments. *Organic Geochemistry* **30**, 379–383 (1999).
130. Fischer, W. W. & Pearson, A. Hypotheses for the origin and early evolution of triterpenoid cyclases. *Geobiology* **5**, 19–34 (2007).
131. Abe, I. Enzymatic synthesis of cyclic triterpenes. *Natural Product Reports* **24**, 1311–1331 (2007).

132. Thoma, R. *et al.* Insight into steroid scaffold formation from the structure of human oxidosqualene cyclase. *Nature* **432**, 118–122 (2004).
133. Füll, C. & Poralla, K. Conserved tyr residues determine functions of Alicyclobacillus acidocaldarius squalene-hopene cyclase. *FEMS Microbiology Letters* **183**, 221–224 (2000).
134. Pale-Grosdemange, C., Feil, C., Rohmer, M. & Poralla, K. Occurrence of Cationic Intermediates and Deficient Control during the Enzymatic Cyclization of Squalene to Hopanoids. *Angewandte Chemie (International Ed. in English)* **37**, 2237–2240 (1998).
135. Poralla, K. The possible role of a repetitive amino acid motif in evolution of triterpenoid cyclases. *Bioorganic & Medicinal Chemistry Letters* **4**, 285–290 (1994).
136. Poralla, K. *et al.* A specific amino acid repeat in squalene and oxidosqualene cyclases. *Trends in Biochemical Sciences* **19**, 157–158 (1994).
137. Frickey, T. & Kannenberg, E. Phylogenetic analysis of the triterpene cyclase protein family in prokaryotes and eukaryotes suggests bidirectional lateral gene transfer. *Environmental Microbiology* **11**, 1224–1241 (2009).
138. Anding, C., Rohmer, M. & Ourisson, G. Nonspecific biosynthesis of hopane triterpenes in a cell-free system from *Acetobacter rancens*. *Journal of the American Chemical Society* **98**, 1274–1275 (1976).
139. Rohmer, M., Bouvier, P. & Ourisson, G. Non-specific lanosterol and hopanoid biosynthesis be a cell-free system from the bacterium *Methylococcus capsulatus*. *European Journal of Biochemistry* **112**, 557–560 (1980).
140. Zundel, M. & Rohmer, M. Prokaryotic triterpenoids. 3. The biosynthesis of 2beta-methylhopanoids and 3beta-methylhopanoids of *Methylobacterium organophilum* and *Acetobacter pasteurianus* ssp. *pasteurianus*. *European Journal of Biochemistry* **150**, 35–39 (1985).
141. Douka, E., Koukkou, A., Drainas, C., Grosdemange-Billiard, C. & Rohmer, M. Structural diversity of the triterpenic hydrocarbons from the bacterium *Zymomonas mobilis*: the signature of defective squalene cyclization by the squalene/hopene cyclase. *FEMS Microbiology Letters* **199**, 247–251 (2001).
142. Horbach, S., Neuss, B. & Sahm, H. Effect of azasqualene on hopanoid biosynthesis and ethanol tolerance of *Zymomonas mobilis*. *FEMS Microbiology Letters* **79**, 347–350 (1991).
143. Bravo, J.-M., Perzl, M., Härtner, T., Kannenberg, E. L. & Rohmer, M. Novel methylated triterpenoids of the gammacerane series from the nitrogen-fixing bacterium

- Bradyrhizobium japonicum USDA 110. *European Journal of Biochemistry* **268**, 1323–1331 (2001).
144. Wendt, K. U. Structure and Function of a Squalene Cyclase. *Science* **277**, 1811–1815 (1997).
145. Lenhart, A., Weihofen, W. A., Pleschke, A. E. . & Schulz, G. E. Crystal Structure of a Squalene Cyclase in Complex with the Potential Anticholesteremic Drug Ro48-8071. *Chemistry & Biology* **9**, 639–645 (2002).
146. Feil, C., Süßmuth, R., Jung, G. & Poralla, K. Site-directed mutagenesis of putative active-site residues in squalene-hopene cyclase. *European Journal of Biochemistry* **242**, 51–55 (1996).
147. le Maire, M., Champeil, P. & Møller, J. V. Interaction of membrane proteins and lipids with solubilizing detergents. *Biochimica et Biophysica Acta - Biomembranes* **1508**, 86–111 (2000).
148. Seddon, A. M., Curnow, P. & Booth, P. J. Membrane proteins, lipids and detergents: not just a soap opera. *Biochimica et Biophysica Acta* **1666**, 105–117 (2004).
149. Duquesne, K. & Sturgis, J. N. Membrane protein solubilization. *Methods in molecular biology (Clifton, N.J.)* **601**, 205–217 (2010).
150. Bringer, S., Thomas, H., Poralla, K. & Sahm, H. Influence of ethanol on the hopanoid content and the fatty acid pattern and continuous cultures of *Zymomonas mobilis*. *Archives of Microbiology* **2**, 312–316 (1985).
151. Ingram, L. O. Microbial tolerance to alcohols: role of the cell membrane. *Trends in Biotechnology* **4**, 40–44 (1986).
152. Hermans, M. a, Neuss, B. & Sahm, H. Content and composition of hopanoids in *Zymomonas mobilis* under various growth conditions. *Journal of Bacteriology* **173**, 5592–5595 (1991).
153. Huang, X. & Miller, W. A time-efficient, linear-space local similarity algorithm. *Advances in Applied Mathematics* **12**, 337–357 (1991).
154. Feng, L. *et al.* Genome and proteome of long-chain alkane degrading *Geobacillus thermodenitrificans* NG80-2 isolated from a deep-subsurface oil reservoir. *Proceedings of the National Academy of Sciences of the United States of America* **104**, 5602–5607 (2007).
155. Ward, N. *et al.* Genomic insights into methanotrophy: the complete genome sequence of *Methylococcus capsulatus* (Bath). *PLoS Biology* **2**, e303 (2004).
156. Nakamura, Y. Complete Genome Structure of the Thermophilic Cyanobacterium *Thermosynechococcus elongatus* BP-1. *DNA Research* **9**, 123–130 (2002).

157. Barabote, R. D. *et al.* Complete genome of the cellulolytic thermophile *Acidothermus cellulolyticus* 11B provides insights into its ecophysiological and evolutionary adaptations. *Genome Research* **19**, 1033–1143 (2009).
158. Copeland, A. *et al.* Complete genome sequence of *Catenulispora acidiphila* type strain (ID 139908). *Standards in Genomic Sciences* **1**, 119–125 (2009).
159. Hsiao, N.-H. & Kirby, R. Comparative genomics of *Streptomyces avermitilis*, *Streptomyces cattleya*, *Streptomyces maritimus* and *Kitasatospora aureofaciens* using a *Streptomyces coelicolor* microarray system. *Antonie van Leeuwenhoek* **93**, 1–25
160. Bignell, D. R. D. *et al.* *Streptomyces scabies* 87-22 contains a coronafacic acid-like biosynthetic cluster that contributes to plant-microbe interactions. *Molecular Plant-Microbe Interactions: MPMI* **23**, 161–175 (2010).
161. Fischbach, M. *et al.* Annotation of *Streptomyces svuceus* ATCC 29083. *Unpublished*
162. Pati, A. *et al.* Complete genome sequence of *Sphaerobacter thermophilus* type strain (S 6022). *Standards in genomic sciences* **2**, 49–56 (2010).
163. Pati, A. *et al.* Complete genome sequence of *Saccharomonospora viridis* type strain (P101). *Standards in Genomic Sciences* **1**, 141–149 (2009).
164. Yang, J. C. *et al.* The complete genome of *Teredinibacter turnerae* T7901: an intracellular endosymbiont of marine wood-boring bivalves (shipworms). *PLoS One* **4**, e6085 (2009).
165. Azuma, Y. *et al.* Whole-genome analyses reveal genetic instability of *Acetobacter pasteurianus*. *Nucleic Acids Research* **37**, 5768–5783 (2009).
166. Oda, Y. *et al.* Multiple genome sequences reveal adaptations of a phototrophic bacterium to sediment microenvironments. *Proceedings of the National Academy of Sciences of the United States of America* **105**, 18543–18548 (2008).
167. Copeland, A. *et al.* Complete sequence of *Syntrophobacter fumaroxidans* MPOB. *Unpublished*
168. Aklujkar, M. *et al.* The genome of *Pelobacter carbinolicus* reveals surprising metabolic capabilities and physiological features. *Unpublished*
169. Yang, S. *et al.* Improved genome annotation for *Zymomonas mobilis*. *Nature Biotechnology* **27**, 893–894 (2009).
170. Seo, J.-S. *et al.* The genome sequence of the ethanologenic bacterium *Zymomonas mobilis* ZM4. *Nature Biotechnology* **23**, 63–68 (2005).

171. Abe, T. & Hoshino, T. Enzymatic cyclizations of squalene analogs with threo- and erythro-diols at the 6,7- or 10,11-positions by recombinant squalene cyclase. Trapping of carbocation intermediates and mechanistic insights into the product and substrate specificities. *Organic & Biomolecular Chemistry* **3**, 3127–3139 (2005).
172. Yoder, R. A. & Johnston, J. N. A case study in biomimetic total synthesis: polyolefin carbocyclizations to terpenes and steroids. *Chemical Reviews* **105**, 4730–4756 (2005).
173. Johnson, W. S., Lindell, S. D. & Steele, J. Rate enhancement of biomimetic polyene cyclizations by a cation-stabilizing auxiliary. *Journal of the American Chemical Society* **109**, 5852–5853 (1987).
174. Johnson, W. S., Telfer, S. J., Cheng, S. & Schubert, U. Cation-stabilizing auxiliaries: a new concept in biomimetic polyene cyclization. *Journal of the American Chemical Society* **109**, 2517–2518 (1987).
175. Van Tamelen, E. E. Bioorganic chemistry: sterols and acrylic terpene terminal epoxides. *Accounts of Chemical Research* **1**, 111–120 (1968).
176. Van Tamelen, E. E. Bioorganic chemistry. Total synthesis of tetra- and pentacyclic triterpenoids. *Accounts of Chemical Research* **8**, 152–158 (1975).
177. Wendt, K. U., Schulz, G. E. & Corey, E. J. Mechanismen der enzymatischen Bildung polycyclischer Triterpene. *Angewandte Chemie* **112**, 2930–2952 (2000).
178. Uyanik, M., Ishibashi, H., Ishihara, K. & Yamamoto, H. Biomimetic synthesis of acid-sensitive (-)-caparrapi oxide and (+)-8-epicaparrapi oxide induced by artificial cyclases. *Organic letters* **7**, 1601–1604 (2005).
179. Ishihara, K., Ishibashi, H. & Yamamoto, H. Enantio- and Diastereoselective Stepwise Cyclization of Polyprenoids Induced by Chiral and Achiral LBAs. A New Entry to (-)-Ambrox, (+)-Podocarpa-8,11,13-triene Diterpenoids, and (-)-Tetracyclic Polyprenoid of Sedimentary Origin. *Journal of the American Chemical Society* **124**, 3647–3655 (2002).
180. Surendra, K. & Corey, E. J. Highly enantioselective proton-initiated polycyclization of polyenes. *Journal of the American Chemical Society* **134**, 11992–4 (2012).
181. Koga, T., Aoki, Y., Hirose, T. & Nohira, H. Resolution of sclareolide as a key intermediate for the synthesis of Ambrox®. *Tetrahedron: Asymmetry* **9**, 3819–3823 (1998).
182. Ohloff, G. 75 Jahre Riechstoff- und Aroma-Chemie im Spiegel der Helvetica Chimica Acta. Teil II. *Helvetica Chimica Acta* **75**, 2041–2108 (1992).



183. Ohloff, G., Giersch, W., Pickenhagen, W., Furrer, A. & Frei, B. Significance of the Geminal Dimethyl Group in the Odor Principle of Ambrox. *Helvetica Chimica Acta* **68**, 2022–2029 (1985).
184. Escher, S., Giersch, W., Niclass, Y., Bernardinelli, G. & Ohloff, G. Configuration-Odor Relationships in 5b-Ambrox. *Helvetica Chimica Acta* **73**, 1935–1947 (1990).
185. Fráter, G., Bajgrowicz, J. A. & Kraft, P. Fragrance chemistry. *Tetrahedron* **54**, 7633–7703 (1998).
186. Mori, K. & Tamura, H. Triterpenoid total synthesis, I. Synthesis of ambrein and Ambrox®. *Liebigs Annalen der Chemie* **1990**, 361–368 (1990).
187. Barrero, A. F., Herrador, M. M., Arteaga, P., Arteaga, J. F. & Arteaga, A. F. Communic acids: occurrence, properties and use as chirons for the synthesis of bioactive compounds. *Molecules* **17**, 1448–1467 (2012).
188. Poigny, S., Huor, T., Guyot, M. & Samadi, M. Synthesis of (-)-Hyatellaquinone and Revision of Absolute Configuration of Naturally Occurring (+)-Hyatellaquinone. *The Journal of Organic Chemistry* **64**, 9318–9320 (1999).
189. Talpir, R., Rudi, A., Kashman, Y., Loya, Y. & Hizi, A. Three new sesquiterpene hydroquinones from marine origin. *Tetrahedron* **50**, 4179–4184 (1994).
190. de la Torre, M. C., García, I. & Sierra, M. A. Straightforward synthesis of the strong ambergris odorant  $\gamma$ -bicyclohomofarnesal and its endo-isomer from R-(+)-sclareolide. *Tetrahedron Letters* **43**, 6351–6353 (2002).
191. Boukouvalas, J., Wang, J.-X., Marion, O. & Ndzi, B. Synthesis and stereochemistry of the antitumor diterpenoid (+)-zerumin B. *The Journal of Organic Chemistry* **71**, 6670–6673 (2006).
192. Xu, H.-X., Dong, H. & Sim, K.-Y. Labdane diterpenes from *Alpinia zerumbet*. *Phytochemistry* **42**, 149–151 (1996).
193. Boukouvalas, J. & Wang, J.-X. Structure revision and synthesis of a novel labdane diterpenoid from *Zingiber ottensii*. *Organic Letters* **10**, 3397–3399 (2008).
194. Hinder, M. & Stoll, M. Odeur et constitution IV. Sur les epoxydes hydroaromatiques e odeur ambroxe. *Helvetica Chimica Acta* **33**, 1308–1312 (1950).
195. Stoll, M. & Hinder, M. Odeur et Constitution III. Les substances bicyclohomofarnesiques. *Helvetica Chimica Acta* **33**, 1251–1260 (1950).
196. Schumacher, J. N., Maurey, H. W. & Teague Jr., C. E. Two stage oxidation of sclareol. US Patent 3,050,532 (1962).

197. Gerke, T. & Bruns, K. Process for producing sclareolide. EP0506776 (1994).
198. Schneider, M., Stalberg, T. & Gerke, T. Process for the production of sclareolide. US Patent 5,525,728 (1996).
199. Barton, D., Parekh, S., Taylor, D. & Chi-lam, T. Preparation Of Ambrox. US5463089 (1995).
200. Barton, D., Taylor, D. & Chi-lam, T. Production Of (-)-dodecahydro-3a,6,6,9a-tetramethyl-naphtho[2,1-b]Furan. US Patent 5,473,085 (1995).
201. Whitesides, G., Rene, D. & Ferdinand, N. Novel Hydroperoxide And Use Of Same As Intermediate For The Preparation Of 3a,6,6,9a-tetramethylperhydronaphtho. US patent 4814469 (1989).
202. Farbood, M., Morris, J. & Downey, A. Process For Producing Diol And Lactone And Microorganisms Capable Of Same. US patent 4970163 (1990).
203. Farbood, M. & Willis, B. Process For Producing Diol And Furan And Microorganism Capable Of Same. US patent 4798799 (1989).
204. Cambie, R., Joblin, K. & Preston, A. Chemistry of the Podocarpaceae. XXX. Conversion of 8 $\alpha$ ,13-Epoxyabd-14-ene into a compound with an ambergris-type odour. *Australian Journal of Chemistry* **24**, 583–591 (1971).
205. Decorzant, R., Vial, C., Näf, F. & Whitesides, G. M. A short synthesis of ambrox® from sclareol. *Tetrahedron* **43**, 1871–1879 (1987).
206. Schneider, M., Stalberg, T. & Gerke, T. Process for producing sclareolide. WO/1993/021174 (1993).
207. Barrero, A. F., Altarejos, J., Alvarez-Manzaneda, E. J., Ramos, J. M. & Salido, S. Synthesis of Ambrox® from communic acids. *Tetrahedron* **49**, 6251–6262 (1993).
208. Verstegen-Haaksma, A. A., Swarts, H. J., Jansen, B. J. M. & de Groot, A. Total synthesis of (-)-Ambrox® from S-(+)-carvone (part 6). *Tetrahedron* **50**, 10095–10106 (1994).
209. Cortés, M., Armstrong, V., Reyes, M. E., López, J. & Madariaga, E. Formal Synthesis of Ambrox® and 9-Epiambrox. *Synthetic Communications* **26**, 1995–2002 (1996).
210. Kutney, J. P. & Cirera, C. The chemistry of thujone. XX. New enantioselective syntheses of Ambrox and epi -Ambrox. *Canadian Journal of Chemistry* **75**, 1136–1150 (1997).
211. Koyama, H., Kaku, Y. & Ohno, M. Synthesis of (-)-ambrox from  $\ell$ -abietic acid. *Tetrahedron Letters* **28**, 2863–2866 (1987).
212. Nishi, Y. & Ishihara, K. Synthesis of (-) -Ambrox (R) from (-) -Levopimaric Acid. *Journal of Japan Oil Chemists' Society* **38**, 276–279 (1989).

213. Barrero, A. F., Alvarez-Manzaneda, E. J., Altarejos, J., Salido, S. & Ramos, J. M. Synthesis of Ambrox® from (-)-sclareol and (+)-cis-abienol. *Tetrahedron* **49**, 10405–10412 (1993).
214. Baker, R., Evans, D. A. & McDowell, P. G. Mono- and sesquiterpenoid constituents of the defence secretion of the termite *Amitermes evuncifer*. *Tetrahedron Letters* **19**, 4073–4076 (1978).
215. Schmitz, F. J., McDonald, F. J. & Vanderah, D. J. Marine natural products: sesquiterpene alcohols and ethers from the sea hare *Aplysia dactylomela*. *The Journal of Organic Chemistry* **43**, 4220–4225 (1978).
216. Hlubucek, J. R., Aasen, A. J., Almquist, S.-O. & Enzell, C. R. Structures and Syntheses of a Nor- and a Seco-terpenoid of the Drimane Series Isolated from Tobacco. *Acta Chemica Scandinavica B* **28**, 18–22 (1974).
217. Barrero, A. F., Alvarez-Manzaneda, E. J., Chahboun, R. & Coral Páiz, M. A new enantiospecific route toward monocarbocyclic terpenoids: Synthesis of (-)- caparrapi oxide. *Tetrahedron Letters* **39**, 9543–9544 (1998).
218. Lombardi, P. *et al.* Synthesen der diastereoisomeren Caparrapioxide. *Helvetica Chimica Acta* **59**, 1158–1168 (1976).
219. Kametani, T., Kurobe, H., Nemoto, H. & Fukumoto, K. Stereoselective olefin cyclization mediated by the selenyl group; direct formation of a selenyl caparrapi oxide. *Journal of the Chemical Society, Perkin Transactions 1* **22**, 1085–1087 (1982).
220. Kametani, T., Fukumoto, K., Kurobe, H. & Nemoto, H. Stereoselective olefinic cyclization assisted by the selenyl group — biogenetic-type synthesis of caparrapi oxide. *Tetrahedron Letters* **22**, 3653–3656 (1981).
221. Ishibashi, H., Ishihara, K. & Yamamoto, H. A new artificial cyclase for polyprenoids: enantioselective total synthesis of (-)-chromazonarol, (+)-8-epi-puupehedione, and (-)-11'-deoxytaondiol methyl ether. *Journal of the American Chemical Society* **126**, 11122–3 (2004).
222. Yajima, I., Sakakibara, H. & Ide, J. Volatile flavor components of watermelon (*Citrullus vulgaris*). *Agricultural and Biological Chemistry* **49**, 3145–3150 (1985).
223. Rapior, S., Marion, C., Pélissier, Y. & Bessièrè, J.-M. Volatile Composition of Fourteen Species of Fresh Wild Mushrooms ( Boletales ). *Journal of Essential Oil Research* **9**, 231–234 (1997).

224. Lewinsohn, E. *et al.* Carotenoid pigmentation affects the volatile composition of tomato and watermelon fruits, as revealed by comparative genetic analyses. *Journal of Agricultural and Food Chemistry* **53**, 3142–3148 (2005).
225. Ferezou, J. P. *et al.* 6,10,14-Trimethylpentadecan-2-one and 6,10,14-trimethyl-5-trans, 9-trans, 13-pentadecatrien-2-one from the androgenic glands of the male crab *Carcinus maenas*. *Experientia* **33**, 290 (1977).
226. Duru, M. *et al.* Chemical composition and antifungal properties of essential oils of three *Pistacia* species. *Fitoterapia* **74**, 170–176 (2003).
227. Lee, A.-L., Malcolmson, S. J., Puglisi, A., Schrock, R. R. & Hoveyda, A. H. Enantioselective synthesis of cyclic enol ethers and all-carbon quaternary stereogenic centers through catalytic asymmetric ring-closing metathesis. *Journal of the American Chemical Society* **128**, 5153–5157 (2006).
228. Arica, A. N., Andreeva, I. Y. & Vlad, P. F. Transformations of sclareol oxide by bromination. Synthesis of driman-8?, 11-diol from sclareol oxide. *Russian Chemical Bulletin* **45**, 2644–2648 (1996).
229. Alvarez-Manzaneda, E. J. *et al.* Diels-Alder cycloaddition approach to puupehenone-related metabolites: synthesis of the potent angiogenesis inhibitor 8-epipuupehedione. *The Journal of Organic Chemistry* **72**, 3332–3339 (2007).
230. Bourguet-Kondracki, M.-L., Lacombe, F. & Guyot, M. Methanol Adduct of Puupehenone, a Biologically Active Derivative from the Marine Sponge *Hyrtios* Species. *Journal of Natural Products* **62**, 1304–1305 (1999).
231. Ravi, B. N. *et al.* Recent research in marine natural products: the puupehenones. *Pure and Applied Chemistry* **51**, 1893–1900 (1979).
232. Piña, I. C., Sanders, M. L. & Crews, P. Puupehenone congeners from an indo-pacific *hyrtios* sponge. *Journal of Natural Products* **66**, 2–6 (2003).
233. Prestwich, G. D., Whitfield, F. D. & Stanley, G. Synthesis and structures and dihydroedulan I and II trace components from the juice of *passiflora edulis* sims. *Tetrahedron* **32**, 2945–2948 (1976).
234. Linares-Palomino, P. J., Salido, S., Altarejos, J., Noguerras, M. & Sánchez, A. Synthesis and odour evaluation of stereoisomers of octahydrobenzopyran derivatives. *Flavour and Fragrance Journal* **21**, 659–666 (2006).

235. Kawanobe, T., Kogami, K. & Matsui, M. New Syntheses of ( $\pm$ )-Ambrox, ( $\pm$ )-Ambra Oxide and Their Stereoisomers(Organic Chemistry). *Agricultural and Biological Chemistry* **50**, 1475–1480 (1986).
236. Bolster, M. G., Jansen, B. J. . & de Groot, A. The synthesis of Ambra oxide related compounds starting from (+)-larixol. Part 3. *Tetrahedron* **58**, 5275–5285 (2002).
237. Oritani, T. & Matsui, M. Chemical Studies on Ambergris. *Agricultural and Biological Chemistry* **30**, 659 (1966).
238. Pohl, M. Diploma thesis, ITB: Squalen-Hopen Zyklenen: Biotransformation von nicht natürlichen Substraten und Charakterisierung der entsprechenden Produkte. 1–87 (2012).
239. Vik, A. *et al.* Antimicrobial and cytotoxic activity of agelasine and agelasimine analogs. *Bioorganic & Medicinal Chemistry* **15**, 4016–4037 (2007).
240. Duez, S., Coudray, L., Mouray, E., Grellier, P. & Dubois, J. Towards the synthesis of bisubstrate inhibitors of protein farnesyltransferase: Synthesis and biological evaluation of new farnesylpyrophosphate analogues. *Bioorganic & Medicinal Chemistry* **18**, 543–556 (2010).
241. Cocker, W., Geraghty, N. W. A., McMurry, T. B. H. & Shannon, P. V. R. An investigation of the thermal decomposition of the methoxyhydroxides and methoxydeuterio-oxides of some 5-N,N-dimethylaminopent-1-enes. *Journal of the Chemical Society, Perkin Transactions 1* 2245–2254 (1984).
242. Cermak, D. M., Wiemer, D. F., Lewis, K. & Hohl, R. J. 2-(Acyloxy)ethylphosphonate analogues of prenyl pyrophosphates: synthesis and biological characterization. *Bioorganic & Medicinal Chemistry* **8**, 2729–2737 (2000).
243. Takagi, R. *et al.* Stereoselective syntheses of (+)-rhopaloid acid A and (–)-ent- and ( $\pm$ )-rac-rhopaloid acid A. *Journal of the Chemical Society, Perkin Transactions 1* 925–934 (1998).
244. Schenk, H. R., Gutmann, H., Jeger, O. & Ruzicka, L. Zur Kenntnis der Diterpene. 65. Mitteilung. Ueber einen Ambrarichstoff aus Manool. *Helvetica Chimica Acta* **37**, 543–546 (1954).
245. Schenk, H. R., Gutmann, H., Jeger, O. & Ruzicka, L. Zur Kenntnis der Diterpene. 62. Mitteilung. Ueber eine neue, ergiebige Partialsynthese des Ambreinolids. *Helvetica Chimica Acta* **35**, 817–824 (1952).
246. Vlad, P. F., Ungur, N. D. & Perutskii, V. B. Superacid cyclization of homo- and bishomoisoprenoid acids. *Chemistry of Heterocyclic Compounds* **27**, 246–249 (1991).

247. Aryku, A. N., Mironov, G. N., Koltsa, M. N. & Vlad, P. F. Products of the ozonolysis of isoabienol. *Chemistry of Natural Compounds* **27**, 42–45 (1991).
248. Ekman, R. *et al.* Isoabienol, the Principal Diterpene Alcohol in *Pinus sylvestris* Needles. *Acta Chemica Scandinavica* **31b**, 921–922 (1977).
249. Mäki-Arvela, P. *et al.* Cyclization of citronellal over zeolites and mesoporous materials for production of isopulegol. *Journal of Catalysis* **225**, 155–169 (2004).
250. Bhuiyan, M. N. I., Begum, J., Sardar, P. K. & Rahman, M. S. Constituents of Peel and Leaf Essential Oils of *Citrus Medica* L. *Journal of Scientific Research* **1**, 387–392 (2009).
251. Paik, S.-Y., Koh, K.-H., Beak, S.-M., Paek, S.-H. & Kim, J.-A. The Essential Oils from *Zanthoxylum schinifolium* Pericarp Induce Apoptosis of HepG2 Human Hepatoma Cells through Increased Production of Reactive Oxygen Species. *Biological & Pharmaceutical Bulletin* **28**, 802–807 (2005).
252. Silva, M. I. G. *et al.* Gastroprotective activity of isopulegol on experimentally induced gastric lesions in mice: investigation of possible mechanisms of action. *Naunyn-Schmiedeberg's Archives of Pharmacology* **380**, 233–245 (2009).
253. Silva, M. I. G. *et al.* Central nervous system activity of acute administration of isopulegol in mice. *Pharmacology, Biochemistry, and Behavior* **88**, 141–147 (2007).
254. Etzold, B., Jess, A. & Nobis, M. Epimerisation of menthol stereoisomers: Kinetic studies of the heterogeneously catalysed menthol production. *Catalysis Today* **140**, 30–36 (2009).
255. Brenna, E., Fuganti, C. & Serra, S. From commercial racemic fragrances to odour active enantiopure compounds: the ten isomers of irone. *Comptes Rendus Chimie* **6**, 529–546 (2003).
256. Chuah, G. Cyclisation of Citronellal to Isopulegol Catalysed by Hydrous Zirconia and Other Solid Acids. *Journal of Catalysis* **200**, 352–359 (2001).
257. Cortés, C. B., Galván, V. T., Pedro, S. S. & García, T. V. One pot synthesis of menthol from ( $\pm$ )-citronellal on nickel sulfated zirconia catalysts. *Catalysis Today* **172**, 21–26 (2011).
258. Yongzhong, Z., Yuntong, N., Jaenicke, S. & Chuah, G. Cyclisation of citronellal over zirconium zeolite beta - a highly diastereoselective catalyst to isopulegol. *Journal of Catalysis* **229**, 404–413 (2005).
259. Arata, K. & Matsuura, C. Isomerizations of citronellal to isopulegol and geraniol to linalool catalyzed by solid acids and bases. *Chemistry Letters* **10**, 1797–1798 (1989).

- 
260. Jacob, R. G., Perin, G., Loi, L. N., Pinno, C. S. & Lenardão, E. J. Green synthesis of (-)-isopulegol from (+)-citronellal: application to essential oil of citronella. *Tetrahedron Letters* **44**, 3605–3608 (2003).
261. Takeshi, I., Okeda, Y. & Hori, Y. Process for producing isopulegol. JP2001010527 (2002).
262. Akutagawa, S. Enantioselective isomerization of allylamine to enamine: practical asymmetric synthesis of (-)-menthol by Rh-BINAP catalysts. *Topics in Catalysis* **4**, 271–274 (1997).
263. McCarrity, J. F. *et al.* *Asymmetric Catalysis on Industrial Scale*. (Wiley-VCH Verlag GmbH & Co. KGaA: Weinheim, FRG, 2003).
264. Heydrich, G., Gralla, G., Ebel, K., Krause, W. & Kashani-Shirazi, N. Continuous process for preparing menthol in pure or enriched form. EP2008/059657 (2008).
265. Heydrich, G. *et al.* Method for producing optically active, racemic menthol. US 2010/0249467 A1 (2010).
266. Maeda, H., Yamada, S., Itoh, H. & Hori, Y. A dual catalyst system provides the shortest pathway for L-menthol synthesis. *Chemical Communications* **48**, 1772–1774 (2012).
267. Poralla, K., Kannenberg, E. & Blume, A. A Glycolipid containing hopane isolated from the acidophilic, thermophilic *Bacillus acidocaldarius*, has a cholesterol-like function in membranes. *FEBS Letters* **113**, 107–110 (1980).
268. Seckler, B. & Poralla, K. Characterization and partial purification of squalene-hopene cyclase from *Bacillus acidocaldarius*. *Biochimica et Biophysica Acta - General Subjects* **881**, 356–363 (1986).
269. Steiner, L. Bachelor thesis, ITB: Zyklase-katalysierte Synthese von Naturstoffderivaten. 1–58 (2012).
270. Seitz, M. *et al.* Substrate specificity of a novel squalene-hopene cyclase from *Zymomonas mobilis*. *Journal of Molecular Catalysis B: Enzymatic* **84**, 72–77 (2012).
271. VCCLAB, Virtual Computational Chemistry Laboratory, <http://www.vcclab.org>, 2005.
272. Tetko, I. V. Computing chemistry on the web. *Drug Discovery today* **10**, 1497–1500 (2005).
273. Tetko, I. V. *et al.* Virtual computational chemistry laboratory--design and description. *Journal of Computer-Aided Molecular Design* **19**, 453–463 (2005).

274. Monera, O. D., Sereda, T. J., Zhou, N. E., Kay, C. M. & Hodges, R. S. Relationship of sidechain hydrophobicity and alpha-helical propensity on the stability of the single-stranded amphipathic alpha-helix. *Journal of Peptide Science* **1**, 319–329
275. Siedenburg, G. *et al.* Activation-independent cyclization of monoterpenoids. *Applied and Environmental Microbiology* **78**, 1055–62 (2012).
276. Siedenburg, G., Breuer, M. & Jendrossek, D. Prokaryotic squalene-hopene cyclases can be converted to citronellal cyclases by single amino acid exchange. *Applied Microbiology and Biotechnology* DOI: 10.1007/s00253-012-4008-1 (2012).
277. Katoh, K. & Toh, H. Improved accuracy of multiple ncRNA alignment by incorporating structural information into a MAFFT-based framework. *BMC Bioinformatics* **9**, 212–225 (2008).
278. Katoh, K., Kuma, K., Toh, H. & Miyata, T. MAFFT version 5: improvement in accuracy of multiple sequence alignment. *Nucleic Acids Research* **33**, 511–518 (2005).
279. Itokawa, H. *et al.* Cytotoxic diterpenes from the rhizomes of *Hedychium coronarium*. *Planta Medica* **54**, 311–315 (1988).
280. Katoh, K. MAFFT: a novel method for rapid multiple sequence alignment based on fast Fourier transform. *Nucleic Acids Research* **30**, 3059–3066 (2002).
281. AIST, C. MAFFT alignment. at <<http://mafft.cbrc.jp/alignment/server/>>
282. Swiss Institute of Bioinformatics LALIGN. (2012).at <[http://www.ch.embnet.org/software/LALIGN\\_form.html](http://www.ch.embnet.org/software/LALIGN_form.html)>
283. Hammer, S. C., Dominicus, J. M., Syrén, P.-O., Nestl, B. M. & Hauer, B. Stereoselective Friedel–Crafts alkylation catalyzed by squalene hopene cyclases. *Tetrahedron* **68**, 7624–7629 (2012).
284. Laemmli, U. K. Cleavage of Structural Proteins during the Assembly of the Head of Bacteriophage T4. *Nature* **227**, 680–685 (1970).
285. Toyota, M. & Asakawa, Y. Sesqui- and triterpenoids of the liverwort *Conocephalum japonicum*. *Phytochemistry* **32**, 1235–1237 (1993).
286. Upar, K. B. *et al.* Efficient enantioselective synthesis of (+)-sclareolide and (+)-tetrahydroactinidiolide: chiral LBA-induced biomimetic cyclization. *Tetrahedron: Asymmetry* **20**, 1637–1640 (2009).
287. Scanlon, J. T. & Willis, D. E. Calculation of flame ionization detector relative response factors using the effective carbon number concept. *Journal of Chromatographic Science* **23**, 333–340 (1985).



# 11 Supplementary data

## 11.1 Abbreviations

× g	gravitational acceleration
°C	degree celsius
μL	microliter
μm	micrometer
<sup>13</sup> C NMR	Carbon-13 NMR
<sup>1</sup> H NMR	Proton-NMR
aa	amino acid
<i>Aaci</i> SHC	<i>Alicyclobacillus acidoterrestris</i> squalene-hopene cyclase
<i>Aac</i> SHC	<i>Alicyclobacillus acidocaldarius</i> squalene-hopene cyclase
<i>Ace</i> SHC	<i>Acidothermus cellolyticus</i> squalene-hopene cyclase
<i>Apa</i> SHC1	<i>Acetobacter pasteurianus</i> squalene-hopene cyclase 1
<i>Apa</i> SHC2	<i>Acetobacter pasteurianus</i> squalene-hopene cyclase 2
approx.	approximately
<i>Bam</i> HI	restriction enzyme from <i>Bacillus amyloliquefaciens</i> , recognition site (G'GATCC)
BINOL	binaphthol
bp	base pair
BSA	bovine serum albumin
<i>Cac</i> SHC	<i>Catenulispora acidiphila</i> squalene-hopene cyclase
CDCl <sub>3</sub>	deuterated chloroform
CHAPS	3-[(3-cholamidopropyl)dimethylammonio]-1-propanesulfonate hydrate
cm/sec	centimeters per second
cmc	critical micelle concentration
COSY	<sup>1</sup> H- <sup>1</sup> H correlated spectroscopy
ddH <sub>2</sub> O	double demineralized water
dH <sub>2</sub> O	demineralized water
DMAPP	dimethylallyl diphosphate
DNA	deoxyribonucleic acid
DxDD	conserved motif in SHCs
<i>E. coli</i>	<i>Escherichia coli</i>
ECN	effective carbon number

---

EDTA	ethylenediaminetetraacetic acid
eV	electron volt
FID	flame ionization detector
final temp.	final temperature
FPP	farnesyl diphosphate
g	gram
GC	gas chromatography
GC-FID	gas chromatography coupled with flame ionization detector
GC-MS	gas chromatography coupled with mass spectrometry
GFPP	geranylarnesyl diphosphate
GGPP	geranylgeranyl diphosphate
GPP	geranyl diphosphate
<i>GthSHC</i>	<i>Geobacillus thermodentrificans</i> squalene-hopene cyclase
h	hour
H <sub>2</sub>	hydrogen
HCl*aq	hydrochloric acid
HMBC	heteronuclear multiple bond coherence
HREIMS	high resolution electron impact mass spectrometry
<i>HsaOSC</i>	human lanosterol synthase
HSQC	heteronuclear single quantum coherence
IPP	isopentenyl diphosphate
IPTG	isopropyl- $\beta$ -D-thiogalactopyranoside
ISTD	internal standard
kb	kilo-base pair
kDa	kilo Dalton
LB	lysogeny broth
LBA	Lewis acid-assisted chiral Brønsted acid
MAD route	mevalonate-dependent route
MAI	mevalonate independent
<i>McaSHC</i>	<i>Methylococcus capsulatus</i> squalene-hopene cyclase
MeOH	methanol
mg	milligram
MgCl <sub>2</sub>	magnesium chloride
MHz	Megahertz
min	minute
mL	milliliter
mM	millimolar

MS	mass spectrometry
NaCl	sodium chloride
NaOH	sodium hydroxide
<i>Nde</i> I	restriction enzyme from <i>Neisseria denitrificans</i> , recognition site (CA <sup>+</sup> TATG)
NMR	nuclear magnetic resonance
no.	number
NOESY	nuclear Overhauser effect spectroscopy
OD <sub>600</sub>	optical density measured at 600 nm
OSC	oxidosqualene cyclase
part. purified	partially purified
<i>Pca</i> SHC1	<i>Pelobacter carbinolicus</i> squalene-hopene cyclase 1
<i>Pca</i> SHC2	<i>Pelobacter carbinolicus</i> squalene-hopene cyclase 2
PMSF	phenylmethanesulfonyl fluoride
RF	relative response factors
Rf	retention factor
<i>Rpa</i> SHC1	<i>Rhodopseudomonas palustris</i> squalene-hopene cyclase 1
<i>Rpa</i> SHC2	<i>Rhodopseudomonas palustris</i> squalene-hopene cyclase 2
rpm	rounds per minute
RT	room temperature
<i>Sco</i> SHC	<i>Streptomyces coelicolor</i> SHC squalene-hopene cyclase
SDS	sodium dodecyl sulfate
SDS-PAGE	sodium dodecyl sulfate polyacrylamide gel electrophoresis
<i>Sfu</i> SHC1	<i>Syntrophobacter fumaroxidans</i> squalene-hopene cyclase 1
<i>Sfu</i> SHC2	<i>Syntrophobacter fumaroxidans</i> squalene-hopene cyclase 2
SHC	squalene-hopene cyclase
<i>Ssc</i> SHC	<i>Streptomyces scabiei</i> squalene-hopene cyclase
<i>Ssv</i> SHC	<i>Streptomyces sviveus</i> squalene-hopene cyclase
<i>Sth</i> SHC	<i>Spherobacter thermophilus</i> squalene-hopene cyclase
<i>Svi</i> SHC	<i>Saccharomonospora viridis</i> squalene-hopene cyclase
TB	terrific broth
<i>Tel</i> SHC	<i>Thermosynechococcus elongatus</i> squalene-hopene cyclase
TLC	thin layer chromatography
Tris	Tris(hydroxymethyl)-aminomethane
TSMSh	trimethylsulfonium hydroxide
<i>Ttu</i> SHC	<i>Teredinibacter turnerae</i> squalene-hopene cyclase
WT	wildtype

xxDC	conserved motif in OSCs
<i>ZmoSHC1</i>	<i>Zymomonas mobilis</i> squalene-hopene cyclase 1
<i>ZmoSHC2</i>	<i>Zymomonas mobilis</i> squalene-hopene cyclase 2

## 11.2 Sequences and other informations about the SHCs

**Table 11.1: Overview of the SHCs discussed and characterized in the present work.**

name	original host	information	available at ITB?	ITB no.
<i>Aaci</i> SHC	<i>Alicyclobacillus acidoterrestris</i>	GI: 927384; CAA61950.1	yes	ITB286
<i>Aac</i> SHC	<i>Alicyclobacillus acidocaldarius</i>	GI: 2851526; P33247.4	yes	ITB285
<i>Ace</i> SHC	<i>Acidothermus cellolyticus</i>	GI: 117928904; YP_873455.1	yes	ITB287
<i>Apa</i> SHC1	<i>Acetobacter pasteurianus</i>	GI: 258541105; YP_003187836.1	yes	ITB312
<i>Apa</i> SHC2	<i>Acetobacter pasteurianus</i>	GI: 258541296; YP_003186729.1	no	-
<i>Cac</i> SHC	<i>Catenulispora acidiphila</i>	GI: 256395787; YP_003117351.1	yes	ITB288
<i>Gth</i> SHC	<i>Geobacillus thermodentrificans</i>	GI: 138895534; YP_001125987.1	yes	ITB162
<i>Mca</i> SHC	<i>Methylococcus capsulatus</i>	GI: 53804820; YP_113312.1	yes	ITB164
<i>Pca</i> SHC1	<i>Pelobacter carbinolicus</i>	GI: 77544139; ABA87701.1	no	-
<i>Pca</i> SHC2	<i>Pelobacter carbinolicus</i>	GI: 77544053; ABA87615.1	yes	ITB313
<i>Rpa</i> SHC1	<i>Rhodopseudomonas palustris</i>	GI: 115526460; YP_783371.1	yes	ITB314
<i>Rpa</i> SHC2	<i>Rhodopseudomonas palustris</i>	GI: 90421528; YP_531598.1	no	-
<i>Sco</i> SHC	<i>Streptomyces coelicolor</i>	GI: 21225057; NP_630836.1	yes	ITB315
<i>Sfu</i> SHC1	<i>Syntrophobacter fumaroxidans</i>	GI: 116698484; ABK17672.1	yes	ITB316
<i>Sfu</i> SHC2	<i>Syntrophobacter fumaroxidans</i>	GI: 116699226; ABK18414.1	no	-
<i>Ssc</i> SHC	<i>Streptomyces scabiei</i>	GI: 260645368; CBG68454.1	yes	ITB289
<i>Ssv</i> SHC	<i>Streptomyces sviveus</i>	GI: 197784692; YP_002207454.1	yes	ITB290
<i>Sth</i> SHC	<i>Spherobacter thermophilus</i>	GI: 269838031; YP_003320259.1	yes	ITB291

<i>Svi</i> SHC	<i>Saccharomonospora viridis</i>	GI: 257056311; YP_003134143.1	yes	ITB292
<i>Tel</i> SHC	<i>Thermosynechococcus elongatus</i>	GI: 22299852; P_683099.1	yes	ITB171
<i>Ttu</i> SHC	<i>Teredinibacter turnerae</i>	GI: 254787171; YP_003074600.1	yes	ITB320
<i>Zmo</i> SHC1	<i>Zymomonas mobilis</i>	GI: 56552444; YP_163283.1	yes	ITB104
<i>Zmo</i> SHC2	<i>Zymomonas mobilis</i>	GI: 6466213; AAF12829.1	yes	ITB283
<i>Zmo</i> SHC1_F486Y	-	-	yes	ITB294
<i>Aac</i> SHC_Y420C	-	-	yes	ITB304
<i>Zmo</i> SHC1_Loop	-	-	yes	ITB322

### 11.2.1 Wildtype SHCs

The amino acid sequences of the SHCs characterized in the present work are shown in this paragraph. For the DNA sequence and further information, see supporting information on the CD-ROM.

#### **ZmoSHC1**

MGIDRMNSLSRLLMKKIFGAEKTSYKSPASDTIIGTDTLKRPNRRPEPTAKVDKTIIFKTMGNS  
LNNTLVSACDWLIGQQKPDGHVWGVAVESNASMEAEWCLALWFLGLEDPRLPRLGNALLEMQ  
REDGSWGVYFGAGNGDINATVEAYAALRSLGYSADNPVLKAAAIAEKGLKNIRVFTRYW  
LALIGEWPWEKTPNLPEI IWFDPDNFVFSIYNFAQWARATMVP IAILSARRPSRPLRPQDRL  
DELFPEGRARFDYELPKKEGIDLWSQFFRTTDRGLHWVQSNLLKRNSLREAAIRHVLEWIIIR  
HQDADGGWGGIQPPWVYGLMALHGEGYQLYHPVMAKALSALDDPGWRHDRGESSWIQATNSP  
VWDTMLALMALKDAAEDRFTPEMDKAADWLLARQVKVKGDWSIKLPDVEPGGWAFEFYANDR  
YPTDDTAVALIALSSYRDKEEWQKGVEDAITRGVNWLIAMQSECGGWGAFDKDNNRSILS  
KIPFCDFGESIDPPSVDVTAHVLEAFGTLGLSRDMPVIQKAIDYVRSEQEAEAGAWFGRWGVN  
YIYGTGAVLPALAAI GEDMTQPYITKACDWLVAHQQEDGGWGESCSSYMEIDSIGKGPPTPS  
QTAWALMGLIAANRPEDYEAI AKGCHYLIDRQEQDGSWKEEEFTGTGFPGYGVGQTIKLDPP  
ALSKRLLQGAELSRAFMLRYDFYRQFFPIMALSRAERLIDLNN

**ZmoSHC2**

MTVSTSSAFHHSPLSDDVEPIIQKATRALLEKQQQDGHVWFEELEADATI PAEYIILLKHYLGE  
 PEDLEIEAKIGRYLRRIQGEHGGWSLFYGGDDLDSATVKAYFALKMIGDSPDAPHMLRARNE  
 I LARGAMRANVFTRIQLALFGAMSWEHVPQMPVELMLMPEWFPVHINKMAYWARTVLVPLL  
 VLQALKPVARNRGILVDELFPDVLPTLQESGDPIWRRFFSALDKVLHKVEPYWPKNMRK  
 AIHSCVHFVTERLNGEDGLGAIYPAIANSVMYDALGYPENHPERAIARRAVEKLMVLDGTE  
 DQGDKEVYCQPCLSPIWDTALVAHAMLEVGGDEAEKSAI SALSWLKPPQI LDVKGDWAWRRP  
 DLRPGGWAFQYRNDYYPDVEDTAVVTMAMDRAAKLSDLHDDFEESKARAMEWTIGMQSDNGG  
 WGAFDANNSYTYLNNIPFADHGALDPPTVDVSARCVMMAQAGISITDPKMKAAVDYLLKE  
 QEEDGSWFRGWVNYIYGTWSALCALNVAALPHDHLAVQKAVAWLKI QNEDGGWGGENCDSY  
 ALDYSGYEPMDSQTAWALLGLMAVGEANSEAVTKGINWLAQNQDEEGLWKEDYYSGGGF  
 PRVFYLRYHGYSKYFPLWALARYRNKKANQP I VHYGM

**AacSHC**

MAEQLV EAPAYARTL DRAVEYLLSCQKDEGYWWGPLLSNVTMEAEYVLLCHILDRVDRDRME  
 KIRRYLLHEQREDGTWALY PGGPDLDTTIEAYVALKY IGMSRDEEPMQKALRFIQSQGGIE  
 SSRVFTRMWLALVGEY PWEKVPMPVPEIMFLGKRMLPNI YEFGSWARATVVALSIVMSRQPV  
 FPLPERARVPELYETDVP PRRRGAKGGGWI FDALDRALHGYQKLSVHPFRRAAEIRALDWL  
 LERQAGDGSWGIQPPWFYALIALKILDMTQHPAFIKGWEGLELYGVVELDYGGWMMFQASISP  
 VWDTGLAVLALRAAGLPADHDLVKAGEWLLDRQITVPGDWAVKRPNLKPGGFQFDNVYY  
 PDVDDTAVVVWALNTLRLPDERRRRDAMTKGFRWIVGMQSSNGGWGAYDVNTSDLPNHIFP  
 CDFGEVTDPPSEEDVTAHVLECFGSFGYDDAWKVI RRAVEYLLKREQKPDGWSWFRGWVNYLYG  
 TGAVVSALKAVGIDTREPYIQKALDWVEQHQNPDGGWGEDCRSYEDPAYAGKGASTPSQTAW  
 ALMALIAGGRAESEAAARRGVQYL VETQRPDGGWDEPYTGTGFPGFYLYGYTMYRHVFP TLA  
 LGRYKQAIERR

**11.2.2 Mutants**

The amino acid sequences of the SHC mutants characterized in the present work are shown in this paragraph. For the DNA sequence and further information, see supporting information on the CD-ROM.

**ZmoSHC1\_F486Y**

MGIDRMNSLSRLLMKKI FGAEKTSYK PASDTIIGTDTLKRPNRRPEPTAKVDKTI FFKTMGNS  
 LNNTLVSACDWLIGQQKPDGHVWGAVE SNASMEAEWCLALWFLGLEDHPLRPLGNLALLEMQ  
 REDGWSGWYFAGAGNDINATVEAYAALRS LGYSADNPVLKKAAWIAEKGLKNI R VFTRYW  
 LALIGEWPEKTPNL PPEI I WFPDNFVFSIYNFAQWARATMVP I AILSARRPSRPLRPQDRL  
 DELFPEGRARFDYELPKKEGIDLWSQFFRTTDRGLHWVQSNLLKRNLSLREAAIRHVLEWII R  
 HQDADGGWGGI QPPVWYGLMALHGEGYQLYHPVMAKALSALDDPGWRHRDRGESSWIQATNSP  
 VWDTMLALMALKDAKAEDRFTPEMDKAADWLLARQVKVKGDSIKLPDVEPGGWAFEFYANDR  
 YPDTDDTAVALIALSSYRDKEEWQKGVEDAITRGVNWLIAMQSECGGWGAYDKDNNSILS  
 KIPFCDFGSAIDPPSVDVTAHVLEAFGTLGLSRDMPVIQKAI DYVRSEQEAEAGAWFRGWVN  
 YIYGTGAVLPALAAIGEDMTQPYITKACDWLVAHQEDGGWGESCS SYMEIDSIGKGP TTPS  
 QTAWALMGLIAANRPEDYEAIAKGC HYLIDRQE QDGSWK EEEFTGTGFPGYGVGQTIKLDDP  
 ALSKRL LQGAELSRAFMLRYDFYRQFFPIMALSRAERLIDLNN

**AacSHC\_Y420C**

MAEQLVEAPAYARTLDRAVEYLLSCQKDEGYWWGPLLSNVTMEAEYVLLCHILDRVDRDRME  
KIRRYLLHEQREDGTWALYPGGPPDLDTTIEAYVALKYIGMSRDEEPMQKALRFIQSQGGIE  
SSRVFTRMWLALVGEYPWEKVPMPVPEIMFLGKRMPINIYEFGSWARATVVALSIVMSRQPV  
FPLPERARVPELYETDVPPIRRRGAQGGGGWIFDALDRALHGYQKLSVHPFRRAAEIRALDWL  
LERQAGDGGSWGGIQPPWFYALIALKILDMTQHPAFIKGWEGLELYGVVELDYGGWMMFQASISP  
VWDTGLAVLALRAAGLPADHDRLVKAGEWLLDRQITVPGDWAVKRPNLKPGGFQFQFDNVYY  
PDVDDTAVVVWALNTLRLPDERRRRDAMTKGFRWIVGMQSSNGGWGACDVNTSDLPNHIFP  
CDFGEVTDPPSEDVTAHVLECFGSFGYDDAWKVIRRAVEYLKREQKPDGGSWFGRWGVNYLYG  
TGAVVSALKAVGIDTREPYIQKALDWVEQHQNPDGGWGEDCRSYEDPAYAGKGASTPSQTAW  
ALMALIAGGRAESEAAARRGVQYLVE TQRPDGGWDEPY YTGTFPGDFYLYGTYMRHVFTPLA  
LGRYKQAIERR

**ZmoSHC1\_Loop**

MGIDRMNSLSRLLMKKIFGAEKTSYKPASDTIIGTDTLKRPNRRPEPTAKVDKTIKFTMGNS  
LNNTLVSACDWLIGQQKPDGHVWVAVESNASMEAEWCLALWFLGLEDHPLRPLGNALLEMQ  
REDGSWGVIYFGAGNGDINATVEAYAALRSLGYSADNPVLKAAAWIAEKGLKNI R VFTRYW  
LALIGEWPEKTPNLPEI I WFPDNFVFSIYNFAQWARATMVPIAIL SAR RPSRPLRPQDR L  
DELFPEGRARFDYELPKKEGIDLWSQFFRTRTDRGLHWVQSNLLKRNLSLEAAIRHVLEWII R  
HQDADGGWGGIQPPVWYGLMALHGEGYQLYHPVMAKALSALDDPGWRHDRGESSWIQATNSP  
VWDTMLALMALKDAKAEDRFTPEMDKAADWLLARQVKVKGDSIKLPDVEPGGWAFEYANDR  
YPTDDTAVALIALSSYRDKEEWQKKGVEDAITRGVNWLIAMQSECGGWGAFDKDNNRSILS  
KIPFCDFGESIDPPSVDVTAHVLEAFGTLGLSRDMPVIQKAIDYVRSEQEAEGAWFGRWGN  
YIYGTGAVLPALAAIGEDMTQPYITKACDWLVAHQQEDGGWGESCSSYMEIDSIGKGP TTPS  
QTAWALMGLIAANRPEDYEAI AKGCHYLIDRQE QDGSWK EEEFTGTGFPRAFMLRYDFYRQF  
FPIMALSRAERLIDLNN









## 12 Curriculum vitae

### Persönliche Daten

Name	Miriam Seitz
Geburtstag	21. Februar 1984 in Rastatt
Familienstand	ledig
Nationalität	deutsch
Anschrift	Wilhelmstr. 11, 70182 Stuttgart
Email	miriam.seitz@gmx.net

### Universitäre Laufbahn

Seit 10/2009	<b>Promotion am Institut für technische Biochemie, Universität Stuttgart</b>  Titel der Arbeit: "Characterization of the substrate specificity of squalene-hopene cyclases (SHCs)"
09/2009	<b>Diplom Lebensmittelchemie, Universität Hohenheim (Note: 1,3)</b>
03/2009 -09/2009	<b>Anfertigen der Diplomarbeit, Universität Vigo, Spanien</b>  Titel der Arbeit: „Development of Immunoaffinity Chromatography (IAC) as an alternative for the Solid-phase Extraction of Polycyclic Aromatic Hydrocarbons (PAHs) in mussels prior to chromatographic analysis (HPLC-FLD and GC-MS)"
10/2006 – 02/2009	<b>Hauptstudium Lebensmittelchemie, Universität Hohenheim</b>
10/2004 – 09/2006	<b>Grundstudium Lebensmittelchemie, Universität Stuttgart (Note: 1,6)</b>

### Schulische Laufbahn und sonstiges

08/2003 – 06/2004	<b>Tätigkeit als Au-Pair, Barcelona, Spanien</b>
07/2003	<b>Abitur, Tulla Gymnasium Rastatt (Note: 1,6)</b>
08/1994 – 07/2003	<b>Tulla-Gymnasium Rastatt</b>